Development of EEG Measurements Coupling with Ocular InformationToward Daily Use Free-Viewing Applications

	Ai　Guangyi
	27
17104	262
URL	http://hdl.handle.net/10228/00006278

Development of EEG measurements coupling with ocular information toward daily use free-viewing applications

Guangyi Ai

Graduate School of Life Science and Systems Engineering,

Kyushu Institute of Technology

Contents

Abstract

As the technique of electroencephalogram (EEG) developed for such many years, its application spreads and permeates into different areas, such like, clinical diagnosis, brain-computer interface, mental state estimation, and so on. Recently, using EEG as a tool for estimate people's mental state and its extensional applications have jump into the limelight. These practical applications are urgently needed because the lack of subjectively estimating methods for the so called metal states, such as the concentration during study, the cognitive workload in driving, the calmness under mental training and so on. On the other hand, the application of EEG signals under daily life conditions especially when eye movements are totally without any constrains under a 'fully free-view' condition are obedient to the traditional ocular artifact suppression methods and how it meets the neuroscience standard has not been clearly expounded. This cause the ambiguities of explaining the obtain data and lead to susceptive results from data analysis.

In our research, based on the basic idea of employing and extending EEG as the main tool for the estimation to mental state for daily life use, we confirmed the direction sensitivity of ocular artifacts induced by various types of eye movements and showed the most sensitive areas to the influence from it by multi zone-of-view experiment with standard neuroscience-targeted EEG devices. Enlightened from the results, we extended heuristic result on the use of more practical portable EEG devices. Besides, for a more realistic solution of the EEG based mental state estimation which is supposed to be applied for daily life environment, we studied the signal processing techniques of artifact suppression on low density electrode EEG and showed the importance of taking

direction/eye position information into account when ocular artifact removal/suppression.

In summary, this thesis has helped pave the practical way of using EEG signals toward the general use in daily life which has irregular eye movement patterns. We also pointed out the view-direction sensitivity of ocular artifact which helps the future studies to overcome the difficulties imposed on EEG applications by the free-view EEG tasks.

Chapter 1　Introduction

1.1. Research background

As time goes by, EEG device and EEG measurement are not the exclusively used appliances any more. More and more EEG application has been expected to help and provide convenience to our everyday life. Especially after the portable EEG device has been invented, researcher and engineers proposed many creative applications of EEG in daily life, for instance, the combination with smart phones to display users' brain activities and EEG spectrums. Moreover, based on the evidences from neuroscience studies, the use of EEG and be expected as hopeful tool for monitoring study efficiency, cognitive workload, patients' home life state and their needs for medical care and so on. The basic ideas of those applications are all based on the portable EEG use concept. Recently, new applications of EEG signals are extensively proposed. They popularity of those new EEG application concepts depends on their needs. As an example, one of the hottest topics in this field is driver's mental state estimation because car accidents have been a serious safety problem in our everyday life. As reported by the National Highway Traffic Safety Administration (NHTSA), over 25% percent of the crashes are related the driver's mental state problems [1]. From another report, it is announced that over all the car crash accidents, driver's mental state actually played a very significant role in all the crashes and near crashes, and this percent can be seem as main factor (78%) [2]. As is shown as typical examples above, the use of EEG to estimate people's brain state has in fact become a huge and highly attractive field. However, every application has its own particularity (e.g. under the condition which is during body movements, or in an almost still state without any motion but intensive brain activities).

Understanding the features used for EEG analysis for that was applications is crucial.However, it is very difficult to work out a general framework which overcomes all the application fields, and including more applications means the meaningful features from EEG signals are not clearly identified, such as which frequency band use or what ERP to test during the practical implications. So it is very important to spacify the original purpose before talking about EEG applications although there may exist some common point between those applications. Drivers' workload estimation is one of the best examples of portable EEG use as it moderately balanced the body movements and brain activities during the EEG recording. So, to clearly identify the daily use condition and avoid the ambiguities, we selected the use of EEG for driver's mental state estimation as the typical example and discussed the issues brought by it in EEG measuring and analysis in the coming parts of this thesis.

On the other hand, the estimation of mental state for daily use is a difficult issue, because usually the mental state is subject was supposed to be a subjective problem which is done by subjects (in our case, drivers) themselves. However, there exists a very big variance by using subjective estimation. The subjective estimation relies on individual judgment and shows a big variance from different subjects, even if they are putting into the same driving environment. Besides, subjective estimation faces the problem of quantitative difficulties. These reasons lead to the necessity of assessing the brain state by means of bio-signals reflecting the inner status concealed beyond the precise assesses by subjective determinations.

The aim of bio-signal based mental state estimation contains the following main tasks:

a) Finding and extracting features representing the metal state changes

b) Quantitatively analyzing the features with predefine metal states or state changes

c) Metal states estimation by the obtained features from real-life data recording

The bio-signal applied for mental state estimation must satisfy the high usability (easy to acquire) and quantitative functions to subjects' inner states or their changes. If the mental state estimation exceeds a certain level of safety concerns, system can alert or provide automatic assistances to the in danger conditions.

The so-called mental state actually comprises a number of factors, for instance, mental workload, fatigue, drowsiness, cognitive distraction and so on. Therefore, it comes with the challenge to deal with the multiple estimation problems, in which it is required to assess as many as the mentioned factors at the same time. As an example, during driving the typical relationship between driver's mental states and the operative performance can be described as the figure below:

Figure 1.1 An example of the typical relationship between mental state and driver's operative performance. The symbols '-' and '+' represent the relationship (negative correlation and positive correlation) between factors in driving tasks.

As we can see from the Figure 1.1, the mental workload is actually acting as a precursor of for the operative performance, but is doesn't affect the operative performance directly. In fact, the situation is one of the straight-forward factors of operative performance. However the deterministic relationship in between bring us the possibilities to setup a measuring system to assess operative performance from brain

actives. According to the negative and positive correlations between mental workload situation awareness and operative performance, an increase in mental workload results in a decrease in situation awareness, then the operative performance decreases with the situation awareness together when the linear constrain holds on. Note, whether their relationship is linear or not and when their relationship can be considered as linear is still not clear. There is a high probability of the existence of non-linear factors and saturation stages. Yet, as shown in the review paper [3], in spite of those doubtable points, the detection of mental stats by bio-signals has been demonstrated with a pretty high precision up to around 90% for off-line use, although the on-line use seems still have a bit far way to go until it can generate satisfactory results. But successful achievements from those off-line systems greatly encourage researchers and the on-line related studies have already caught the tremendous attentions in car-safety system design and related fields.

Therefore, the application of bio-signals in mental state estimation is an extraordinarily hopeful technique which may lead to revolutionary innovations and highly expected to form a practical use system to decrease the accident rate with the necessary alert to drivers or help the intelligent car systems to determine the corresponding operations in time. In another word, this technique places our hope on providing a smart life protector in our developing on-the-car life.

1.2. Bio-signal based mental state estimation

Indeed, mental state estimation can be done from many kinds of bio-signals. The bio-signals has been employed in the mental state estimation include: Electroencephalogram (EEG), Electrooculography (EOG), eye trace, heartbeat rate,

Electromyography (EMG) and so on. Recent researches suggested that many kinds of bio-signals fit the purpose of detecting human brain state, while some of them such as pupil size and skin conductance applied techniques greatly rely on the surrounding environments (e.g. quietness, darkroom, keeping still when testing and so on) and only works for in-lab psychological experiment, the others were able to be extended to the real-life use for state estimations. Some of the popular bio-signals are listed below, as mentioned above the examples are shown with respect to drivers' mental state estimation:

1) Electroencephalogram

It has been as of now exhibited by a few studies that EEG is touchy to fluctuations in carefulness or vigilance and has been suggested as a method to make predictions about the decrease of efficiency or performance because of continuous mental work in operative tasks [4][5].

Relationship between an abatement of human alertness and a kind of degeneration in carefulness and weakness has been found to produce significantly obvious signs in on-going EEG recordings. Those signs are particularly and clearly shown in alpha and theta waves bands [6][7]. With respect to the band power changes, it has been demonstrated that a process of decreasing in vigilance and a gradual decline in operative performance are brought into relation with the spectra increment of EEG band power in theta band and a change in EEG alpha power [8].

In addition, the study of Okogbaa et al. [9] suggested that arousal and alertness have a correlation with an increase phenomenon take place in the EEG power spectrum. And the increase they found was in beta band. They also pointed out that the alpha band's

power increase happens when the subjects were in relaxed conditions, with decreased attention, and suffer from drowsiness. However, during the wakeful stage, no significant alpha features were found. In comparison to alpha wave, theta waves show a strong tendency of occurring when sleeping. Conversely, an observation that the alpha activity shows at the parietal area decreases with the change of the predefined gradually increasing working memory load or multi task level [10]–[12].

It is also necessary to note that at parietal areas an increase of theta power has also been reported as a response to increased task demands [13]. With respect to the tasks in which attention level goes up, theta activities also can be observed in frontal head [14]. This provides a very good clue to measure mental stress or workload in driving conditions for drivers.

Previous researches also studied the relationship between time pressure task and EEG power. As an instance, in the research of Slobounov's [15], they found an increase in theta band during the time pressure task. The electrodes clearly showing the tendency were located in frontal head and central scalp. Boksem [12] testify the influence from fatigue accumulation. They also found theta band power increase by comparing the theta power at the end and the started time of tasks.

It has been reported that during a task with complex and high cognitive demands the EEG power in alpha band decreased. The power decrease was proved to appear in different areas over scalp, and the regions of frontal-central and parietal were suggested showing stable decreasing patterns [13][15].

During the change process from a common state to a fatigued state, EEG also shows corresponding changes. This kind of power change was observed increasing in delta band [16]. As is reviewed by Borghini [3], in many studies, the EEG power decrease in

alpha band and the increase in theta band were usually paired in tasks.

Recently, the increase in theta band was also found during the well-designed tasks that attracts subjects' sustained attention. The same pattern were reported via simultaneous multi task based EEG measuring experiments as were mentioned in [10][13]. However, in multi task experiments, whether the sensitivity of EEG power changes is adequate enough to make a complexity level estimation are still staying unclear.

EEG studies on pilots' training and real-driving have done as well as car drivers' recently. The interesting conclusion was that during the training sessions, pilots' theta power was not affected, whereas the changes in real-driving were significantly observed.

2) Heart rate

The cardiovascular response can thus be used to evaluate the mental load of a task in aviation. However, the variation of HR is also linked to different factors besides mental workload, including the fatigue of the subjects (in terms of muscular efforts). Another important variable that can be linked to mental fatigue using cardiovascular responses is the Fourier transform of the HR signal, known as Heart Rate Variability (HRV).

Several studies have shown that if the internal, external and initial conditions are kept constant, HR and HRV are measures of task demands, since such variables demonstrated a very high correlation with questionnaires and behavioral tasks [17][18].

3) Electrooculography

It is a common experience that when a particular task involves the use of visual

attention, subject becomes more concentrated and decreases the time spent with the eye closed for blinking, i.e., their blink frequency decreases. Researchers have investigated whether such phenomena could lead to valid indications about the mental workload for tasks requiring high visual attention, such as driving. As a result, eye blink data has been collected in highly realistic settings of driving. Different parameters characterizing the blink, such as the Blink Rate (BR), the Blink Duration (BD), and the Blink Latency (BL) have been analyzed and used as workload measures in a series of studies [19][20].

Blink patterns can be used to provide information about the subjects' response to different stimuli and thus SA, and the latency measure has been found to increase with memory demands. A general conclusion that can be drawn is that

A general conclusion that can be drawn is that the blink rate maybe most related to visual information requirements and fatigue. Blink duration and blink latency could be also measures of work-load. Wilson and Fisher [19] have demonstrated the advantage of using both HR and eye blink data in the analyses of pilots' mental workloads. Fewer and shorter blinks have been associated with increased workload, in tasks such as city driving, reading and aircraft weapon delivery [21].

In this study, our choice of bio-signal used to detect mental state is EEG. Among all the bio-signals, EEG is highly preferred as a powerful tool to assess inside brain neuron activities because EEG is directly related to the brain and neuron activities.

Along with the hardware technology development, the portable EEG devices with high sampling frequency and long battery life are not only an assumption in theoretical research anymore. Portable EEG devices has already been invented and commercialized now. Its high usability of EEG gains the popularity in applications and is pushed to a real-life utilization stage.

However, here are some issues and limitations of EEG based mental state estimation. Those difficulties to real-life application induced the main objectives of this thesis:

1.3. Thesis Objectives

Although EEG based mental state estimation has been proved efficient and practical, it still suffers from some well-known problems, for instance, the most prominent problems of suppression of artifacts and lack of robust and stable algorithms for low density, low sampling frequency portable EEG devices. Another important issue is that, most of the experiments are done in laboratory environment with only EEG measurement. This is risky because of two reasons. The first, the information collected by a single system may not be able to provide adequate proofs to reflect the real inside-brain state. If there are some biases or systematic errors, it will be very difficult to realize by simply investigating the one-sided data recordings. A very good example is, when a potential level changed in a single-channel recording system, it is almost not possible to tell whether it belongs to eye movement artifact or induced by heartbeat or some other non-brain activities. The second, in-lab environment experiment, especially for EEG experiments, there are many factors cannot be well simulated. For example under driving condition ,the light condition, weather, passengers, and the vibrations in the cockpit, and relative speed caused by car acceleration and so on, all these factors occupy a considerable proportion of real driving, and there it is not necessarily that there are uncorrelated to EEG recordings and mental states.

Taking aim at improving the practicability of EEG measuring for a real-world use, in this thesis, the study was focused on ocular artifact suppression under daily use conditions which is totally in a free-view working environment. The difference between

laboratory conditions and real life environment causes significant distinctions of ocular artifact in magnitude and amount. To solve the problem of such kind of free-view artifact suppression, the characteristic of free-view eye movements must be well analyzed. To improve the practicability of EEG with real-world environment, this thesis is mainly focused on the following crucial jobs:

1) Prominent artifact (ocular artifacts) analysis with eye tracker by standard neuroscience research instruments

Differing from the neuron science tasks which are basically performed in laboratory environment with well-designed stimulations and fixation instructions, it is impossible to avoid or restrain eye movements. The eye movements may also exceed the reasonably defined distance/angles in traditional EEG experiments. Furthermore, under conditions outdoor, subjects' blink frequency may extremely overtake the common frequency measuring in a comfort environment where the common EEG or BCI experiments are carried out.

In this way, the eye artifacts were constrained with the number of the limitations. For example, the eye movement frequency and the eye moment distance during the EEG measuring tasks. Before experiment, all subjects usually get instructed with some explanation that not to know their body and all eyes doing the experiment. Although many researchers investigated the relationship between eye movement and the invoked potentials over scalp for neuroscience experiments (e.g. ERP analysis) [22]–[24], BCI use [25], all of them were focused on data center fixed it EOG pattern, that the eye rotation happen in literal side or the random area have not been well researched yet. Maybe in the traditional neuroscience experiments, it doesn't matter how the eye

rotations happen in a random area generate influence to EEG signals, because the eye rotation was constrained with some predefined limitations, for example the fixation cross in the center of the stimulation screen. In a real life environment, it's crucial because there is no assurance that the users' eyes stare at the predefined area. To overcome the problem of this, it is urgently necessary to know how the free eye movement the fact the EEG signals. In this part of our research is focused on this issue. The main target in this part is to investigate whether there are significant effects existing and which parts on the scalp or affected strongly or almost nothing not to be affected from the free eye moment. Hopefully, we can identify the areas being safe (not contaminated by strong ocular artifacts) under free view condition. The study for this purpose would be profound in-lab, and to get a precise data set, some limitations used it in neuroscience researches would be combined.

In this section, the nature of ocular artifacts in EEG recordings would be analyzed combining an eye tracking system. In this way, the redundant data from eye tracking system would provide benefits for the analysis to EEG data. Provided the eye trace data, the EEG caused by eye moment can be more precisely identified and well segmented with the time information with respect to eye moments.

2) Practical ocular artifact suppression method evaluations and finding out a smart method for portable EEG device

The EEG measurement suffers from high amplitude artifacts such as the EMG, line noise which is caused by power supply, and ocular artifacts which induced by blink or eye movements. So, at certain, it is a very important task to solve the problem of artifact suppression. To reconstruct the true EEG signals or the EEG signals only contain a very

low level artifact, the algorithm ran for data analysis and de-noising is vital. There are many methods have been proposed recently [26], every of them were proved to be efficient in signal de-noising. However, because the true EEG signal and artifacts cannot be separated when measuring, there are no criterions and evidences of what is the actual EEG signal.

However, it doesn't mean that it is not necessary to analysis the factors which influence the artifact suppression process. Researchers are making great efforts to investigate the factors hidden behind the visible EEG recordings and it has been proved the methods developed under different assumptions or verification theories improved the visibility of the 'under-ground' neuron activates such as event-related potential (ERP), event-related synchronization (ERS) and event-related synchronization (ERD). So the study around the central topic of EEG artifact suppression is still one of the most important steps towering the practical use of EEG signals in real life.

So, one of the main tasks of this research has been set on this purpose. Several existing techniques would be analyzed and evaluated for the use of artifact removal. Actually, there are many kinds of artifacts take place in EEG experiments, such as EMG, line noise, heartbeat, EEG level drifting caused by sweeting and so on. Because the ocular artifact is deemed as one of the most prominent artifact sources, we selected ocular artifact as the main topic in this thesis, and algorithms for suppressing or removing ocular artifacts would be studied too.

In addition, we also study the complexity of all the algorithms, because in a real-life use not all the algorithms designed for theoretical research can be applied, one of the aims of the research was set to find out a simple but efficient method for the artifact suppression in low-density, low sampling frequency possible EEG devices.

3) Evaluation to EEG based mental state estimations with practical use with portable devices

The aim of estimating mental state with the commercial level EEG instruments is not that easy. Because there are potential risks brought by the EEG instruments, in other words, whether the portable commercial EEG devices can provide enough signal quality for our purpose hasn't been investigated or reported from recent researches. We would do the job ourselves by evaluating the performance of the commercial EEG devices with well researched psychological experiments with respect to human mental state in this thesis as well. The result of our research will probably push the EEG experiment from an in-lab environment to the real-life use, because of the on-purpose selected EEG device we used. The eye tracking system used for analyzing eye movements and its nature would also be combined in our EEG experiment. Hopefully, we can also get some other approaches which can help EEG analysis and mental state estimations. Finally, we would demonstrate that combining eye tracker may provide some extra benefits for mental state estimation by providing redundant information that related to the change of mental states.

1.4. The organization of this thesis

In chapter 2, the nature of EEG including the source and the electrical characteristics were studied the sources and properties of artifacts, especially for the ocular artifacts. The traditional way of dealing with ocular artifacts and its limitation in daily use were also discussed in this chapter. Chapter 3 focused on the signal processing methods of suppressing or removing artifacts. In chapter 4, we investigated the direction sensitivity

of eye moment related artifacts and their distribution on topographic maps by a novel systematic experimental design. We also discussed the possibility of improving existing ocular artifacts removal algorithms and opened a new viewpoint about free view EEG experiment design and data analysis. Moreover, our results suggested that by selecting intellectual positions, the problem of ocular artifact in driving experiments can be relieve, so that the common artifact removal algorithm may also get considerable good performance in the data analysis stage. In chapter 6, the performance improvement when taking view-field into account was shown and evaluated by correlation coefficient comparisons. Finally, in chapter 7, the contributions of this thesis and the prospective of conquering the artifacts induced by irregular eye movement in daily life use EEG was summarized.

Chapter 2　EEG measurements and ocular artifacts

2.1. EEG signals, frequency band and EEG measurement

1) EEG signal and collection:

The Electroencephalogram (EEG) is the potentials which observed by noninvasive surface electrode over a head scalp. EEG can be seen as the biological expression in surface potential reflecting the inside brain activities including: oscillation, voltage fluctuations. This kind of signal registers the inside-brain spontaneous electrical changes which induce neuron's firing under skull. The ionic current within the neurons of the brain is deemed as the source of EEG [27]. Whereas a single neuron can only generate very weak electrical changes, when a big cluster of neuron fire together, an observable electrical changes can be measured using an electrode over human's scalp surface. Figure 2.1 and 2.2 show how the EEG signals were generated from neuron activities. So in a sense, EEG signals are the electrical expression of the brain activities under skull and actually the original EEG signals are very weak that without a high gain amplifier the potentials are difficult to obtain. From the pictures we can see, the EEG signals are highly related with cortex structures. Irregular folds of cortex surface may cancel the potential field of neuron activities greatly, thus the neuron activities with the same strength may lead into different EEG potentials depending on the EEG correction positions. Note that people's brain folds are different from one another even on the same cortex. This leads to an ambiguity of explaining EEG signals, so that for the same brain activity, the EEG signals obtained may have differences between subjects. On the other hand, the propagation of EEG signals is actually in the form of spreading from the activity source to near areas over scalp, so that activities from the same source can be

observed in the area around the source position through the volume conductance of brain [28]. Taking this property of EEG into account, it is reasonable to believe that the EEG signals are statistically similar between subjects. This provides the availability of the using EEG signals from different subjects to assess and bring activities with respect to the same stimulation in experiments.

When measuring the EEG signals, the position of electrodes is crucial. As mentioned before, EEG signals may show different tendencies depending on electrode positions, determining electrode positions becomes a vital step in EEG measurements. The most popular way to define electrode positions is international 10-20 system. Figure 2.3 shows an example of international 10-20 system configuration. In this international electrode position configuration, all the electrode positions are defined using the distances of proportions of predefined total length on scalp, and basically the difference between two electrodes are set as 10% or 20% of the circumference of subjects scalp.

This electrode position configuration method has been extended to international 10-5 and 10-10 systems and so on four different purposes.
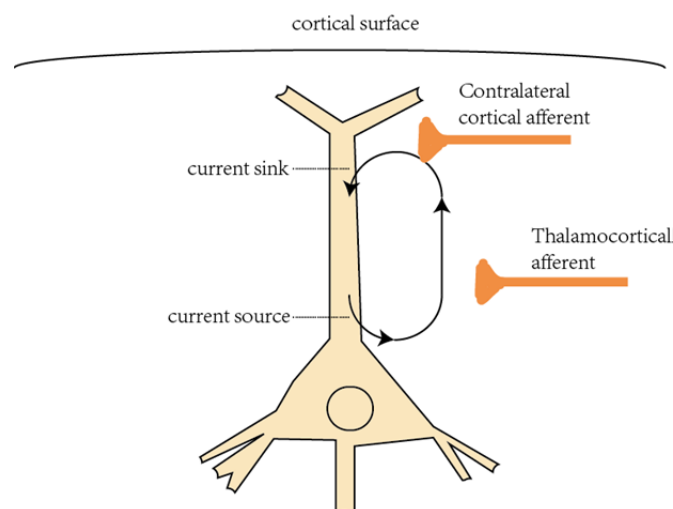

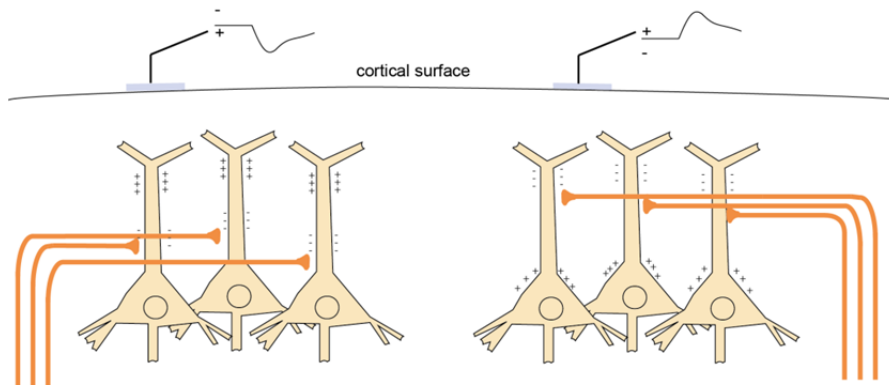Figure 2.1 an example of the pattern of electrical current flow

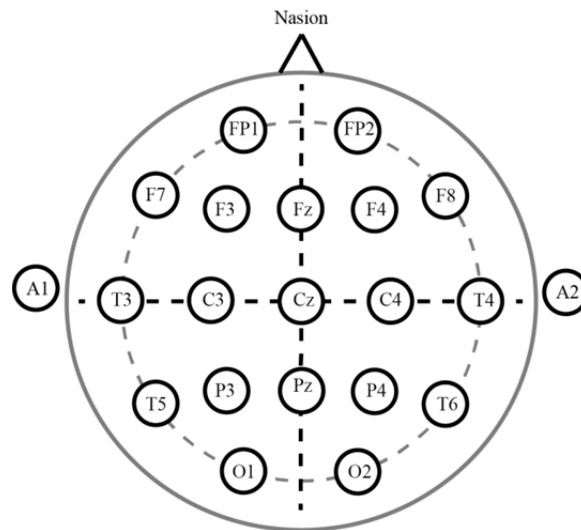Figure 2.2 neuron cluster and surface electrical potential

Figure 2.3 An example of electrode configuration of international 10-20 system

As EEG signals are considerably weak, typically less than 10 µV~100µV [29] from scalp measurement, the acquisition of EEG signals are usually obtained by the amplifier before ADC input. To make the EEG signals observable, the gain of the amplifier is usually set to 10,000 or higher. Figure 2.4 shows a typical EEG correction system structure. Usually the collection device in this figure is flexible depending on implementations. For traditional in-lab in neuroscience researches, big and unhandy professional EEG measuring devices are used; whereas for possible EEG applications,

this part is generally realized by a single structure which contains both the amplifier and ADC functions but with a convenient and possible design so that subjects' motion is not constrained.
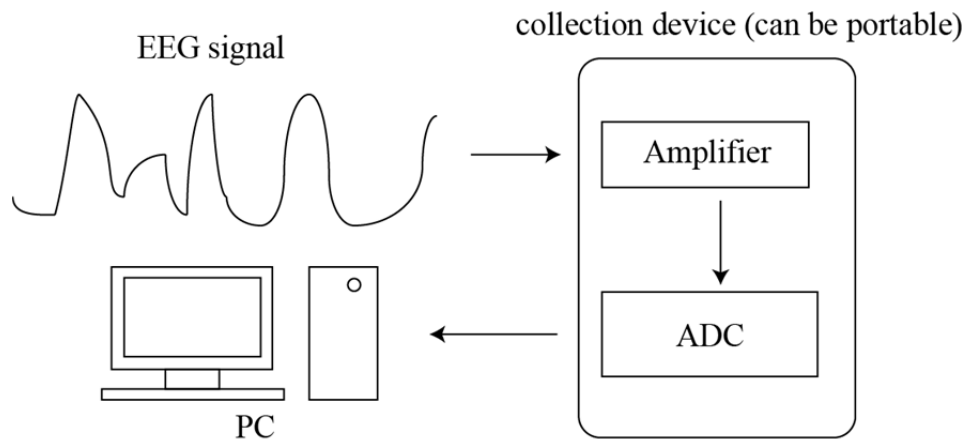

Figure 2.4 Typical EEG collection system

2) Frequency band in EEG signal:

As its oscillation nature of brain activities which is very complicated and usually investigated by dynamic models, EEG signals also show oscillation patterns in different defined events from low-frequency to the higher ones: Delta (<4 Hz), Theta (4~7 Hz), Alpha (8~15 Hz), Beta (16~31 Hz) and Gamma (higher than 31 Hz). In some researches, Mu band is defined as 8~12 Hz frequency band. This kind of definition is usually used for sensorimotor cortex related researches, which is commonly combined with BCI or ERD/ERS topics.

Delta band signals are often detected in frontal head from adult humans and in posterior parts of head from children. EEG signals in this band usually show high amplitudes and relatively smooth changes in comparison to the other EEG signal bands, for instance, the research done by Kirmizi et al. [30]. In their research, the investigated

the potential changes in GO/NoGO tasks. They suggested that delta band power changes are related with continuous attention tasks under certain conditions.

Theta wave is one of the most extensively investigated fields in many researches. In Zhang's research, they reported the traveling theta waves take place in human hippocampus [31]. Because this nature of Theta wave, researchers often presume that theta wave is strongly related to memory process and recognition. It is reported that theta wave are related to working memory process, and its power is usually stronger in children than adults in frontal-midline locations [32]. Interestingly, the locations of theta wave are usually not related to tasks designs. Maglione [33] reported that the EEG spectrum of Theta band changes markedly during car driving tasks when workload or drowsiness varies.

The famous alpha wave has a long history. It is deemed alpha wave was found by Hans Berger, one of the greatest researchers who opened the field of EEG. The easiest way to elicit alpha wave is just closing eyes during EEG recording. Posterior regions such as O1, O2, and Oz usually show the strongest alpha waves in this way of closing eyes. Alpha wave is very frequently used in neuroscience researches, especially is investigated as the main signal for sleeping related researches [34]–[36]. Recently, the relationship between pain and alpha power changes has also been reported [37]. In car driving related studies (e.g. fatigue, drowsiness, workload and so on), alpha wave also plays prominent roles [38]–[41].

Beta wave generally shows a low-amplitude characteristic in EEG signals. High alertness, stress, anxious state and focusing are highly related to the beta spectra fluctuations [42]–[45]. beta wave also had been found and applied to ERD/ERS studies [46]. As one of the most successful applications, most of the motor imagery based BCIs

employ beta wave as a crucial feature [47]–[49]. In addition, the Mu wave should be mentioned together here, because mu suppression is used as the indicator that monitors rest state when subject are not doing anything to elicit motor neurons activities. In most of the BCI applications, mu wave and beta wave are paired.

The last EEG band is gamma band. Gamma band has the widest frequency range. Because the line-noise caused by power supply (usually 50 or 60 Hz) and EMG caused by muscular movements strongly contaminate gamma waves, in many preliminary researches, gamma band was usually only taken from 31 Hz to a frequency lower than 50 Hz to avoid the line noise or abandoned when muscular movements are too much. Another practical method is notch filter with an extremely sharp block frequency band. Gamma band has also been investigated on its correlation with mental workload [50][51], but for car driving topics, it is not frequently mentioned.

3) EEG measuring system

There are several ways to classify EEG instruments because the use or application of EEG instruments differs from each other. Besides, the specifications also affect categorization. Generally, according to amplifier type, EEG measuring devices can be separated into two groups: AC EEG instrument and DC EEG instrument.

In AC-amp systems, the large offset the low-frequency potential is reduced by using high-pass filters before handling the signals by an analog-digital-converter (ADC). In other words, the gain of low-frequency signals is very low, so that the high amplitude low-frequency components were filtered out before data recording. Most of the traditional EEG measuring devices are in this structure, because without a filtering stage, low-frequency signal which contains significantly high potentials may cause saturation

problems to EEG recordings. DC coupled amplifiers solve this problem by a filter techniques, in this way the dynamic range of the ADC can be most efficiently used. However, the negative part of this technique is losing the slowly drifting potential conflicts in EEG recordings. This technique was the only option for EEG acquisition up until approximately 15 years ago. An example of the AC EEG instrument recorded signal is shown below:
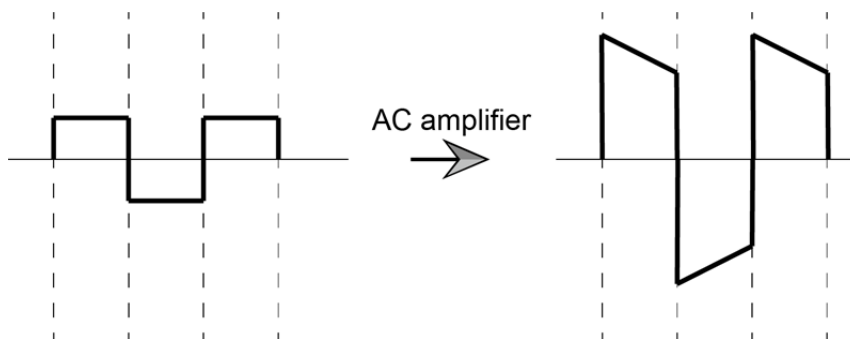

Figure 2.5 EEG recordings collected by AC amplifier

In DC EEG instruments, the amplifier works in a DC mode with a wide-range rail-to-rail the dynamic range so that the offset of the low-frequency components with high amplitude are not necessary to be filled out. Generally, this dynamic range is between +/- 300~450 mVs. DC EEG amplifier is recently developed it is more expensive than the AC EEG devices and has more power consumption at the same sampling rate of AC EEG instruments. But its powerful way to register low-frequency components in EEG experiments makes DC EEG systems the more preferable to collect EEG data. The figure below shows an example of the signals recorded by DC EEG instrument.
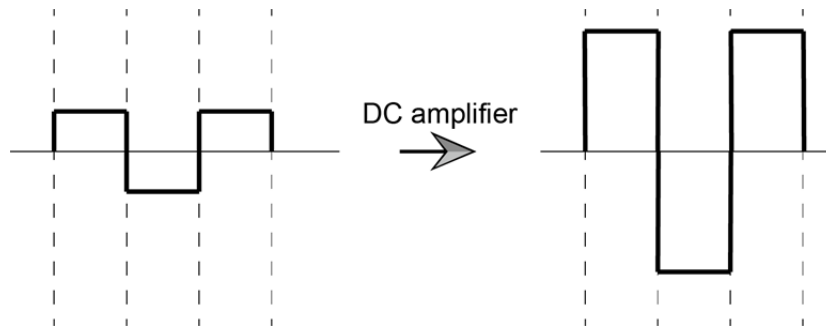
Figure 2.6 EEG recordings collected by DC amplifier

The EEG signals are usually measure by silver electrodes (Ag/AgCl). But in this way, the electrodes should be used with paste or gel to be a media between data centers and them. The preparing stage of this costs a lot of time, and sometimes even causes uncomfortable feelings to subjects. Recently new EEG electrodes have been invented, for example needle electrode and felt electrode is showing below. The previous one is actually a kind of dry electrode which is efficient in touching the bare skin on subjects' head surface, whereas the later one is a kind of semi-dry structure which employs the conductance of liquid media for electrically data collections. Figure 2.7 shows two typical examples of electrodes.
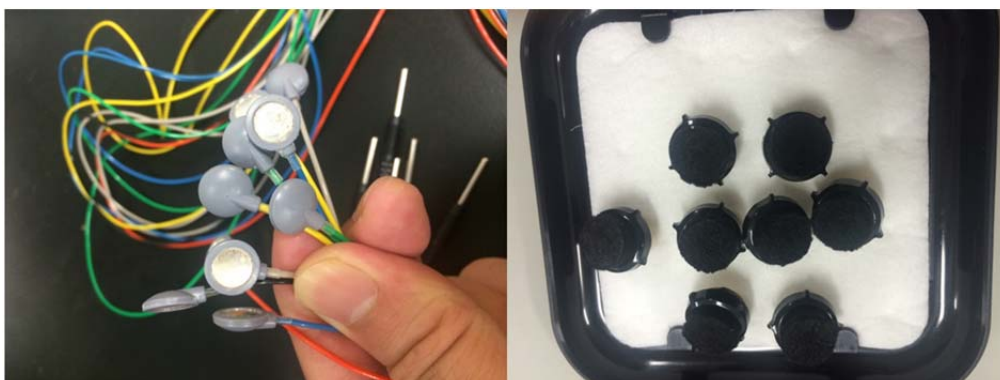

Figure 2.7 Ag/Agcl electrodes and low cost half-dry electrodes

EEG instruments can also be categorized as standard EEG instrument and commercial EEG device. The standard EEG instruments usually has more EEG channels (from 16~256 or more) and higher sampling frequency (~2000 Hz or more). Experiments done with the standard EEG instruments are generally constrained in an in-lab environment; and subjects' motions are extremely limited. While the commercial EEG devices usually have only a few EEG channels can be used sampling frequency (typically ~128 or 256 Hz), but the commercial version of EEG instruments is usually designed for entertainment or portable use. So it provides a more practical way to measure EEG signals in real-life environments. Figure 2.8 and Figure 2.9 display two kinds of EEG measuring devices, a standard EEG instrument and a portable one.
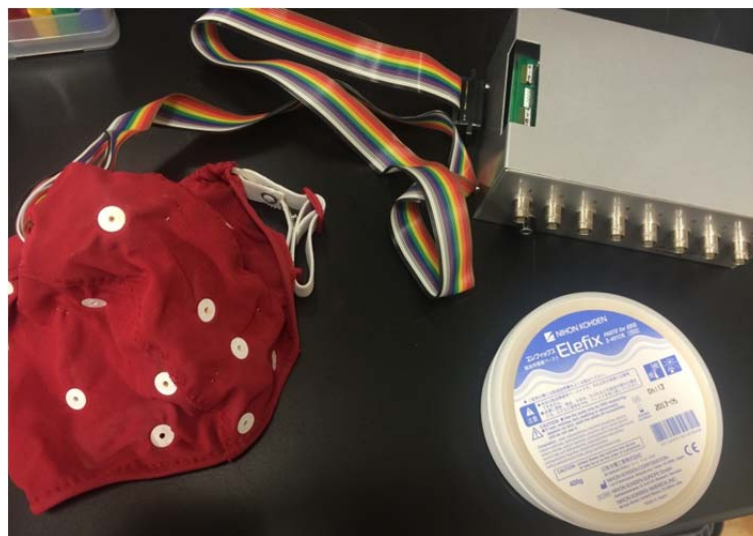

Figure 2.8 Standard EEG device

Figure 2.9 Portable commercial EEG device

According to the type of electrons, they can be separated into two groups: passive electrodes and active electrodes. The passive electrodes are the original type used for EEG instruments. Recently, the electrodes with a little amplifier near the electrode taps have been invented and called as active electrode. The active electrode can efficiently decrease the noise caused by line shakings and has been more and more popularly used in EEG measuring systems.

2.2. Advantages and hindrances of EEG

Because of its noninvasive property, EEG recordings gain the popularity among the brain activity observation technologies. With a long development history, Electroencephalogram (EEG) signal has become one of the most popular ways for observing brain activities. The first time that EEG signals and its properties were described is known as the great job done by Hans Berger, in 1929.

The primary use of EEG was a tool for neuroscientists to investigate

neurophysiological phenomena with respect to brain activities. After so many years development, EEG has become a very popular tool and over the past decades researcher extensively investigated possible applications of EEG and boosted into a technique for various on-line monitoring system, such as brain-computer-interface (BCI), neuro-marketing [52], driver and pilot fatigue monitoring, and training [53].

The success of EEG is well-known, but for the same purpose of brain state observation, actually there are many other suitable techniques. For instance, functional magnetic resonance imaging which can provide precise information of activated brain or cortex area and magnetoencephalography which take advantages of the magnetic field change induce by the current flow.

However, the two well-known techniques, although the functional magnetic resonance and the magnetoencephalography are able to specify activated brain regions deep inside, they have inevitable limitation in body movements and difficulties downsizing into a handheld tool. As they measure brain activities in another way by the magnetic field changes, they usually need power supply system and massive hardware components to assure data precision. Thus, the limitations with respect to those apparatus confine their applications greatly and prevent their use in daily life. Near-infrared spectroscopy (NIRS) is a new attempt and has been grown up to a popular technique for brain activity observation. NIRS employs optical imaging technology to reflect the blood-oxygenation-level of the blood flow, thus can avoid the electrical problems the other systems have for example, noise potentials. This technique is also safe to use. Because of this ascendant reason, it attracts researchers to study young infant's brain activities [54] by using NIRS. However, with the advantage of interference-free with other electric activities, it also has the disadvantages of limited

spatial and temporal resolutions because of relatively slow blood circulation speed. Furthermore, all those instruments mentioned above are so extremely expensive that is impossible to be extended for brain state observation in daily use.

Whereas, EEG can be obtain by considerably cheaper devices. Up to now, there have already existed many kinds of commercialized portable EEG devices, which are targeted to daily life use or for entertainment purposes. Besides, EEG provides high time resolution (typically more than 200 Hz) so that researchers have a strong tendency to combine EEG technique with MRI or MEG together for brain science or neuroscience studies, even for clinical diagnostics. Although its spatial resolution is relatively low, recently researchers reported an amount of evidences of its performance in source localization and source estimation [55] which support EEG as a general research tool in the future.

However, extracting meaningful signals or features from EEG data are still an intractable problem. Extracting meaningful signals from EEG highly relies on the signal quality obtain by EEG devices.

In the typical in-lab experiments, researchers basically impose constrains to subjects so that the signal quality can be improved, although the endogenous artifacts are impossible to be decreased, such as the artifacts generated by heart beats or spontaneous activities.

Actually, the low qualities of EEG signals are caused by two main reasons: Hardware specifications and artifacts.

Hardware problem is significantly prominent in portable EEG devices. The table below shows the difference between typical in-lab EEG instruments and commercial EEG devices:

For in-lab use, devices employed are usually professional EEG instruments; the electrodes used for data recording are usually Ag/Agcl electrode because they can provide high-quality potential collection; the technical sampling frequency is greater than 1000 Hz; the ADC resolution is usually more than 20 bits, and so on.

Whereas for daily use/solutions, the device used are usually portable/commercialized EEG devices. They collect EEG signals by low-cost dry or felt electrodes; sampling frequency is usually less than 256 Hz; the ADC resolution is usually less than 16 bits.

The relatively low specification of portable EEG devices determines the relatively inferior competence in signal quality and data sufficiency. But it is reasonable to believe that this problem can be overcome sooner or later according to the development of hardware technique. Contradictorily, the endogenous problems of various artifacts are more intractable.

2.3 The artifacts in EEG

Artifacts can be understood as the non-brain activities in EEG recordings. This does not mean the artifacts are caused by improper data acquisition or device problems. Artifacts can be grouped as the following two classes.

a) Physiological artifacts:

Ocular artifacts: induced by eye movements, blinks or muscular actions of eyes.

EMG: originates from muscular activities.

ECG: the heartbeat potential recorded in EEG data.

And so on...

b) Non-physiological artifacts:

Bad electrode connection: usually caused by unstable electrode montage and motion during experiments.

D.C. drift: the change of direct current component in EEG recordings.

Line noise: 50/60 Hz noise interference from power supply system.

And so on...

While the non-physiological artifacts may be avoided by adjusting and setting the experimental environment, the physiological artifacts which reflect subjects' physiological activities are not possible to suppress. In spite of the fact that they are deemed not related to brain activities, their amplitude and power spectrum may greatly bigger than the original EEG signals collected from scalp. Future more, because they are non-separable, no one can tell how the true EEG signals look like and how they changes during brain activities. This obscure the meaning of obtained EEG signals a lot.

The latter two physiological artifacts are usually called as ocular artifacts. Removing ocular artifacts is still a problem of EEG analysis for ERP experiments and frequency analyses.

As mentioned before and the ocular artifacts are usually defined as the potentials caused by blinks and eye movements during EEG recordings. These artifacts have tortured EEG researches for many years. Ocular artifacts are usually more than 100 μV which is much higher than common EEG signals, covering the low-frequency band up to about 20 Hz in common [56].

Ocular artifacts, especially the ones happened near stimulation onset distort baseline and the invoked potentials greatly. Although signal averaging can improve signal-to-noise rate, the invoked potentials are usually very weak (e.g. less than 10 μV). Furthermore, ocular artifacts usually do not follow a certain statistical distribution. If

ocular artifacts are involved, much more trials are needed to average out the influences of them.

Because their frequency band is overlapped, during EEG spectrum analysis, it is unclear that the low-frequency changes are caused by ocular artifacts or predefined stimulations.

This problem becomes even more serious in daily EEG applications, because in daily EEG applications eye movements are irregular. In comparison to in-lab experiments, daily EEG applications are special because subjects are not put into a highly constrained environment (e.g. construing of view sights or ranges). In another word, daily EEG applications are basically performed in a completely free-viewing experiment without any fixation lockers/points to guide the subjects' viewing actions. The frequency and magnitude of ocular artifacts may be greatly higher because of the more complicated stimulations from the real-life environment. This problem becomes one of the biggest challenges to boost in-lab EEG achievements to the reliable applications in daily life.

2.4 Electrical model of eyes

In human eyeballs, there exists a potential between the front and the back part. This potential is usually defined as the potential difference between cornea and retina [57]. The electrolysis process is deemed as the reason why this potential exists. When lights pass through eyeballs, the cornea and racial parts of eyeballs are charged positively and negatively respectively, so that the electrical potential difference can be measured between the frontal and back sides. To make it easy to understand, we can describe this model as a charge the battery in a 3-D dimension. Whereas, the potential difference between cornea and retina is far from static. This can be explained as the fact that the

lights passing through eyeballs are highly dependent of the environments and the electrolysis process taking place inside eyeballs. From now on, we use the terminology 'corneo-retinal dipole' to describe this electrical model. This electrical model of eyes explains why the potential from eyeballs propagate is over scalp. It is deemed that the potential of corneo-retinal dipole propagates by volume conductance of brain [25]. Corft and Barry [22] suggested that the amplitude of the propagated potential is inversely related to the distance from eyeballs to the scalp electrode positions. In another word, the further the electrodes positions are, the weaker propagated potentials would be propagated to those electrode positions. Thus, this propagation rate/coefficient can be observed by collecting the EOG (obtained from the electrodes around eyes) and the propagated potentials from different scalp electrodes.

EOG potentials are not static because of the influences of lights and the dynamical electrolysis process taking place inside eyeballs and brain. Whereas, the relationship between EOG signals and the propagated signals over scalp are generally linear, so that it is possible to obtain the linear coefficient representing their relationship. This is the basis of the EOG propagation analysis.

It is very important to know that the electrical model of eyes is also affected by eyelids. As we can see from Figure2.10, when eyelid moves the positively charged with cornea area would be covered partly and this directly based to the potential decrease of the cornea pole. However the decrease of the positive charges doesn't mean that they were canceled out, on the contrary, the covered positive charges contribute to the potential increase of the electrodes located at higher positions. So, usually this effect or described as a kind of shortcut process. Because of shortcut effect from eyelid, the electrodes located higher than eyeballs are actually showing a positive drift after eyelid

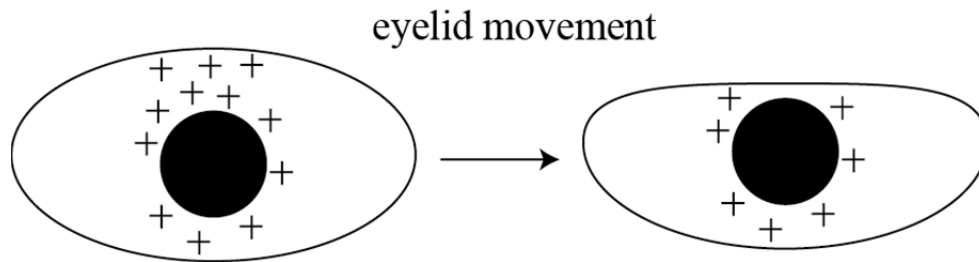goes downward with the constraint that the reference electrodes are not affected by this shortcut effect.

Figure 2.10 eyelid movement and cornea potential

The most typical of a moment is blink. Figure 2.11 shows link potentials during EEG recording. The shortcut effect of eyelid movement explains why the eye link potentials are positive peaks in most of the EEG recordings. Note in this figure, we can see in channel V1D and V2D, the potentials are actually negative. This is because those electrodes or below all eyes.

To simplify the model, the eye movements are usually modeled as a sliding electrode in researches [25]. In summary, the electric model of eyes can be seen as a spatial dipoles which contain both position information and electrical characteristics.
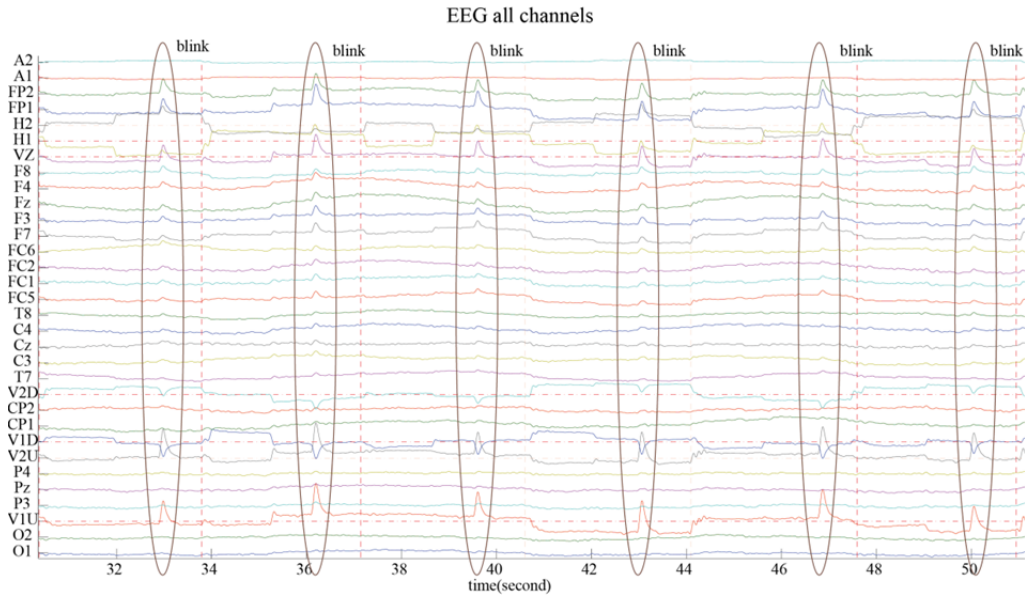
Figure 2.11 Blinks in EEG recording

The electrical model eyeballs considerably simplified propagation potentials in EEG recording. But eye moment processes are usually dynamic and taking place in the three dimension natural space. In this space eye moments can be described as a sum of three elements: horizontal component, vertical component and radial component. And theoretically, any eye moment can be separated into the eye movements of these three components. To model the eye moments consisting different components, Berg and Scherg [58] suggested a 3-D dipole model. In this model, they used six parameters to describe the spatial properties of eyeball dipoles. These six parameters are: x location, y location and z location of dipoles, with their orientation represented by two angular values, and the amplitude of dipoles. In this way, any dynamic changes taking place in eye moments can be described by the changes of those six parameters. In this model, the x,y,z coordinates defined the position of current-dipole in a 3-D space; the amplitude of the dipole is determined by the current strength; and the orientation of the dipole can be

determined by those two angular values.

Indeed, brain activities can also be modeled as 3-D spatial dipoles [59] as suggested by Delorme's research. They pointed out that independent EEG sources having different morphologies over scalp and they can be described by different current dipoles and EEG signals process by independent component analysis (ICA) could be directly modeled as spatial dipoles from those independent components. Although there are an amount of unclear factors such as non-even electrolysis and asymmetric spatial distributions in real EEG, the current-dipoles model can provide a theoretical frame of analyzing brain activities and eye moments efficiently. It also gives heuristic descriptions of how the EEG changes during dynamic processes. Following the 3-D dipole model, EEG potentials can be heuristically predicted morphologically as shown with the Figure 2.12. From the figure, we can see the areas affected by eye moment and speculate their effects on EEG recordings intuitively. Note that in this figure, with only showed the dipoles of the eyeballs. The current-dipoles of brain activities can be inferred similarly.

Combining with the inversely related relationship between distance and the propagated potentials, the ocular artifacts propagated to EEG electrodes in the way expressed by Figure 2.13.

As shown in the figures, the spatial pattern of propagation actually affects difference areas by different strength. In addition, the number of abstracted dipoles of eyeball also affects the patterns. Although it is possible to model the dipole into only one as long as there is not significant differences between the modeling methods.
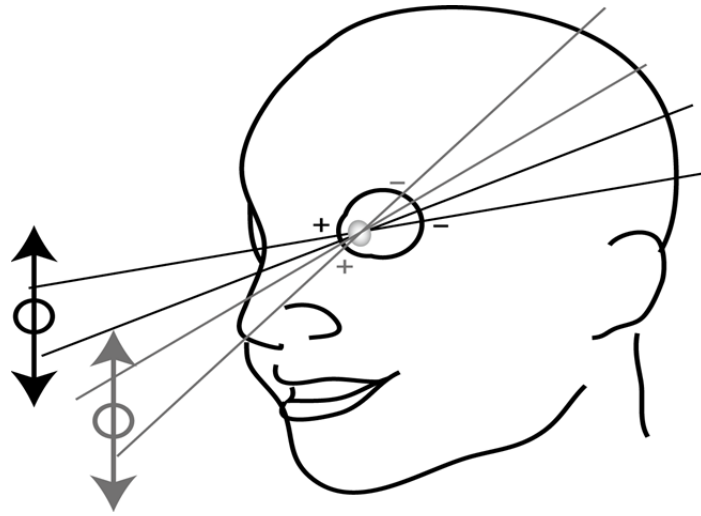
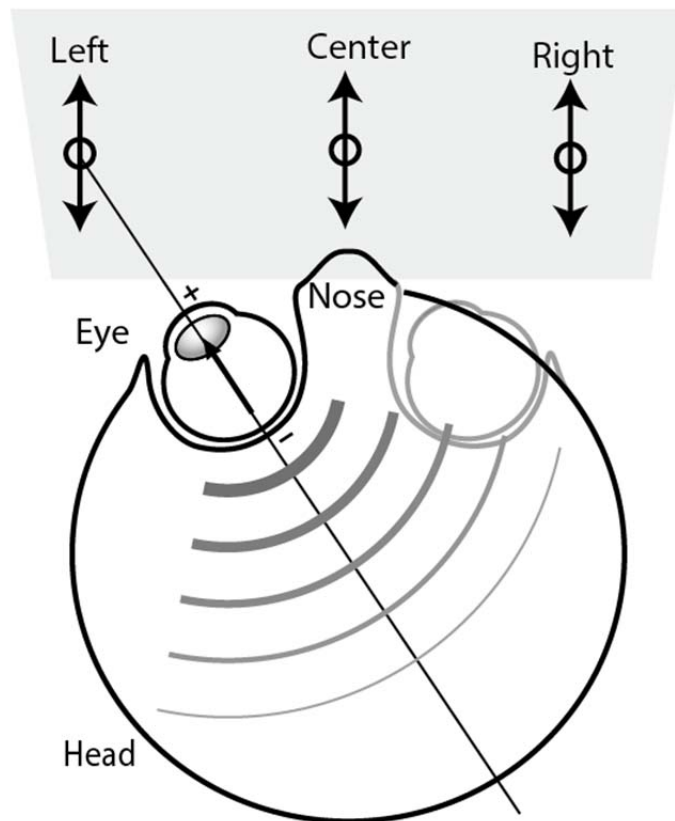Figure 2.12 3-dimension dipole movement

Figure 2.13 ocular artifact propagation and diploe orientation

However this is only the theoretical assumption of the potential propagation of ocular

artifacts. This model faces two problems:

1) Head shape of subjects

As every subject may have an individual head shape, the distance of the current-dipole and scalp electrodes may not be precisely defined. This problem can be solved by using fMRI the source localization technique [60]. However, obviously it is not possible or practical to obtain every subjects' head structure before EEG experiments. Besides, this solution is over-expensive and inconvenient. Thus the dipole model is usually used to roughly estimate ocular artifacts propagation in practice.

2) Unpredictable inside electrolysis process

Without knowing the clear electrolysis process, there is no assurance that the potentials generated by eyeball and is moments propagate smoothly over scalp.

In summary, the 3-D dipole model as a powerful tool for potential propagation estimation, but in practice it may not reflect the real dynamic processes precisely. Thus, the experiments based on the 3-D dipole model combining with a real obtained result would be more persuasive.

3) Determining factors of eye ocular artifacts:

Ocular artifacts can be generally grouped as eyeball movements which are also called cornea-retinal dipole moments, and eyelid movements (typically shown as blinks).

Cornea-retinal dipole moment is the most common eye moment during EEG recordings. Human's eyes never stop moving. This is the nature that keeps humans view

sight. Cornea-retinal dipole moment can be tiny when staring at the specified point (e.g. the fixation point) or very large when subject changes view sight from one to another.

Movement direction is one of the most important factors of cornea-retinal dipole moment. But basically we used for kinds of moving directions to describe cornea-retinal dipole moment: upward, downward, leftward and rightward. Any oblique directions are possibly expressed as the combination of two of those four basic eye movement directions.

Potential propagation that the every direction shows different morphology patterns as suggested by Picton et al. [61]. In their work, they collected eye movement data from 67 subjects and obtained of the topographic pattern of potential propagation by principal component analysis (PCA). They suggested that different kind of eye moments generate different topographic patterns and those patterns can be used for determining ocular artifact types. This is the great progress in ocular artifact removal. After this technique had been developed, component based at techniques jumped into the limelight in ocular artifacts removal/suppression. From EEG recordings, without considering the propagation patterns, eye movement information is usually difficult to determine so that the artifact removal also faces ambiguities at a certain level. Component based methods got a great benefit from Picton's work. As an instance, independent component analysis (ICA) takes advantages of the propagation patterns to determine the corresponding components of ocular artifact.

Eyelid movements are another kind of typical ocular artifact. Principally, the artifact generated by eyelid movement can be seen as a change of the resistance between Ford had and cornea. Eyelid movement causes three kinds of related artifacts: blinks, saccade of eyelids, and another kind of saccadic eyelid movement called post-saccadic

movement. There are generated from the same mechanism.

Blinks may not relate to eye moments, but the other two kinds of the eyelid movements are both highly related to cornea-retinal dipole moment. Eyelid saccade is the process of eyelids' moment along eyeball rotations. The saccade direction depends on the direction of the eyeball rotations. As literally described, the post-saccadic eyelid movement represents the process of the eyelid movements after the rotation of eyeball stopped. This process is reported as a slow slide of eyelid lasting from 30ms to 300ms after eyeball rotation finished [62].

In summary, eye movements are actually a combination of eyeball rotations and eyelid movements. These two parts are the key to analyze ocular artifacts.

Whereas obtaining eyelid movements in practice is a challenge. Although by means of high-speed camera, eyelid movements can be recorded, the recording process usually employs markers pasting on subjects eyelids. Those markers may cause uncomfortable feelings to the subjects and make the recording data biased. As the purpose of this thesis is to establish a way to understand the characteristic of eyeball rotations/saccades in free-viewing environment and their influence of potential propagation, we do not deeply discuss and solve the problem of eyelid movements, and leave this topic as a future work to solve so that we can focus on our main target.

2.5 Suppression/removal of ocular artifacts

Ocular artifacts are endogenous. As mentioned before, small potential changes caused by eyes can also be induced by light conditions or other phenomenon. This implies that it is difficult to separate ocular artifacts from EEG recordings or to obtain an absolutely pure EEG data set without any ocular potential. How to obtain a pure

EEG dataset is still an ongoing problem. But EEG measurements may obtain a data set which does not contain any eye movement or blink in it. Providing an experimental condition with temperature, brightness and other factors kept constant helps suppress artifacts, thus a relatively ocular-artifact-free EEG signal is possible to easily obtain.

Researchers often use the following methods to suppress ocular artifacts during EEG experiment or to improve the cleanness of EEG signal before data analysis:

1) Eye fixation

Eye fixation is a very common strategy to constraining subjects eye moment during EEG experiments. During EEG recording, subjects are usually asked it to stare at the fixation point in a predefined position on stimulation screen. The picture below shows an example of fixation cross during EEG experiment. Figure2.14 shows a typical appearance of eye-fixation stimulation screen.
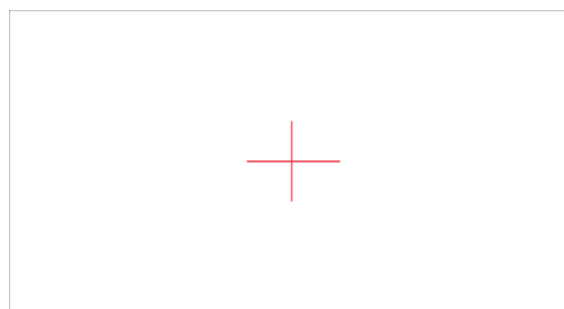

Figure 2.14 An example of fixation-cross on stimulation screen

This strategy guarantees that no big eye movements happen during EEG recording. Most of the in-lab EEG experiments utilize the fixation strategy to suppress ocular artifacts. Especially for ERP experiments, to decrease ocular artifacts and its influences,

fixation is generally used.

The disadvantage of this method is: not all that EEG tasks are compatible without eye moment performed. To extend the use of EEG for measuring subjects' mental state during natural actions, eye movement cannot be constrained because it's one of the most prominent factors influence subjects natural actions. Therefore the uses of the eye fixation method are usually not practical in EEG experiments.

2) Sophisticated experimental design

In well-designed EEG experiments, at a certain ocular artifacts can be suppressed. Using cues to attract subjects' attention, using softer background light to reduce subject eye tiredness are two basic examples of them. The selection to stimulation scenes also plays a very important role in experimental design. Following figures show two examples of experimental designs.

These two figures are picked out from our experiments of driver mental state estimation. In those experiments subjects were asked it to perform driving tasks with voice distractions. The eye tracker was employed to record subjects' eye moments during the whole tasks. Eye movement data was shown by blue points over the figures. As we can see from these figures, using a simple driving scene subjects' eye moments can be concentrated to the center of the stimulation screen. Whereas, when a complicated driving scene was selected, the blue points spread considerably. In this case, ocular artifacts appeared with higher amplitudes in our EEG recordings because of larger saccades.

As shown before the sophisticated designed experiment can greatly suppress ocular artifacts. However, before that EEG experiments performed in natural environments, it

is not possible to change all the things following designers' requests, furthermore for practical use the natural view is one of the factors influence subject reactions.

Figure 2.15 An example of good experimental design

Figure 2.16 An example of bad experimental design

3) Data rejection

Data rejection is a simple strategy to improve the cleanness of EEG data by rejecting all the data sacraments suspected of being contaminated by ocular artifacts. Figure2.17 shows an example of data rejection process. Usually the data sacraments being rejected are selected by eye manually.

As shown in the figure all the suspected data segments were marked by blue color. Before data analysis on the market data sacraments would be deleted to make sure the data set used for EEG analysis are clean enough.
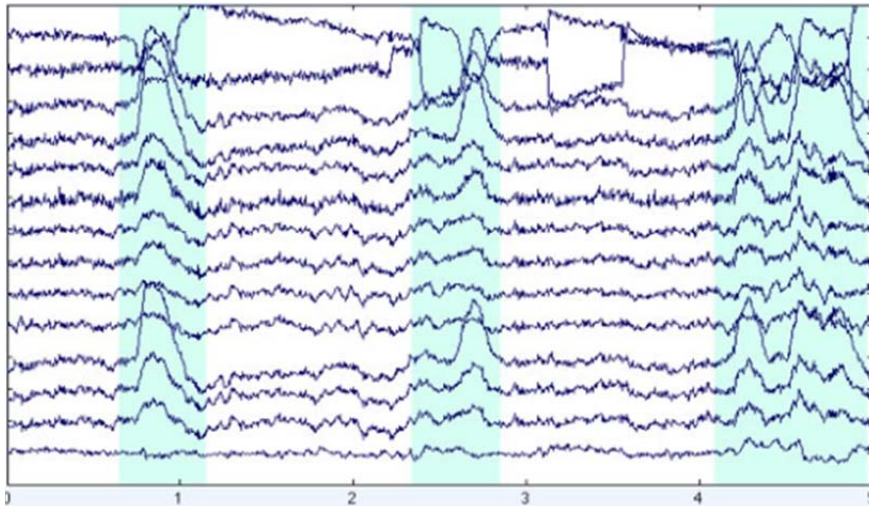

Figure 2.17 An example of data rejection

A skilled EEG analyzer can greatly improve data quality by rejection method. However as shown in Figure 2.17, this method causes a great amount of data loss, which may cause the problems the statistical analysis.

4) Filtering

Filtering method is inclined to be a data processing strategy. It can also be realized in the data recording stage by enabling a hardware filter before data collection. This method can filter out all the frequency components contaminated by ocular artifacts. However because of the overlapping property of ocular artifacts in original EEG signals, the filtering method also keeps low-frequency EEG signals out.

All these disadvantages of the above ocular artifact suppression methods lead to the

way of the dealing with this problem by signal processing techniques. Actually most of the recent researches are focused on this field. Various signal processing techniques have been developed in the purpose of the ocular artifact suppression/removal [26]. Some techniques like to regression-based methods [22][63] and data ICA can be used for general purpose. On the other hand, other signal processing techniques have been developed for special purposes such as adaptive filtering techniques for monitoring bring activities online [64]; single-channel EEG analysis technique for monitoring stages of sleep [65]; singular spectrum analysis (SSA) the trending and frequency extracting [66] and so on. These signal analysis techniques opened a new era of constraint-free EEG measurements.

On the other hand, these techniques are still in the ongoing state because of the complicated physiological principles of artifacts.

One of the problems is that after ocular artifact removal, because of lack of standard reference, it is difficult to estimate the performance of the artifact removal process. Up to now, unfortunately, there is no standard reference can be used to compare how much ocular artifact is contained in an EEG data set. Furthermore, there are no any efficient methods can extract artifact-free EEG signals during recording the stage. Thus, most of the researches use simulated data to evaluate the performance of the ocular artifact removal processes and algorithms or by visual inspections to the corrected EEG data. Moreover, there is generally no report about quantitatively verified assessment to how much the ocular artifacts should be removed and how much the residual of ocular artifacts distort recorded EEG signals. This causes a problem of estimating the real underlying brain sources from EEG data.

However, it doesn't mean that it is not necessary to analysis the factors which

influence the artifact suppression process. Researchers are making great efforts to investigate the factors hidden behind the visible EEG recordings and it has been proved the methods developed under different assumptions or verification theories improved the visibility of the 'under-ground' neuron activates. In addition, by means of summing and averaging, the signal-to-noise rate can be improved depending on the number of trials used for averaging procedure. If the number of trials exceeds a significant value, the nonrelated signals can be canceled out whereas time locked information of EEG signals would be unscrambled. Although this is a traditional method, it still plays an important role in EEG analysis. By using this method, we can also estimate artifacts and their properties stochastically.

According to our previous research review, we found a common point of all the previous researches. Except some techniques based on adaptive strategies, all the signal processing techniques supposed to that the coefficient or propagation pattern of ocular artifacts does not change during the whole EEG recording procedure, but only rare works of them clearly explained the reason why to assume those constant coefficients and propagation patterns. This fact motivated us to investigate the nature of eye moments and whether ocular artifacts propagated constantly for all conditions.

Chapter 3　Regression based solutions to ocular artifact

suppression or removal in EEG

So far, EEG still is ones of the most prominent and dominant technologies to observe the brain activity under natural conditions reproduced as an activity of daily life. Contamination of artifacts and unintended signal resources, are inevitable in any measurement method and principle and ocular and myographic potentials are major artifacts in EEG measurements. Since EEG signals are considerably weak to exhibit the potentials in micro-voltage level, which are far less than muscular potentials, and ocular potentials induced by eyeball and eyelid movements, the removal of ocular artifacts has been studied intensively. As a practical treatment in experiments in neuroscience studies, subjects are requested to gaze at a fixed point with the head clamped for the sake of reduction of a certain level of ocular artifacts. On the other hand, recently highlighted in neuro-engineering studies, the applications of EEG such as brain-machine-interface (BCI), EEG signals are recorded under constraint-free conditions. Thus it is highly expected in the purpose of analyses on-going brain states [67]. Yet the complete ocular artifact removal still remains unsolved especially in free-viewing EEG studies [68]–[70].

Several simple but efficient methods have already existed. Filtering method of specific frequency bands is the simplest way to remove low frequency components involving ocular artifacts from recorded signals, which has a risk of deleting target EEG components involved in the same frequency range [56]. Similarly, epoch rejection method removing the data fragments suspected of severe contamination of ocular

artifacts also has a serious risk of losing large amount of recording data for statistical analysis.

Because of the disadvantages and difficulties of those traditional methods (e.g. eye fixation, sophisticated experiment design, data rejection and filtering) in practical use, researchers recently started focusing on the way the signal processing to suppress or removal of ocular artifacts from EEG recordings.

According to the morphology of eyeballs and the electrophysiology of extraocular muscles, the cornea-retinal potential is charged with tens millivolt range [71] and monitored as hundreds micro-voltage level from electrodes attached around eyes known as electrooculography (EOG) recording [72][73]. In spite of the low pass filter effect in the measurement equipment, the ocular potential ideally stays at the certain level depending on the degree of eyeball rotations, which was examined in saccade tasks [74] and demonstrated in an approximately linear relationship between the rotation degree and the ocular potential [73]. With respect to those electrophysiological evidences, the impact of ocular artifacts on EEGs were explained in the dipole model that is spatially located inside the scalp to provide a non-negligible influence to extracranial EEG recordings [58], and the measured EEGs were conventionally modeled as a linear summation of true EEGs and EOGs multiplied by coefficient values as the ratio of the contamination [22][23] under the assumption of signal independence with each other, i.e. less nonlinear interferences. The mechanism of ocular artifacts were considered to be different depending on types (saccade eye movements or blinks), which were respectively caused by a change of ocular dipoles' orientation or the interaction between eyeballs and eyelids which can be seen as a sliding electrode [61].

Current ocular artifact correction methods mainly consist of two prominent

approaches, regression based methods and component based methods [26]. Regression based methods have a long history in research on signal processing and ocular artifact correction [22][23][75][76]. Based on the linear model to describe recorded EEG signals as a linear combination of true EEGs and artifacts, the target problem is the calculation of the ocular artifact propagation coefficients. Providing the coefficients are successfully obtained in the calibration stage in prior to the main observation stage, this correction procedure can be a simple and powerful tool to estimate real EEGs for online monitoring by subtracting the product of EOGs and the obtained propagation coefficients, without any complicated statistical treatments. The technique to calculate the coefficients is an important issue, such as the mean slope algorithm [23], aligned-artifact average (AAA) solution [77], Bayesian adaptive regression splines (BARS) [78]–[80] and so on. Component based methods or blind source separation (BSS) is employed to deal with problems of general signal decomposition with knowledge of probabilistic models in the framework of matrix factorization [81]. Component based method is a way to find a new reduced and structured representation for the observed signal that can be interpreted as meaningful and minimized (subspace) coding, such as independent component analysis (ICA) and principle component analysis (PCA). In the purpose of EEG de-noising, PCA and singular value decomposition (SVD) algorithms correct artifacts by removing components suspected as artifacts based on orthogonalization calculated in the framework of matrix factorization [82]. It has been effectively used for large amplitude EOG artifacts removal and topographic pattern analysis [61]. Independent component analysis (ICA) [83]–[85] is a more reasonable way based on a widely accepted assumption that the sources forming the measured EEG recordings are independent from each other. If EEG

data is obtained from enough number of channels, independent components can be effectively separated using this method, but after the separation process the specification of which components are artifacts is the issue. The discrimination can be done using topographic distribution and morphological differences manually or automatically [86].

Although many approaches have been proposed and applied in ocular artifact removal up to now, whether they fit the purpose of daily life EEG applications (free-viewing EEG recording conditions) is still unclear yet. To determine the suitability of the proposed approaches and how to revise them for real-life applications, it is extremely crucial to understand the basic principles of them. In this chapter, the basic principles of the several prominent methods are introduced as examples. There are advantages and disadvantages are also analyzed to make a comprehensive evaluation to their availabilities in daily life EEG applications.

3.1 General model of EEG signals

All the signal processing techniques for ocular artifact removal are based on a widely accepted mathematic model of EEG. In this model EEG signals are described as the linear combination of a number of components.

$$mEEG_{m \times n} = \vec{a}_{m \times 1} * comp1_{1 \times n} + \vec{b}_{m \times 1} * comp2_{1 \times n} + \vec{c}_{m \times 1} * comp3_{1 \times n} + \cdots \text{ (3-1)}$$

Where $mEEG$ is an m-by-n matrix representing the m-hannel measured EEG signals with data length n. The coefficient vectors $\vec{a}, \vec{b}, \vec{c}$ and so on represent the weights of projection from components space to EEG channels. Every component in this formula is a 1-by-n vector according to data length. These components can be grouped as brain activity components and non-brain activity components. Whereas brain activity components represent the 'true underlying EEG signals', non-brain activity components

represent the recorded data that are not related to bring activities such as the potential changes caused by various physiological artifacts, line noise, potential shifting induced by sweating and so on. The physiological artifacts here include ocular artifacts, EMG, amplifier saturation and so. In our research, because we're focusing on ocular artifact removal, other kinds of artifacts are assumed to be zero for simplifying the problem framework.

3.2 Regression based approaches

Regression approaches are similar to the work of analog ocular artifact removal done by Girton and Kamiya in 1973 [87]. In their research, they realized an analog circuit to correct ocular artifacts online. They used attenuators connecting to EOG channels, and then the direct feedbacks (EOG potentials) of those attenuators were used as the reference for artifact removal. They asked subjects to perform extremely large eye moments while adjusting the transfer rate (correction coefficient) by subtracting the output from the attenuator (i.e. EOG) from EEG signals via an analog subtracting circuit. They tuned the parameters of the subtracting circuit until no eye movement related potential changes can be visually observed. This method is a great try of ocular artifact removal, although it is inferior to the modern digital signal processing techniques.

Lately proposed regression-based ocular artifact removal approaches made a significant improvement to the criterion for determining correction coefficients, which are also called as propagation coefficients. Under the framework of linear regression, the measured EEG signals can be expressed by the sum of assumed real EEG signal and the products of EOG components and their propagation coefficients. The following formula shows their mathematical expressions:

$$mEEG_{m \times n} = rEEG_{m \times n} + \sum_{i=1}^{M} \vec{b_i}_{m \times 1} * mEOG_{i_{1 \times n}} \qquad (3\text{-}2)$$

where $rEEG_{m \times n}$ represents the true underlying EEG signal without any contamination from ocular artifacts (i.e. propagated EOG potentials). M represents how many EOG components are used in this regression model. M is usually set to 1 or 2 depending on model selection. For instance, when only the vertical EOG is taken into account, M equals one and $\vec{b_i}$ corresponds to the propagation coefficients of vertical EOG to all EEG channels. Usually, both vertical EOG (vEOG) and horizontal EOG (hEOG) are utilized during ocular artifact correction. Oblique eye movements can be treated as the combination of vertical eye movements and horizontal eye movements, so does the relationship between EOG potentials. Only in few researches, decomposition of EOG into vertical, horizontal and radial totally three components are proposed [22][76][77] based on the fact that eye movements take place in a 3-D space. However, theoretically the collection of radial EOG component is considerably difficult as mentioned in [25]. On the other hand, Plöchl *et al.* [68] reported that actually the usage of the radial component cannot improve the performance of regression method, inversely when the radial component were added into the regression model performance even got worse. In summary, it is a wise choice to use to component based the regression method for ocular artifact removal.

The criterion used in regression approaches was 'least square'. In stochastic analysis, this criterion is also called as ordinary least squares (OLS) method. Figure 3.1 shows the basic principle of least square method by a one dimension (i.e. only one regressor used) example.
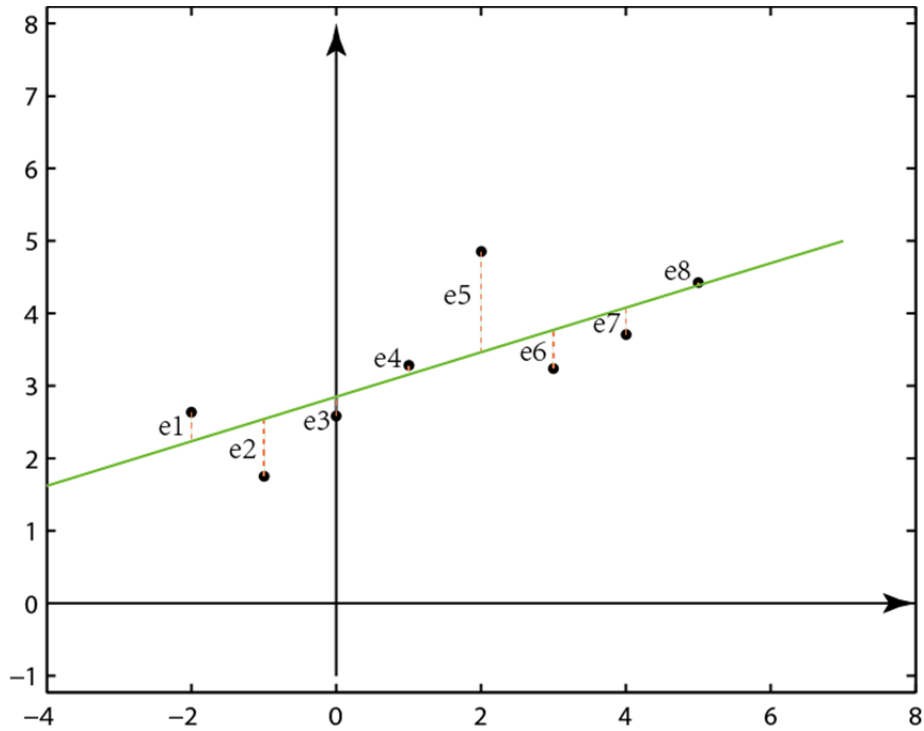
Figure 3.1 An example of simple one-regressor linear regression

Given a training dataset (output value and regressor) with a linear model (in this example $= a * x + b$), OLS can lead to a line fit the training dataset optimally in a sense of least square. This best fit line minimizes the sum of squares of all error terms (shown as e1~e8 in this example).

Applying this linear model to ocular artifact removal faces the problem. As we can see from the linear model, the output data is actually expressed as some products of coefficients and regressors plus a constant term. In EEG model the term is not constant; instead, it is the real EEG signals we are going to estimate. So, there are some limitations of using regression method to obtain propagation coefficients. Croft and Barry [22] pointed out that it is possible to apply a similar linear model in form of $y = b * x + d$ directly, where b is a vector and $d = estEEG + C$, where estEEG

represents the estimated EEG and C is a constant. But the dataset should be collected only during large eye moments, otherwise the estEEG and b would be biased. This means, when the real EEG signal is very weak, and EOG is considerably large, the propagation coefficients b can be calculated by sample data and their mean values as the formula shown below:

$$b = \frac{\sum(x_i - \bar{x})(y_i - \bar{y})}{\sum(x_i - \bar{y})^2} \tag{3-3}$$

Where x_i and y_i represent the EOG and EEG potential at time i; $\bar{x}$ and $\bar{y}$ are the mean values of EOG and EEG respectively. In a more intuitive way, the formula can be reformed by:

$$b = r_{xy} * \frac{std_y}{std_x} \tag{3-4}$$

Where r_{xy} stands for the co-relation coefficient between EOG and EEG; std_y and std_x represent the standard deviation of EEG and EOG. Following the above formula, all the propagation coefficients can be obtained for a single EOG component regression model channel by channel. Then the estimated real EEG signal can be obtained:

$$estEEG = mEEG - \vec{b} * EOG - C \tag{3-5}$$

Obtained $estEEG$ is the optimal estimation in the sense of least square. C in this formula stands for the constant term (also called slope) in regression model, which is calculated as:

$$C = \bar{y} - (\bar{x} * b) \tag{3-6}$$

To be more practical, the calculation of propagation coefficients is usually done with two EOG components, as mentioned previously, vertical eye movement component (vEOG) and horizontal eye movement component (hEOG). In this case, the calculation of coefficients should be done as follows:

$$b_1 = \left(\frac{r_{y,x1} - r_{y,x2}\, r_{x1,x2}}{1 - r_{x1,x2}^2}\right) * \left(\frac{std_y}{std_{x1}}\right) \qquad (3\text{-}7)$$

$$b_2 = \left(\frac{r_{y,x2} - r_{y,x1}\, r_{x1,x2}}{1 - r_{x1,x2}^2}\right) * \left(\frac{std_y}{std_{x2}}\right) \qquad (3\text{-}8)$$

In this equation set:

x_1 and x_2: vEOG and hEOG.

b_1 and b_2: the coefficients corresponding to the vEOG and hEOG respectively.

$r_{y,x1}$ and $r_{y,x2}$: the correlation coefficients between measured EEG and two EOG components.

$r_{x1,x2}$: the correlation coefficient between vEOG and hEOG.

std_y, std_{x1} and std_{x2}: the standard deviation of measured EEG signals, vEOG and hEOG.

While the single component regression can be expressed by a line in a 2-dimensional space, the regression with two components is corresponding to a square in a 3-dimension space. Figure 3.2 shows a graphical description of two components regression with simulation data. In this figure the red lines indicate the points are under the optimal fit square; the green lines indicate the corresponding points are over the optimal fit square. Coefficient calculation followed the general multivariate linear model: $y = a * x1 + b * x2 + c$. In this model, c is a constant value, x1, x2 and their coefficients a and b span a square under constraint of OLS.
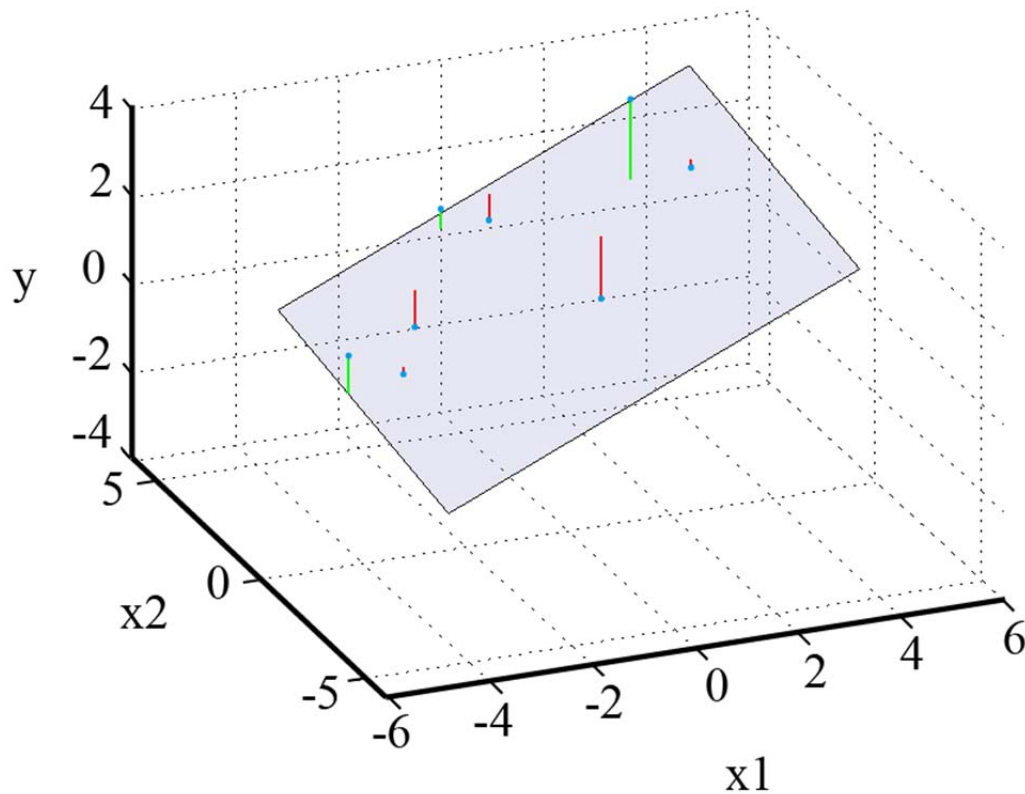
Figure 3.2 An example of 2-D regression (two regressors)

There is another way to explain the calculation of the linear regression by matrices. The base model can be expressed as:

$$\vec{y} = \vec{S} + \sum_{i=1}^{M} \vec{x_i} * b_i \qquad (3-9)$$

in which $\vec{y}$ is the output data, $\vec{x_i}$ is input variable (regressor) and b_i represents the coefficients of regressors. And $\vec{y}$, $\vec{x_i}$ and $\vec{S}$ are column vectors. So, this equation can be rewritten to:

$$\vec{y} = \vec{S} + X * \vec{b} \qquad (3-10)$$

where X is a matrix whose columns are the same vectors as $\vec{x_i}$.

Unlike the general model used to in previous explanations, in this model, the extra term S can be a variable other than a constant. But to make this equation solvable, S is

assumed nonrelated to input variables so that $X^T * \vec{S} = 0$.

It is easy to get the following derivation:

$$X^T * \vec{y} = X^T * \vec{S} + X^T * X * \vec{b} \qquad (3\text{-}11)$$

and

$$X^T * \vec{y} - X^T * X * \vec{b} = X^T * \vec{S} = 0 \qquad (3\text{-}12)$$

$$X^T * \vec{y} = X^T * X * \vec{b} \qquad (3\text{-}13)$$

thus, the coefficient vector

$$\vec{b} = (X^T * X)^{-1}(X^T * \vec{y}) \qquad (3\text{-}14)$$

$(X^T * X)^{-1}$ is the the auto-covariance measures of X and $(X^T * \vec{y})$ is the cross-covariance matrix of X and $\vec{y}$. In this example, $\vec{y}$ and $\vec{S}$ are vectors, and they can be extended into matrices by combining several channels of output $\vec{y}$ and $\vec{S}$ together.

3.3 Limitations and issues of regression method

1) Collinearity

Collinearity is also called as multicollinearity in statistics. It is a phenomenon of high correlation between two or more regressors. In the worst-case, the correlation between regressors equals 1, which means one regressor can be expressed by another regressor times the constant K, the regressors used for the regression are actually decreased about one, because that regressor can be completely explained by the other one although they are different in amplitude. Collinearity may influence the convergence of OLS algorithm. $\vec{b} = (X^T * X)^{-1}(X^T * \vec{y})$ does not exist in case of a perfect collinearity happens. Although the perfect collinearity does not exist because of the noise in

recorded dataset, it may highly dilate the results of regression coefficients.

An intuitive example in EEG is when vertical eye movements and horizontal eye movements take place at the same time. In this case, vEOG and hEOG which are used as the regressors in the regression model are highly correlated. Thus the propagation coefficients cannot be obtained correctly. For this reason, all the regression based methods utilize the calibration stage before real EEG experiments. In the calibration stage, subjects are usually asked to perform simple eye moments, such as upward, downward, leftward and rightward eye movement respectively. The recorded EOG and EEG signals in this stage are used for the calculation of propagation coefficients. Schlogl [45] proposed a new method to avoid collinearity. In his research, the subjects were asked to perform round eye movements instead of the simple direction eye moments. This method has been proved efficient in collinearity prevention and propagation coefficient calculations. In addition, this method has been integrated into the BioSig open source software library [88] for ocular artifact removal.

2) non-constant property or correlation between regressors and the extra term in regression model

If the actual term d and $\vec{S}$ in previously described generally models does not stay in a relatively constant value or highly related to regressors, linear regression method faces another problem. These extra terms are actually responding to the sum of a constant value and the estimated EEG signals. Hence, the eye movements used for calibration must be large enough. In practice, usually the eye moments larger than $10°$ angular difference are used in the calibration stage.

3.4 Applications of regression method to EEG signal

1) EOG collection

As EOG signals are used as the regressor in regression model, the way of getting EOG signals are crucially important. Generally, there are two ways of obtaining EOG signals.

A common way to obtain EOG signals advocate in many researches [22][63][68][77][89]–[91]. They utilize the seven electrodes structure to obtain EOG signals.

In this electrode configuration, vEOG is usually defined as the average of left vEOG and right vEOG:

$$vEOG = ((V1u - V1d) + (V2u - V2d))/2 \qquad (3\text{-}15)$$

hEOG is defined as the potential difference between H1 and H2;

$$hEOG = H1 - H2 \text{ or } H2 - H1 \qquad (3\text{-}16)$$

Vz in this configuration is usually used for assistance, for example in case of obtaining radial EOG in some researches. Calibrations use vEOG and hEOG recorded from simple straight-line (i.e. upward, downward, leftward and rightward) eye movements, and then calculate propagation coefficients by linear regression. Electrode positions of pairwise bipolar electrode configuration are shown in Figure 3.3.

Triangular configuration is proposed by Schlogl [25]. He suggested that the necessary number of eye electrodes should be no more than and no less than three, because eye movements can be decomposed into three components theoretically in a three dimension space. More electrodes might be better but may not be necessary, while lack of the electrodes cannot collect enough information for the decomposition. This

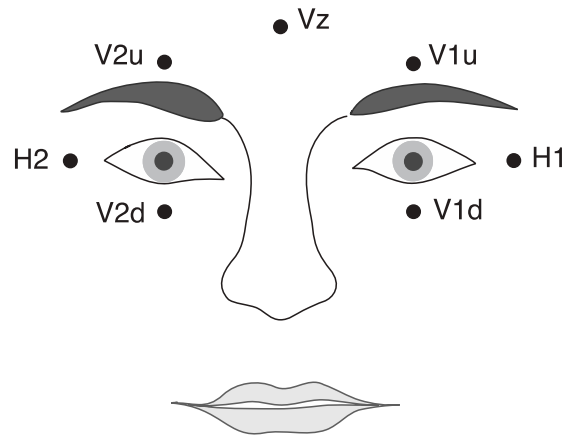kind of configuration is shown as by Figure 3.4.

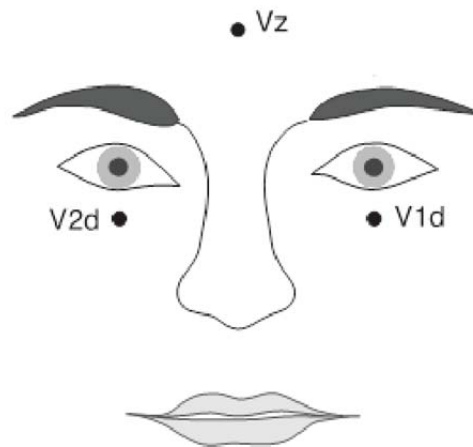Figure 3.3 Pairwise bipolar electrode configuration

Figure 3.4 Triangular configuration

In his work, he did not separate EOG into components like vEOG and hEOG and perform simple straight-line eye moment for calibration. Instead, subjects were asked it to perform round eye movements, and the potentials of those electrodes were used to calculate propagation coefficients directly without considering eye movement

directions.

The calibration stage and its flow can be described by Figure 3.5. Before the real EEG experiment, subjects are asked to perform simple eye movements with EEG and EOG signals collected. From the EEG and EOG recordings, the propagation coefficients (usually $\vec{b_h}$ and $\vec{b_v}$ for both vertical component and horizontal component) are obtained. These propagation coefficients will be used to remove the ocular artifacts in the coming real EEG experiments.

2) Regression strategies

Gratton proposed a regression strategy for ocular artifact removal in ERP recordings [23][24]. In this method, all the collect EEG and EOG trials were linked together respectively, forming two signal series of EEG and EOG. After that, those two series were sent to regression (calibration stage) to obtain propagation coefficients. Once the propagation coefficients were obtained, all the following EEG recordings use those coefficients to correct/remove ocular artifacts with predefined vEOG and hEOG collected from the electrodes. Figure 3.6 shows the example of one component calibration by Gratton style.

Unlike Gratton's method, Croft and Barry proposed a novel solution of calibration named aligned-artifact average(AAA) [77]. In AAA, contracted trial data are averaged firstly, and then send to regression. Croft and Barry suggested that calibrations done in this way can obtain better performance which has a smaller variance in propagation coefficient value by means of both simulation data and really EEG recordings. Figure3.7 shows the procedures of this method:
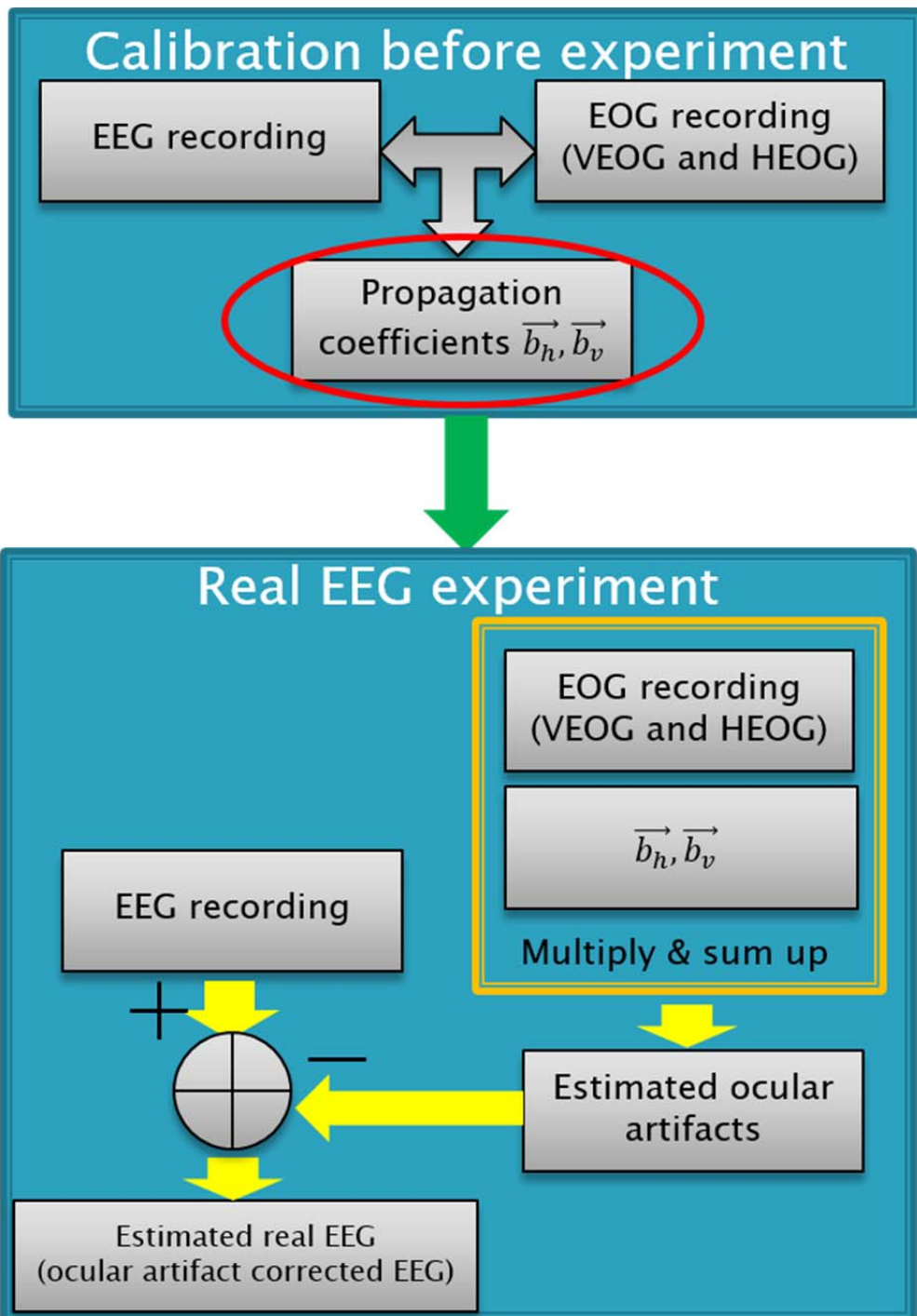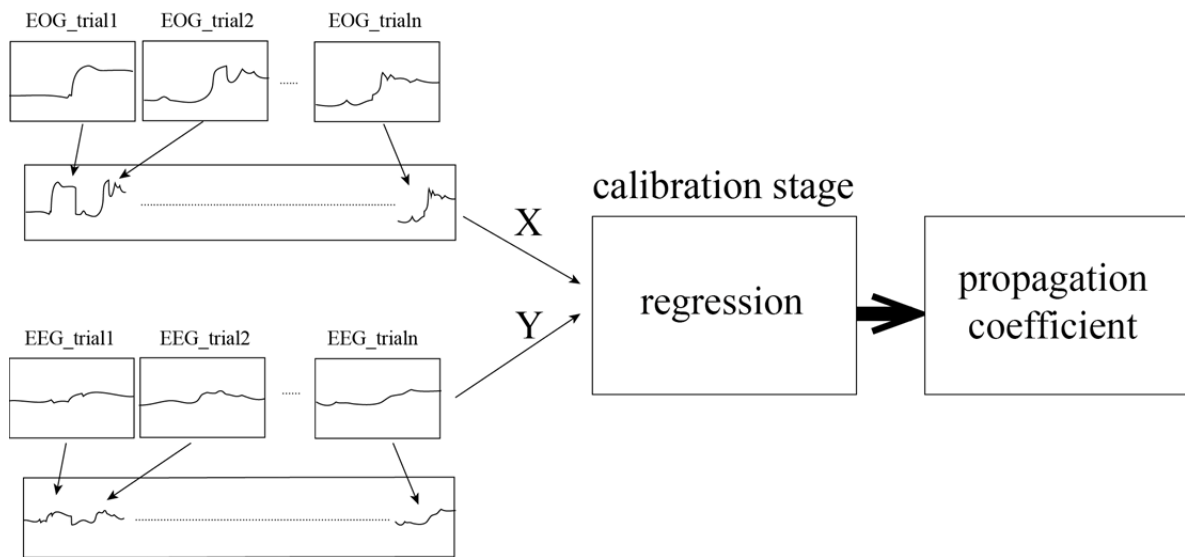
Figure 3.5 flow of calibration

Figure 3.6 Gratton style calibration

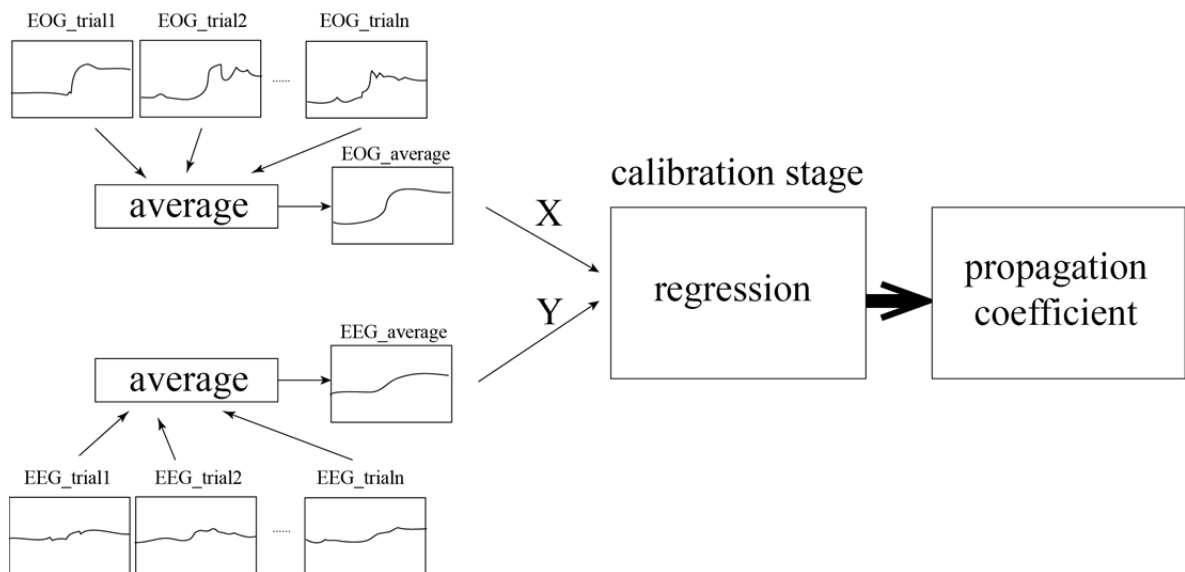

Figure 3.7. Calibration in Aligned-artifact average(AAA)

There are many alternative strategies can be used for calibrations. In fact, the only thing change is the way of generating data series for regression model, for example, lately developed Bayesian adaptive regression splines (BARS) [78]–[80] and so on. All these methods differ by the way of organizing calibration data/training data for

regression, while the basic flows are all the same. Because they are not the main topic of this thesis, the details of those specialized method are not stated here.

3) Relationship between propagation coefficients and propagation patterns

Propagation coefficients are directly related to propagation patterns suggested by Picton in 2000 [61]. Although in Picton's work a component based method PCA was used to extract propagation patterns, if the propagation coefficient vectors which contain propagation coefficient to every channel are projected to a topographic head map, exactly the same or similar topographies can be obtained. Figure 3.8 shows an example of the upward eye movements topographic. The topographic pattern obtained from propagation coefficient vector demonstrates the appearance as the ones described by ICA and PCA research articles [84][86][92][93].
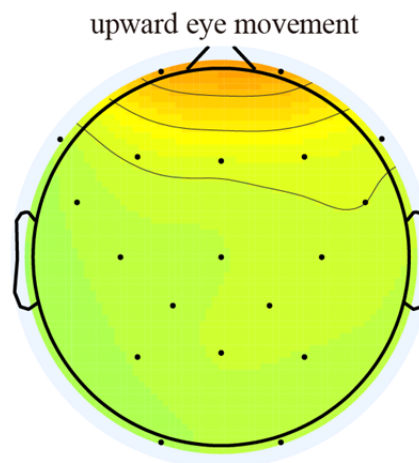

Figure 3.8 An example of topographic made from propagation coefficients (bs)

As the real EEG is not possible to obtain, thus, using real experimental data is not convincible to explain whether the method work well or not. Here we show an example

made from simulated dataset in Figure 3.9. In this dataset the real EEG is a 10 Hz sin wave to simulate an alpha activity; the real EOG is double peak triangular wave simulating blink EOG. Figure 3.9, measured EEG is the linear combination of real EEG, real EOG and a white noise series; measured EOG is simply the sum of real EOG and a white noise. We can see the EEG signal distorted by blink EOG and white noise are corrected by regression method efficiently, although there is still a little distortion the influence from blink EOG are greatly decreased. Therefore, as shown here, regression based method is efficient for ocular artifacts removal/suppression.

1.5 Why not component based methods?

Recent years as the signal processing techniques' development, component based methods have become more and more popularly in this field. For instance, principle component analysis (PCA) and independent component analysis (ICA). There is a common point among all those methods: there use spatial propagation pattern to distinguish brain activity related EEG and artifacts related EEG. Then reject the artifact components after they are identified.

PCA acts as a foundation for present-day signal processing, however, it appears to be a method that was frequently used yet inadequately understood. PCA is being credited as one of the most precious result via applied linear algebra, and was amply applied in the field of neuroscience and image processing due to its effectiveness in obtaining pertinent information from huge groups of mystifying datasets. It minimizes composite data into significant pattern, which serves for better features understanding.
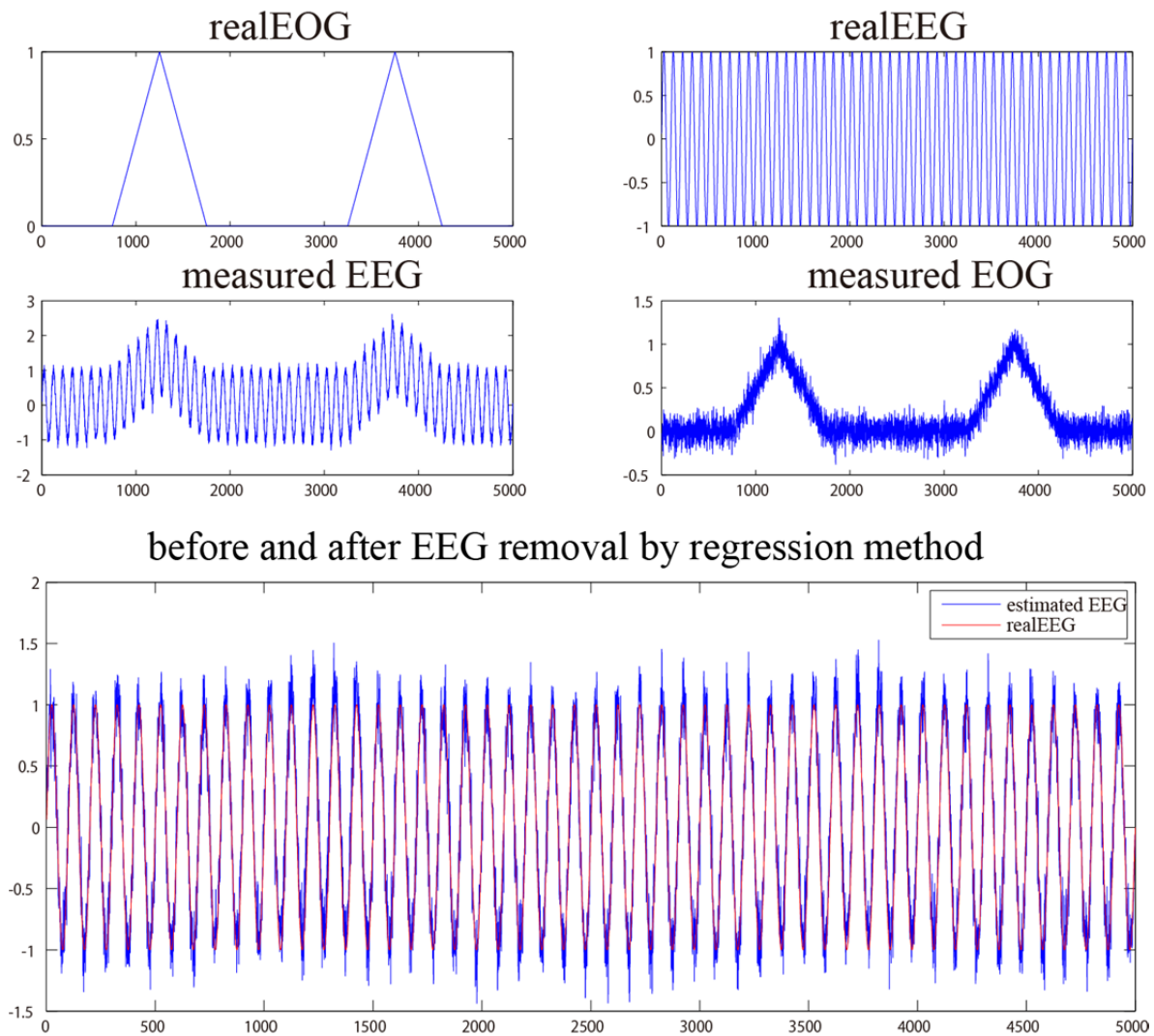
Figure 3.9 Regression on simulation data

PCA is a statistical procedure that uses orthogonal transformation to convert set of observations of correlated variables in to set of values of linearly uncorrelated variables (Principle Components). Number of components is less than or equal to number of original variables.

PCA makes one stringent but powerful assumption: linearity. Linearity vastly simplifies the problem by restricting set of potential bases and formalizing implicit assumption of continuity in dataset. PCA is now limited to re-express data linear

combination of its basis vectors. PCA was mainly expressed by the formula below.

$$Y = P * X \qquad (3\text{-}17)$$

X is the original dataset; Y is the represented data while P is the weightage of principal components, whereby each rows of P are orthogonal to one another. Besides that, P can also be explained as a matrix transformation that relates X and Y, a rotation and a stretch that transform X into Y and set of new basis vectors for expressing columns of X.

$$PX = \begin{bmatrix} \overrightarrow{P1^T} \\ \overrightarrow{P2^T} \\ \overrightarrow{P3^T} \\ . \\ . \\ . \\ \overrightarrow{Pm^T} \end{bmatrix} \begin{bmatrix} \overrightarrow{x1} & \overrightarrow{x2} & \overrightarrow{x3} & . & . & .\overrightarrow{xn} \end{bmatrix} \qquad (3\text{-}18)$$

Thus,

$$Y = \begin{bmatrix} p_1 * x_1 & \cdots & p_1 * x_n \\ \vdots & \ddots & \vdots \\ p_m * x_1 & \cdots & p_m * x_n \end{bmatrix} \qquad (3\text{-}19)$$

The P in above equations are the key of PCA. To obtain P, PCA algorithm actually calculate the eigen vectors of the semi-positive-definete Sx as shown in the formula below:

$$Sx = \frac{1}{n-1} XX^T \qquad (3\text{-}20)$$

ICA is based on the assumption of the independence between different sources. Indeed, the so-call the whitening or sphering step of ICA do the same job as PCA. Whereas, ICA use the independent assumption to extract components rather than the eigen vectors that represent the maximum-variance directions. The observation in ICA is seen as a linear combination of different independent sources:

$$X = W * S \qquad (3\text{-}21)$$

So that if W can be estimated, W^{-1}, the inverse matrix of projection weight matrix

W can be used to un-mix the independent components. Hence, after components corresponding to ocular artifacts are rejected (whole data series set to zero), the ocular-artifact-free EEG can be reconstructed.

As is mentioned above, this component based methods utilize matrix calculations and stochastic analysis to obtain the expected results. Basically, they have high computational consumptions, which is not possible to be easily implemented in real-life used devices. Although some of the previous researches claimed that they outperform the regression based the strategies; some others declared that not huge differences can be found and the assumptions (i.e. orthogonality and independence) are too strong.

On the other hand, both regression based methods and component based methods can be seen from the same point of view, the propagation patterns. Whereas using regression based method, the quantified coefficients can be obtained, component based methods take advantage of the relative ratio between those coefficients. Hence, at a certain, they result in the same analytic pattern.

For the original purpose of applying EEG signals for daily use, obviously, regression based method is the better choice. Thus, in this thesis, we selected regression based method as the way to analyze and deal with ocular artifacts. Note that, even if their might be some performance difference, generally the tendencies must stay the same.

Chapter 4　Measuring EEG with eye-tracking system

The present problem is to estimate real EEG signals because EEGs are very weak in the range of microvolts and are easily contaminated by artifacts from ocular and myographic electric potentials exceeding a certain voltage level. The eye movement-related potential, which is recorded in Electrooculography (EOG), is a major artifact called ocular artifact. In traditional EEG experiments, subjects are required to gaze at a fixed position on the screen to reduce the artifact [68], while it is difficult in terms of engineering applications to help daily human activities accompanied with frequent eye movements.

Ocular artifacts can be explained using spatial dipole models [22][25] to represent how electric potentials are generated with respect to cornea-retinal rotations. As for the previously-reported methods for ocular artifact removals, some methods dealt with three dimensional properties of eyeball rotations in the linear model of EEGs and EOGs [22][25], while gaze-of-zone related eye movement EOG influences in EEGs were rarely noticed in traditional methods [26]. Plöchl et al. [68] introduced a combined analysis of EEG and eye-tracking data used to monitor saccade onset timings when eyeballs start to move. Recent technological advancement allows us to use a high-spec eye-tracking system with a 500 Hz sampling rate close to that of the EEG recording system, leading to an effective combined analysis. EOGs can be observed directly by using electrodes attached at regular positions around eyes to achieve simultaneous recording with EEGs, while electrodes around eyes is a serious burden to experimental subjects and thus a strong restriction to engineering applications. For engineering purposes [3][67], daily-use devices with a limited number of recording channels are

getting popular. If the high-speed eye-tracking system enables to pursue eye movements, EOG information could be estimated accurately from cumbersome electrodes around eyes.

How much an accurate tracking of eye movements contributes to the artifact removal is still unclear. Plöchl et al. [68] demonstrated a large offset between conditions of upward and downward saccades, which means a comparison of opposite vertical directions, whereas a comparison in horizontal saccades and an effect of saccade movement length is not clearly observed as a significant different in the analysis of ERP topographic maps.

In the present study, we proposed a concept to complement the EOG artifact removal from EEGs with the eye-tracking system, and studied preliminary investigated EOG influences in the EEG topographic pattern analysis depending on viewing-area of eye movements. This combination provides a favor in understanding the nature of eye movement and establishing the intuitions of the relationship between eye movements and EEG signal. An extra benefit is that by only EEG signals onset is difficult to determine but with eye-tracking system, the onset of EEG can be decided according to the timing of interest. The original purpose of this experiment is to get a preliminary understanding to the nature of eye movements and its potential properties in EEG. In addition, we hypothesized that EOG influences in the EEGs are different depending on viewing-areas, which can be called 'zone-of-gaze dependency' and we tried to observe the differentiations of propagation topographic patterns related to the area to gaze and when pursuing visual targets. We simply designed several tasks to test the EEG changes during various eye movements and the zone-of-gaze dependency by vertical saccade movements in different zones would also be testified by dividing view-sight into three

viewing areas horizontally.

4.1. Experiment Design and Method.

In this analysis, EEG measurement data was obtained from three subjects under the following experimental conditions. All subjects sat and their heads were fixed by the head support frame as shown in Figure 4.1. The head height was adjusted to the level for each subject to look at the center of the monitor screen with their eyes straightforwardly. Figure 4.2 shows the experiment scene after chin and view sight adjusted. EOG were obtained by using seven electrodes around eye (Figure 4.3). Visual stimulus was displayed by a 40×30cm CRT monitor with a distance of 75cm from the subject (Figure 4.4) and subjects were instructed to keep quiet positions to prevent the jaw and clenching artifacts. A simultaneous recording of EEGs and EOGs were monitored by 32-channel electrodes of International 10-20 System (BrainAmp amplifier, Brain Products GmbH) with the 1000 Hz sampling rate. For comparison with EOGs, eye movement data were obtained by a 500 Hz high-speed eye-tracking system (Eyelink CL, SR Research).

4.2 Task design

For investigations on the zone-of-gaze dependency of EOG influences in EEG recording data, we focused on vertical saccade movements in different zones that divided into three areas horizontally as an important step for further systematic analysis.
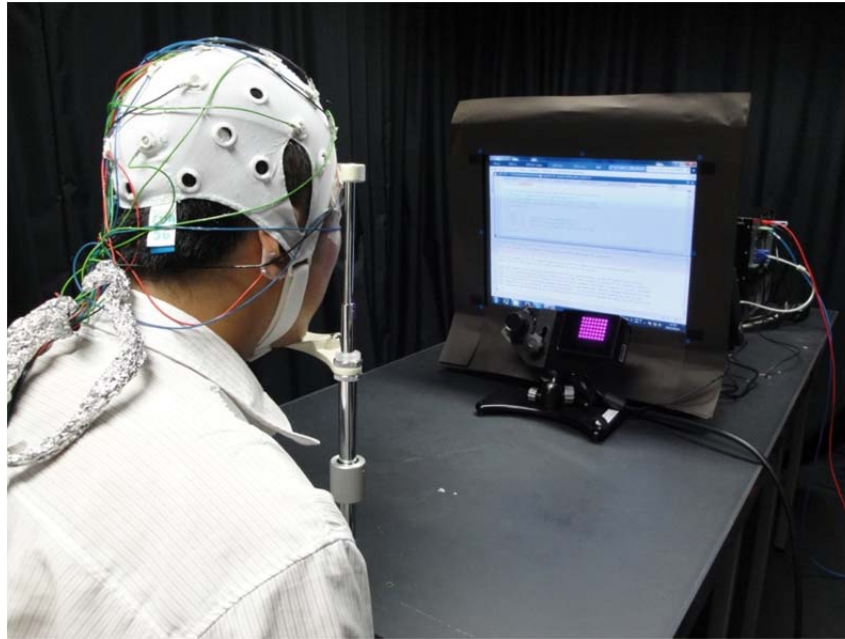
Figure 4.1 Experiment scene: Subjects were set to an environment with stable and even light condition. A chin support was used to reduce subject's head movements. The eye tracker under the monitor is adjusted to a good position to record eye movement with its best performance.
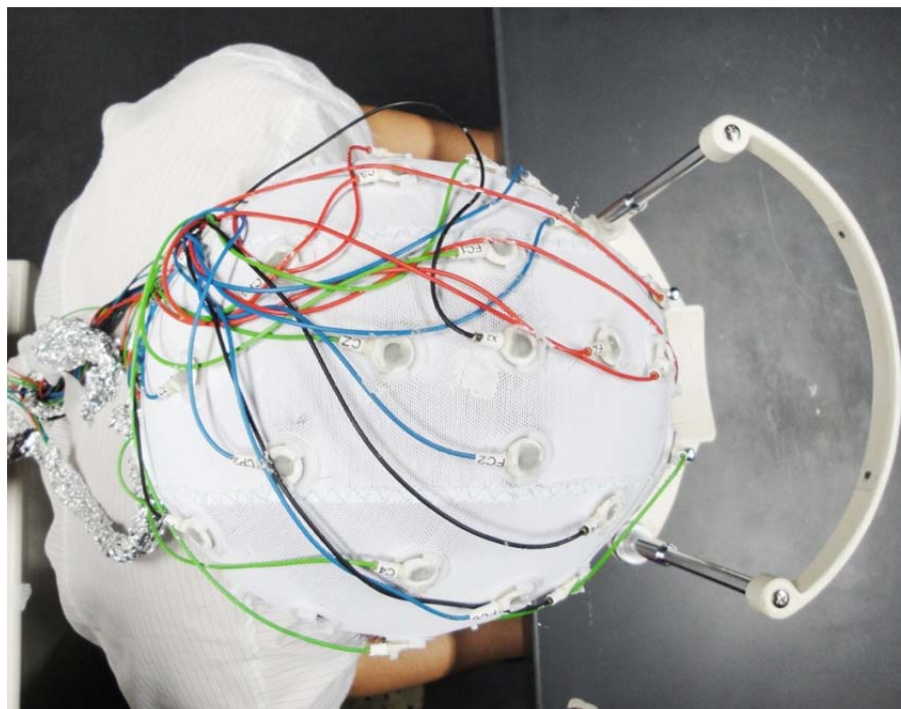

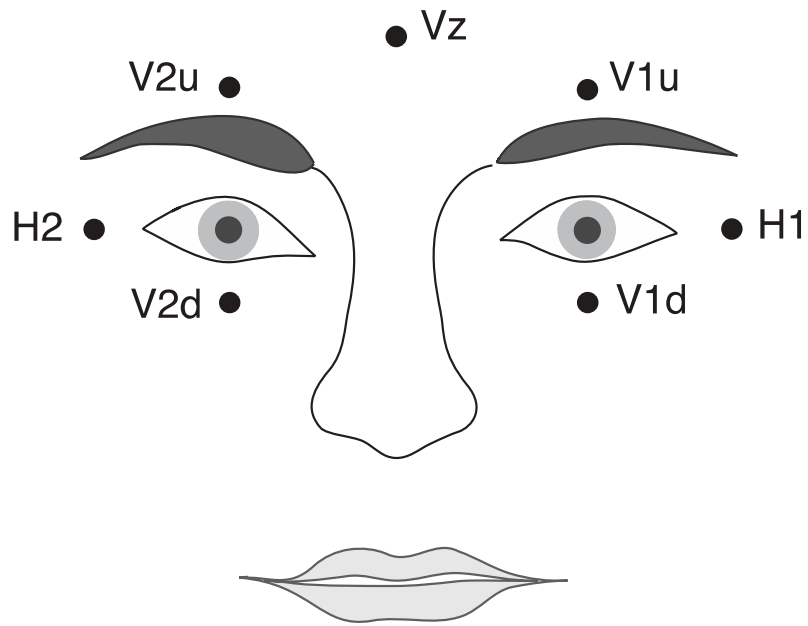Figure 4.2 EEG channels and the chin support from a top view sight
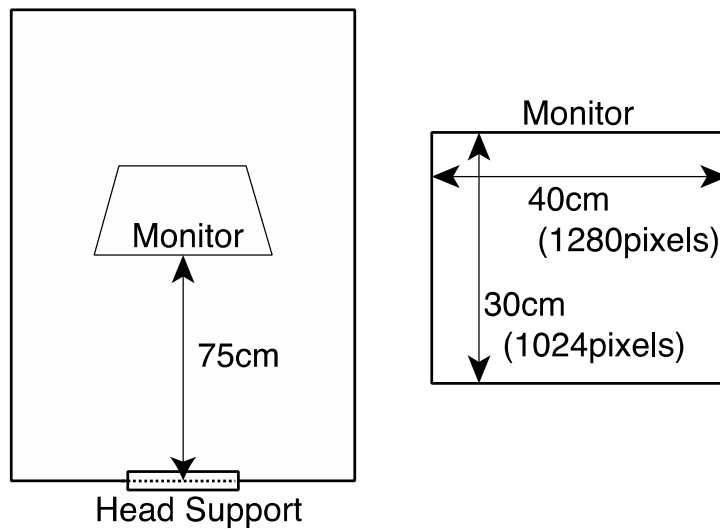
Figure 4.3 EOG electrode positions

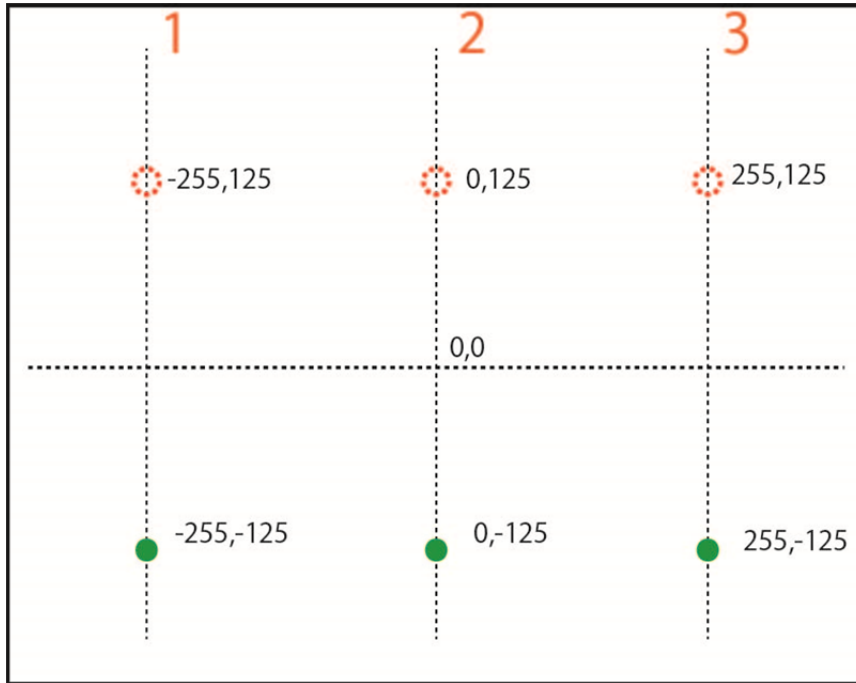Figure 4.4 Experimental setting of the distance to the screen and its size

Figure 4.5 Vertical type stimulation

In the task, three zones ('left', 'middle', 'right' in Figure 4.5) were selected semi-randomly in every session. Individual session starts by showing a red-cross mark at the bottom position in the selected zone (a filled circle in the figure) and the subject gazes it for 1.5s. After that, a filled red circle appears at the top position in the same zone (open circle in the figure) and the appearance lasts for 1s to induce the upward saccade movement and the gaze, and then the filled circle is displaced at the bottom position and stays for 1s to induce the downward saccade and the gaze. The same protocol repeats once again. With respect to experimental setting (Figure 4.4), fixation and target positions in right and left zones are aligned horizontally as $\pm 9°$ saccade angle from the middle, and vertical movement ranges are aligned a $12°$ rotation angle from the origin. Since upward and downward saccade movements are obtained two times in each session of this task, total 48 sessions including 16 sessions for each zone

are performed by each subject.

4.3 Methods for ocular artifact correction.

Various algorithms for EEG artifact removal and noise component detections have been proposed [26][83][85]. Components based algorithms have been widely used, such as Principle components analysis (PCA) which decomposes multiple channel EEG signals into orthogonal components by second order statistics, and Independent component analysis (ICA) which enhances the component detection by making use of higher order statistics. In ICA, non-gaussianity or mutual information is used to decompose the EEG into equivalent number of independent components as signal channels [83][85]. Even if the computational costs were set aside the discussion, ICA component rejection has the disadvantage of having a certain amount of hands-on experience, because the rejection criterions are only empirically specified and therefore the full automation of ICA is still unsolved. In contrast, regression based methods reduce the burden by calculating EOG influences in the form of propagation coefficients based on simple statistics. After the propagation coefficients are calculated, 'real' EEG signals can be estimated from a subtraction of EOG components and multiplied by the coefficients from all EEG channels. Although the method subtracts EOG influences proportionally with less adaptiveness for temporal and spatial variations, it is still a popular method because of its simplicity [22][25][77][80], which is expected to have wide application in on-line analyses.

In the present study, we examined the zone-of-gaze dependency by using a revised regression method known as 'AAA' [77] and ICA [85][94] integrated in EEGlab [95].

4.4 Analysis method

1) Regression based method:

In agreement with the previous researches [22][25][77][80], the model of EEG and EOG can be described by a linear model:

$$mEEG_{m \times n} = rEEG_{m \times n} + \sum_{i=1}^{M} \vec{b}_{i_{m \times 1}} * mEOG_{i_{1 \times n}} \qquad (3\text{-}21)$$

where $mEEG$ is measured EEG signal, $rEEG$ is the 'real' EEG signal, $mEOG_i$ is the i-th EOG component, and b_i represents the propagation coefficient. The regression method by Schlögl $et\ al.$ [25] assumes that EEG and EOG are independent, and then b_i can be calculated by the inner product of the inverse matrix and the auto-variance matrix of EOG signals with the cross-variance matrix between EEG and EOG signals. After the propagation coefficients are calculated, the 'real' EEG signal can be estimated by the following equation:

$$rEEG_{m \times n} = mEEG_{m \times n} - \sum_{i=1}^{M} \vec{b}_{i_{m \times 1}} * mEOG_{i_{1 \times n}} \qquad (3\text{-}22)$$

where b_i represents how much EOG is transferred from eyes to the i-th channel placed over the head map, b_i can be used to explain EOG influences as propagation patterns.

Croft and Barry [22] suggested that 3 EOG components (i.e. vertical, horizontal and radial) are necessary for EEG correction as the eye movements actually take place in a 3-D space and the influence from eyelid may also be related or can be described as a one or a combination of different components. However, vertical and horizontal EOG components are used conventionally, because of the difficulty of extracting the radial EOG [25]. Consistently, the two EOG component model were inherited by following analyses.

2) Independent component analysis (ICA):

ICA is a well-known method for solving blind-source-separation problems. For the signals assumed as a linear combination of multiple independent components and containing up to a Gaussian signal, ICA can provide an inference of weights of components based on high order statistics. The model can be described as:

$$WA = S \tag{3-23}$$

where A is the only known data matrix of size number of channels-by-number of data length. S represents the source matrix which contains components no more than the number of channels in A. In most cases, whitening or sphering is done to unify the data variance through all the dimensions before solving the statistics. By maximizing the entropy or maximizing the mutual information between the inputs and the output, ICA provides an estimated un-mixing matrix with following ambiguities [85]: 1) the order of the independent components is no deterministic, and 2) the variance (in a sense of energy) of the components cannot be determined. The spatial distribution which can be obtained from the un-mixing matrix directly represents the propagation patterns. Since neuronal and non-neuronal source signals are assumed to be independent, target topographies of Independent component (IC) can be selected manually based on expert knowledge. ICA was used as a preliminary analysis for extracting the propagation patterns of EOG.

4.5 Experimental result and analysis.

Recorded data from three subjects with 144 sessions were used in this analysis, which totally contains 576 eye movements.

1) EOG and eye-tracking data:

Example of recorded EOG, eye tracking data and EEG were shown in Figure 4.6 and Figure 4.7. In the part of data for 15s demonstrated that the correlation of upward and downward movements in the vertical EOG (V-EOG) obtained by the equation of ((v1u-v1d)+(v2u-v2d))/2 and session-to-session transitions in every 5.5s were observed in the horizontal EOG (H-EOG) by H1-H2, shifting from the middle to right and then left. The eye-tracking data (X-ETS and Y-ETS) exhibited consistent changes depending on V- and H-EOGs. With the assistance of the high-sampling rate eye-tracker system, eye movements were accurately estimated in a comparison with temporal sequences of EOGs. As shown in Figure 4.6, the eye movement pursued the visual target, which can be divided into two phases: 1) A quick saccade with a large amplitude change in 40~60ms is observed as a long-distance jump, if the movement exceed the target position (or to be short until the target) 2) an eye position is adjusted to reach the target position with a small amplitude change. The eye movement around 4s in the figure exhibited an overrun-and-return, and movements around 10s represented a shortage-and-adjust behavior. This observation suggests that it is possible for the eye-tracking system to estimate the EOG information, which is powerful enough for artifact removals, such as linear regressions and ICA.

Figure 4.7 showed temporal sequences of potentials in frontal EEG channels as FP1 and FP2 after band filtered with a 0.1~30 Hz FIR band pass filter. Activities in the channels were largely influenced depending on vertical EOG changes. In following sections, EOG influences depending on the viewing-area, or gaze-of-zone, were analyzed in the propagation coefficient and EEG event-related topographic maps in

ICA.

2) Linear regression analyses:

In the result of the regression analysis, propagation coefficients were obtained on every channel based on the procedure discussed in regression based method and applied to the first motion of the upward saccade in every session. Resultant coefficient values of frontal channels of FP1 and FP2 were shown in Figure 4.8. While EEG channels are expected with a large influence from EOGs, in this experiment, the differences were not statistically significant. However, in the result, a little viewing-area sensitive differences were observed under the left and right conditions in comparison with the middle. Intuitively, maybe increasing the angular distance of saccades can lead to a significant difference between viewing-areas. For all the conditions, FP2 propagation coefficients are slightly larger than FP1's, which needs further systematic analyses with multiple combinations of eye-movement directions and zones, and possibilities of bias effects of electrode positions or other asymmetric conditions in EEG channels can be considered.
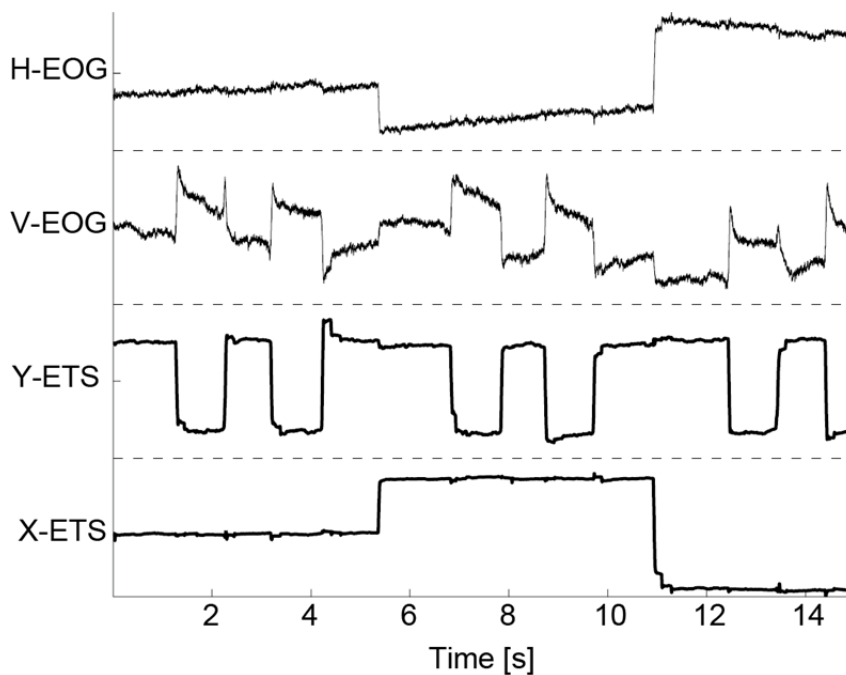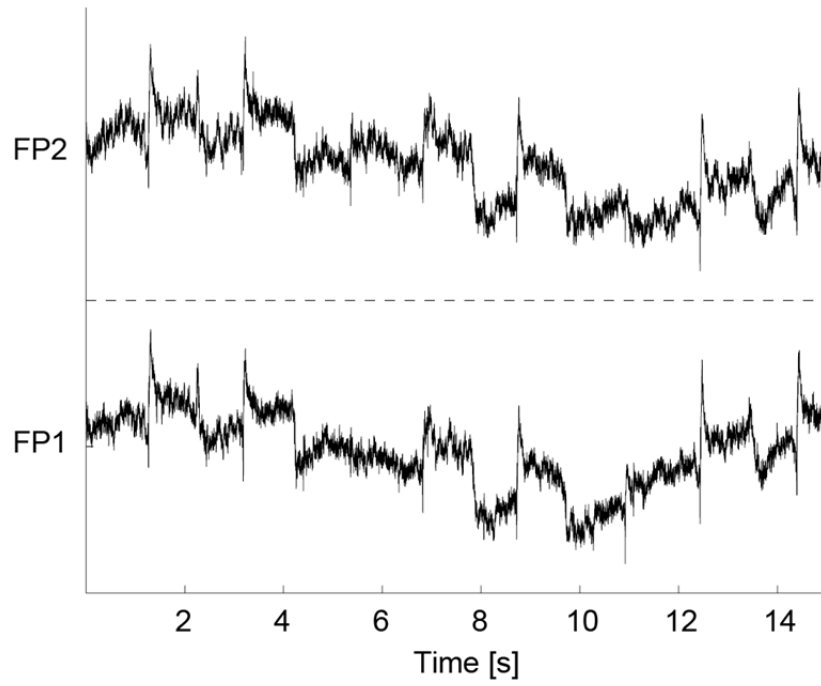

Figure 4.6 EOG and eye-tracking data

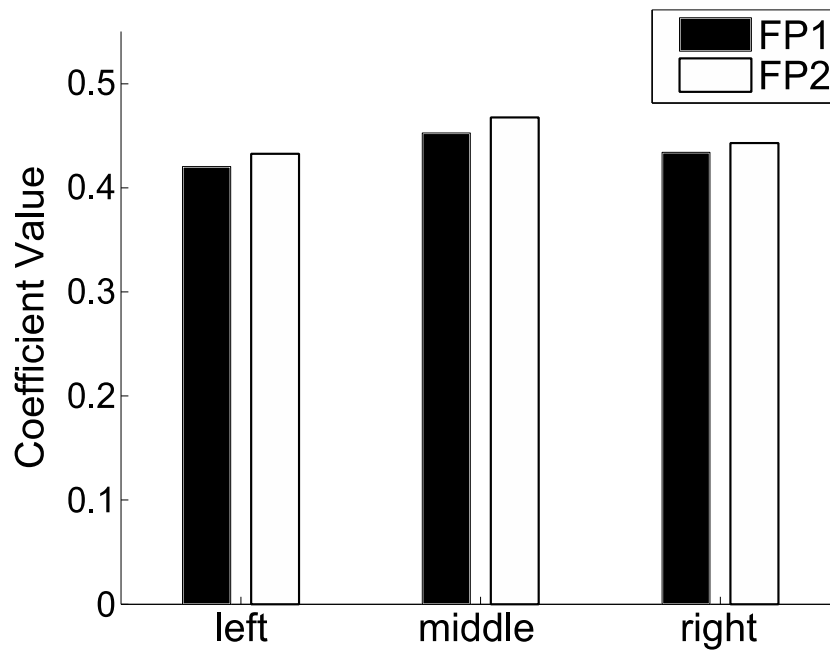Figure 4.7 EEG raw data from channels of FP1 and FP2

Figure 4.8 Propagation coefficients of different zones (upward saccade)

3) ICA analyses:

In ICA analyses, we investigated EOG influences in EEGs after the separation of eight cases that consist of two groups (upward and downward movements) and zone-of-gaze dependency (left, middle right, and all zone-of-gaze combination conditions). Recording data was preprocessed with a 1~30 Hz FIR band pass filter and down sampling into 500 Hz to fit to the eye-tracker data. Independent Components (ICs) were obtained by ICA, and applied to each epoch defined as the period [-400ms ~ 600ms] with respect to the eye movement onset timing, which was defined by the time point with a maximum speed of eye-tracking data in the epoch. As an example, the topographies of EOG component were shown in Figure 4.9. Figure 4.10 showed a sample of ICs in eight epochs of the downward eye movement in the combination case. Dotted line and solid line denote epoch period and onset timing respectively.

In Figure 4.9, the influence of zone-of-gaze dependency in EEGs appeared as differences of topographic maps in left and right conditions compared with the middle condition. In the combination case of the topographic map, a relatively smooth propagation pattern was observed with a symmetric pattern, while our zone specific analyses revealed non-negligible differences depending on the viewing area both in results of the linear regression method and ICA based topographic maps consistently. Those results indicated a risk of ignorance of the EOG zone-of-gaze dependency in EEG analyses and ocular-artifact corrections.

left middle right combination

(a) downward eye movement

left middle right combination
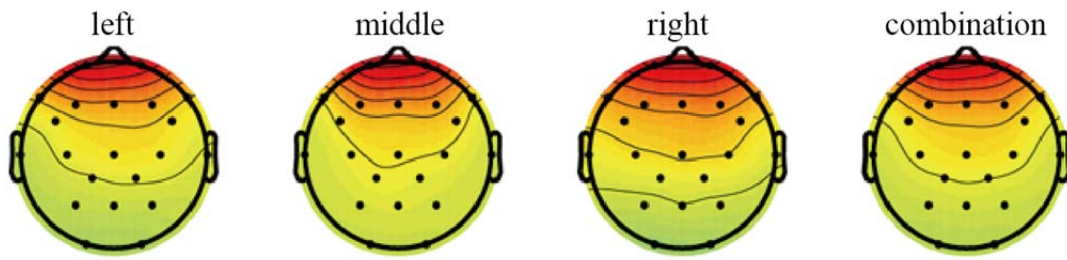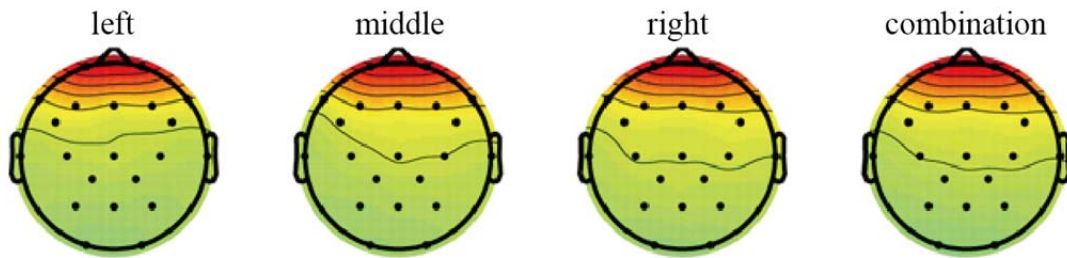
(b) upward eye movement

Figure 4.9 Topographic head map of the independent components representing ocular artifacts

Figure 4.10 An example of ICA component decompositions (downward saccade)

Our hypothesis of the EOG influence in EEGs in the viewpoint of zone-of-gaze dependency was preliminarily examined by the experiment with simultaneous recording of EOG, eye tracking and EEG recordings. In quantitative analyses with regression coefficient and ICA topographies, the results demonstrated a general tendency of the differences to testify the hypothesis. Our result indicates that the real eye movement analysis is important for improvements of artifact corrections by calculating the linear regression coefficients and ICA topographies separately depending on the gaze-of-zone, which have been considered as a naive assumption in traditional ocular artifact removals, yet it extends the availability of the high-spec eye tracking system effectively. Effects of initialized positions to gaze, its range of angle and directions are considerable factors, which should be analyzed in the further investigation.

Chapter 5　Direction and viewing area-sensitive influence of EOG artifacts revealed in the EEG topographic pattern analysis

In chapter four, an intuitive experiment result showed that there seems to be some propagation difference both under regression based analysis and ICA topographic patterns. For practical use, a quantitative is preferable. Thus, in this chapter, a new experiment is designed to obtain a quantitative analysis to the influence and significance caused by zone-of-gaze.

We investigated the influence of eye movement related artifacts on Electroencephalography (EEG) measurements of human subjects who were requested to perform a direction/viewing area depending saccade task. In this task, the subject gazed at a fixed point in a specific area of a screen and pursued with eyes depending on the instructed target to guide its direction either horizontally or vertically. Ocular electric potentials recorded as electro-oculography (EOG) were generated by making saccadic eye movements towards visual targets that were spatially located and aligned with the two possible directions of motion in the display. Traditionally, removal methods of EOG artifacts contaminated in EEGs have been studied under the assumption of a linear combination model, which indicates that the signals are superimposed with different strength to be described as coefficients of the linear model. The coefficient identification is the issue to minimize the error in the real EEG estimation, and eye movement-related differences were rarely noticed in those methods. We therefore designed a systematic protocol to evaluate the dependency and studied the coupling

effect of eye-movement direction and viewing area in the framework of the linear regression analysis for EOG corrections. In our experimental results, event-related potential (ERP) topographic patterns to evaluate EOG influences in the EEG head map were observed as a reversal structure in the coupling condition between horizontal-rightward and –leftward eye movements and consistently in the coupling condition between vertical-upward and –downward eye movements. Surprisingly, EOG influences are different in comparison between top-viewing and bottom-viewing areas in the horizontal movement and consistently are different between right-viewing and left-viewing areas in the vertical movement. The result demonstrated that the propagation coefficients were affected differently by the EOG changes depending on viewing fields and the eye movement directions, suggesting the non-trivial contribution to the EOG artifact removal if the coefficient identification will be done separately depending on the coupling condition of the viewing area and its direction. The maximum difference depending on conditions exceeded 10% percent change in propagation coefficients in the regression model, and the electrodes with significant difference in propagation coefficients were also shown in our result by pairwise T-test over all subjects ($t(7) > 2.3646$; $p < 0.05$).

5.1 Eye movement related artifacts and their spatial sensitivities

Owing to accumulations of the experimental evidences, understandings of ocular potential mechanisms are growing as a patchwork in this field, yet there are still unknown effects have not been interpreted, and the comprehensive ocular removal remains unsolved [56][61][68][96].

Recent advancements of eye-tracking systems make it possible to obtain a high

spatial-temporal resolution with a comparable sampling rate as EEG signals. This may lead to a fundamental improvement in the specification of EOG potential changes without electrodes surrounding eyes. Observation of accurate eyeball movements may predict spatial diploe changes that spread over EEG channels with a spatial distribution of EOG influences, thus may effectively help ocular artifact removal. Traditionally, the EOG propagation is treated as a static spatial distribution decreasing monotonically from a frontal area around eyeballs to occipital areas, which can be used for regression based methods for its validation and component based methods in a topographic discrimination whether independent components are ocular artifacts or not. Coincidentally, Plöchl et al. [68] noted future potentials of simultaneous recording EEGs and eye-tracking observations, such as a proposal to use the eye-tracker for determining the onset timing of the eye movement in saccade event-related potentials (ERPs), contributing for opening discussion on the eye movement dependent EOG specificity with the corneo-retinal dipole changes and their influence to EEG measurements. In an early stage investigation, Schlögl et al. [25] testified the EOG influence in the tasks requiring subjects to perform clockwise and counter-clockwise eye movements (large circular eye movements without moving their head) and Plöchl et al. [68] investigated eight types of eye movements centered in the middle of a big stimulation screen. As a preliminary investigation, they demonstrated a topographic difference of ERPs in comparison between upward and downward eye movements but they found there is no topographic pattern difference in comparison between small and large saccade movements. It suggests the directional selectivity of ocular artifacts and an important clue to the presence of the sensitivity of viewing area in a framework beyond traditional center-fixed saccade tasks.

In the purpose of resolving the ambiguity in the center-fixed saccade analysis task, we focused on viewing area depended ocular artifact generation in the background of the directional selectivity, proposed a novel systematic task comparing vertical and horizontal eye movements performed in different areas in the field of view and investigated twelve types of eye movements with varying fixation positions. The fixation positions are left, middle and right in the vertical (rightward/leftward) eye movements and top, middle and bottom in the horizontal (upward/downward) eye movements. Our aim was to test the actual topographic differences and their impact to the existing ocular artifact removal methods involving the difference in directions/viewing-areas and our experimental results was validated by propagation pattern analyses based on the linear regression coefficients. In following sections, methods and data analysis were introduced in Section 2, and experimental results was shown in Section 3. Discussion and conclusion were followed in Section 4 and 5.

5.2 Methods and Data Analysis

In the systematic analyses of EOG influence by extending the concept of Plöchl et al. [68], which demonstrated large offsets between different fixation positions. Figure 5.1 illustrated a possible influence of corneo-retial dipole changes to the head map of the event-related brain potentials. It is expected that even in the same kind of eyeball movements, different influences can be observed depending on the areas on the screen. In the present study, the linear regression method was used for the validation to the effect and analyses of differentiation of EOG influences depending on conditions, which means an extension of the fixed propagation coefficients obtained by the whole recording data to condition-dependent coefficients.
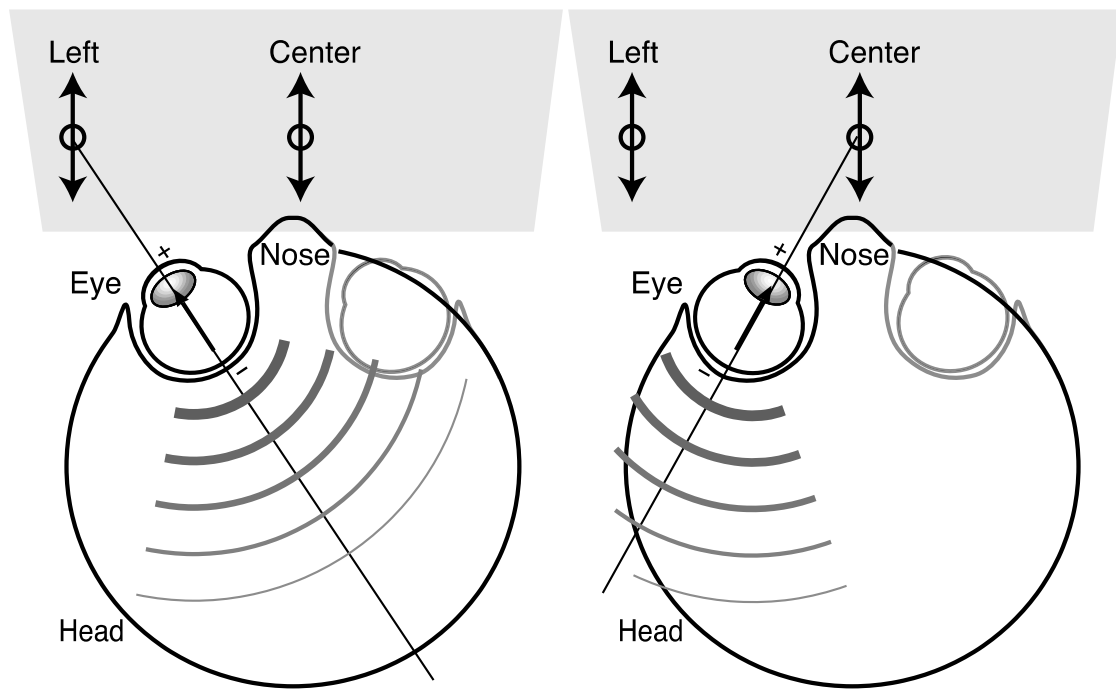
Figure 5.1 Schematic illustration of corneo-retinal dipole changes depending on viewing areas. (left) Condition seeing the left side. (right) Condition seeing the center.

1）Participants:

In this study, we recorded EOG and EEG data from 7 electrodes surrounding eyes and 23 scalp electrodes (Figure 5.2) with 12 different eye movement conditions (Figure 5.3a) from 8 subjects with a mean age of 26.1 years old (age range from 21 to 45 years old; 7 male and1 female) and without any signs of medical or psychiatric illness. All the subjects were normal sight or corrected-to-normal. All the subjects signed consent after being clearly informed of the purpose and procedures of the experiment. The experiment protocol was approved by the Ethics Committee in Future University Hakodate.
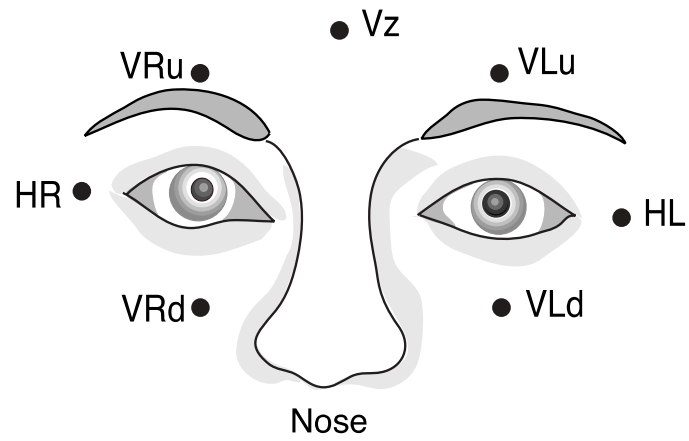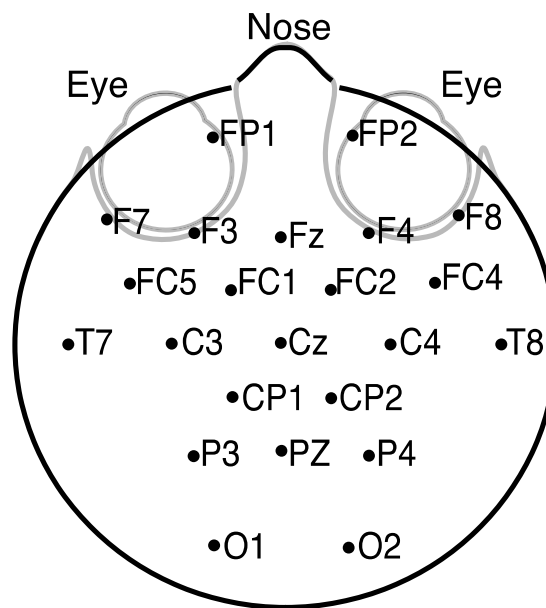
Figure 5.2 EOG electrode positions and EEG channel locations in the head map. (a) EOG electrodes attached on the face with 7 channels. (b) 23 EEG channels attached on the scalp using a EEG cap.
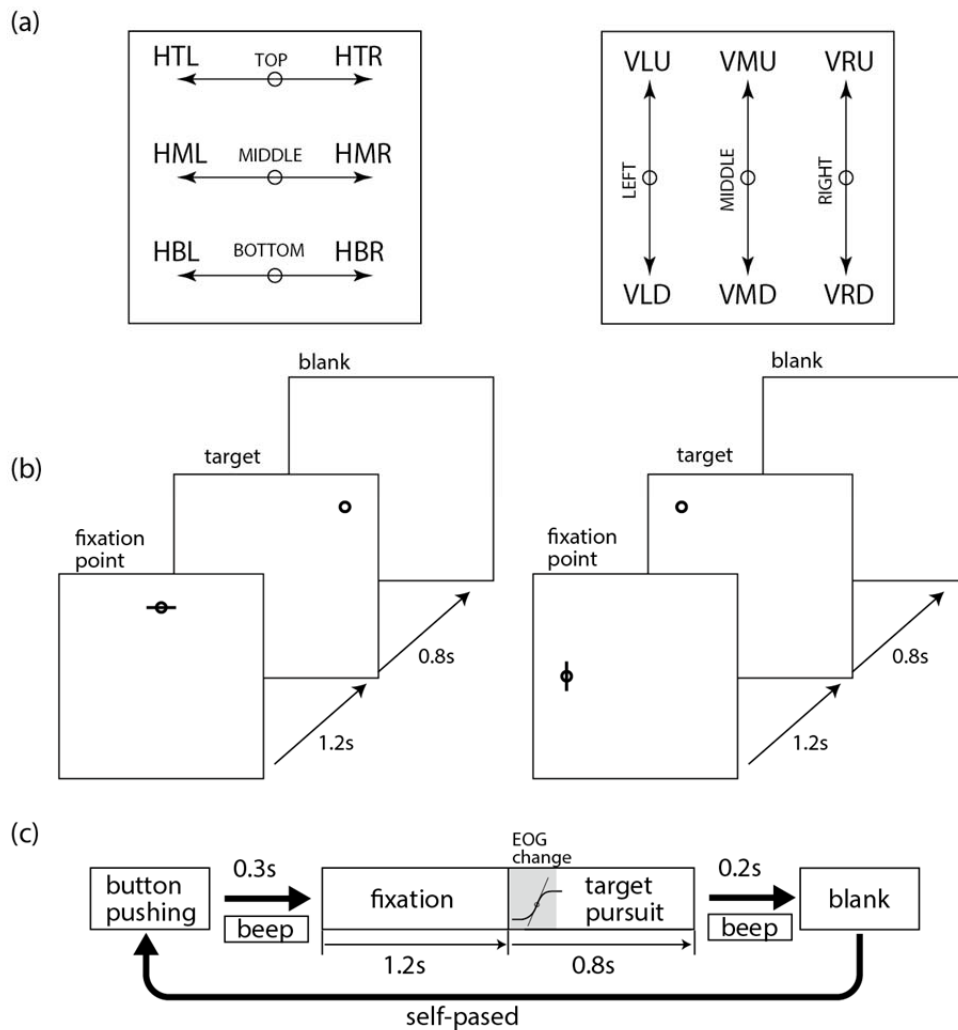
Figure 5.3 Task design and task scheduling. (a) Horizontal eye movement conditions segregated into three viewing areas horizontally (left) and vertical eye movement conditions segregated into three viewing areas vertically. (b) Timing to shift from the fixation, target and blank screen. (c) Task design as a self-paced saccade eye movement.

2) Stimuli and experimental procedure:

The subjects sat in a comfortable arm chair in front of a 21-inch CRT monitor (Sony, CPD-G520, refresh rate 85 Hz, 1024×768 pixels). An ophthalmic chin rest was used to support the subject's head to prevent irregular head movements. As shown in Figure 5.3b, all the subjects were instructed to stare at the fixation point in the screen and

follow a target point with their eyes after the target is presented in the screen (Figure5.3b), and subjects were requested not to blink during the task. To maximize the effect of the prevention of blinks, a 'my-pace' handy button was used for letting the subject decide the own starting timing during every trial, as self-pace task scheduling (Figure 5.3c). Stimuli were presented on a black background using MATLAB (MathWorks, USA) with the Psychophysics Toolbox extensions designed by Brainard [97].

During the experiment, subjects performed horizontal and vertical eye movements according to the stimuli pattern: the eye movement was cued to perform from different fixation points shown as a circle in the central position of arrowed-lines in the Figure 5.3a, which illustrates horizontal and vertical eye movement conditions separately in the left and right panels. Middle points in horizontal and vertical conditions are given as the exact same position, and the distance or movement width/height between two adjacent points denoted as individual ends of arrowed-lines are the same as 12° eye movement in horizontal or vertical conditions. Fixation points and eye movement directions were selected semi-randomly in the whole sessions and trials. As illustrated in Figure 5.3c, after 'my-pace' button was pressed, a beep sound was played to suggest the start of trial. After 0.3 seconds, a fixation mark appeared in one of the six positions marked by rounds with a bar (Figure 5.3b) to hint the forthcoming eye movement's direction (either horizontal or vertical). The fixation lasted 1.2 seconds and then the fixation mark disappeared and a stimulus point appeared at the location of the end of the arrow according to the selected movement direction. This stimulus point showed 0.8 seconds. And then another is beep was played to tell the subject the trial was over.

Twelve types of eye movement conditions were abbreviated according to horizontal

(H) or vertical (V) as the first letter, the fixation position that was given as Top (T), middle (M) and bottom (D) in the horizontal case and left (L), middle (M) and right (R) in the vertical case were given as the second letter, and finally the movement direction either leftward (L), rightward (R), upward (U) or downward (D) were used as the last letter, such as abbreviations of HMR and VLU.

The whole experiment was divided into 4 sessions. In every session, each subject performed 13 eye movements under every condition. Totally 52 trials of eye movements were recorded under every experimental condition.

3) EEG recording and analysis:

EEG signals were acquired using a 32-channel BrainVision amplifier (BrainProducts, Germany). 23 of the Ag/AgCl electrodes were used for EEG channels (FP1, FP2, F7, F3, Fz, F4, F8, FC5, FC1, FC2, FC4, T7, C3, Cz, C4, T8, CP1, CP2, P3, Pz, P4, O1, O2) according to the international 10-20 system, 7 for electro-oculography (EOG) channels (VRu, VRd, VLu, VLd: 4 vertical EOG (VEOG) electrodes placed on supraorbital and infraorbital rims of each eye; HL, HR: 2 horizontal EOG (HEOG) electrodes were on the left and right outer canthi; Vz: one was on the forehead approximately 25mm above the nasion, as shown by Figure 5.2a), and 2 for earlobes. EEG recordings (0.01–100 Hz bandpass, 500 Hz sampling rate) were referenced to an electrode between Fz and Cz during measurement and re-referenced to linked earlobes for analysis. VEOG are defined as the average of EOG potentials in both eyes given as $[(VRu\text{-}VRd)+(VLu\text{-}VLd)]/2$ and HEOG are defined as the difference between two horizontal EOG electrodes: $HL-HR$.

All EEG recordings were filtered by a 30 Hz FIR low pass filter before data analysis.

In the analysis of the event-related potential of EOGs and EEGs, each onset of the trial was given by the time point of the highest inclination in the EOG change (Figure 5.3c), which was calculated by the largest difference between the value at the present time and value 10ms earlier, and it was reset as $t = 0$. Then ERPs were obtained from -250ms to 400ms for every channel of EEGs and EOGs. Bad trials were rejected by the following simple algorithm based on statistical distribution. The procedure was given as:

- Alignment (mean value removal): $s_i^{ch}(t) = e_i^{ch}(t) - \bar{e}_i^{ch}$ where $\bar{e}_i^{ch}$ is the mean value of the i -th trial and $ch = [EEG_1, EEG_2, \cdots, EEG_{23}, VEOG, HEOG]$ denotes EEG and EOG channels. After the mean value removal, aligned ERP signals $\mathbf{s}_{trial}^{ch}(t) = [s_1^{ch}(t), s_2^{ch}(t), \cdots, s_N^{ch}(t)](i = 1, \cdots, N)$ were obtained in each trial, where N is the number of trials.

- Calculating of the standard deviation σ^{ch} over trials: for the purpose to set a rejection criterion of the improper data, the mean and standard deviation were calculated via the formulas $\mu^{ch}(t) = \sum_i \mathbf{s}_i^{ch}(t)/N (i = 1, \cdots, N)$ and $\sigma^{ch}(t) = \sqrt{\sum_i (\mathbf{s}_i^{ch}(t) - \mu^{ch}(t))^2/(N - 1)}(i = 1, \cdots, N)$ over N trials.

- Bad trial rejection: in our data analysis procedure, proper data is defined as $\mathbf{s}_{G\_trial}^{ch}(t) = \{^{\forall} t, |s_i^{ch}(t)| \le \eta \cdot \sigma^{ch}(t)\}$ and an abnormal trial involves at least one data point exceeding the predefined threshold $\eta \cdot \sigma^{ch}(t)$ such that $\mathbf{s}_{B\_trial}^{ch}(t) = \{^{\exists} t, |s_i^{ch}(t)| > \eta \cdot \sigma^{ch}(t)\}$ where $\eta = 3$ for EOGs and $\eta = 4$ for EEGs. Whichever the EOG or EEG exceeds the predefined threshold, the whole set

of data in the same trial is removed from the analysis.

Figure 5.4, Figure 5.5 and Figure 5.6 showed some examples of the procedure. In Figure 5.4 and Figure 5.5, the mean value was shown as a thick curve in green, and the rejection boundary were marked by thin red dash lines. In Figure 5.6, all the rejected trials are marked by increasing line width and coloring by red.
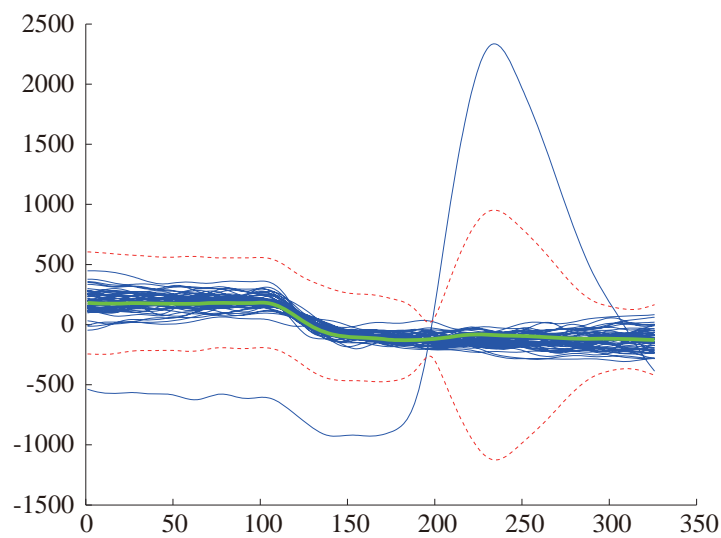

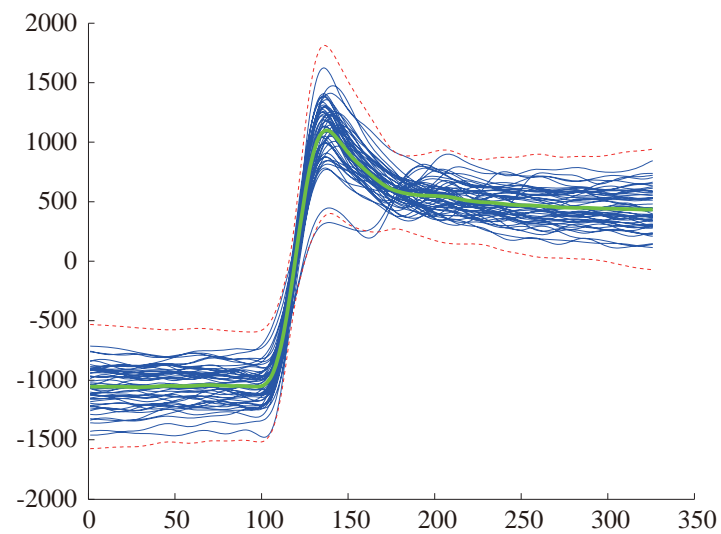Figure 5.4 An example (EOG data) of the dataset containing bad trial of blink

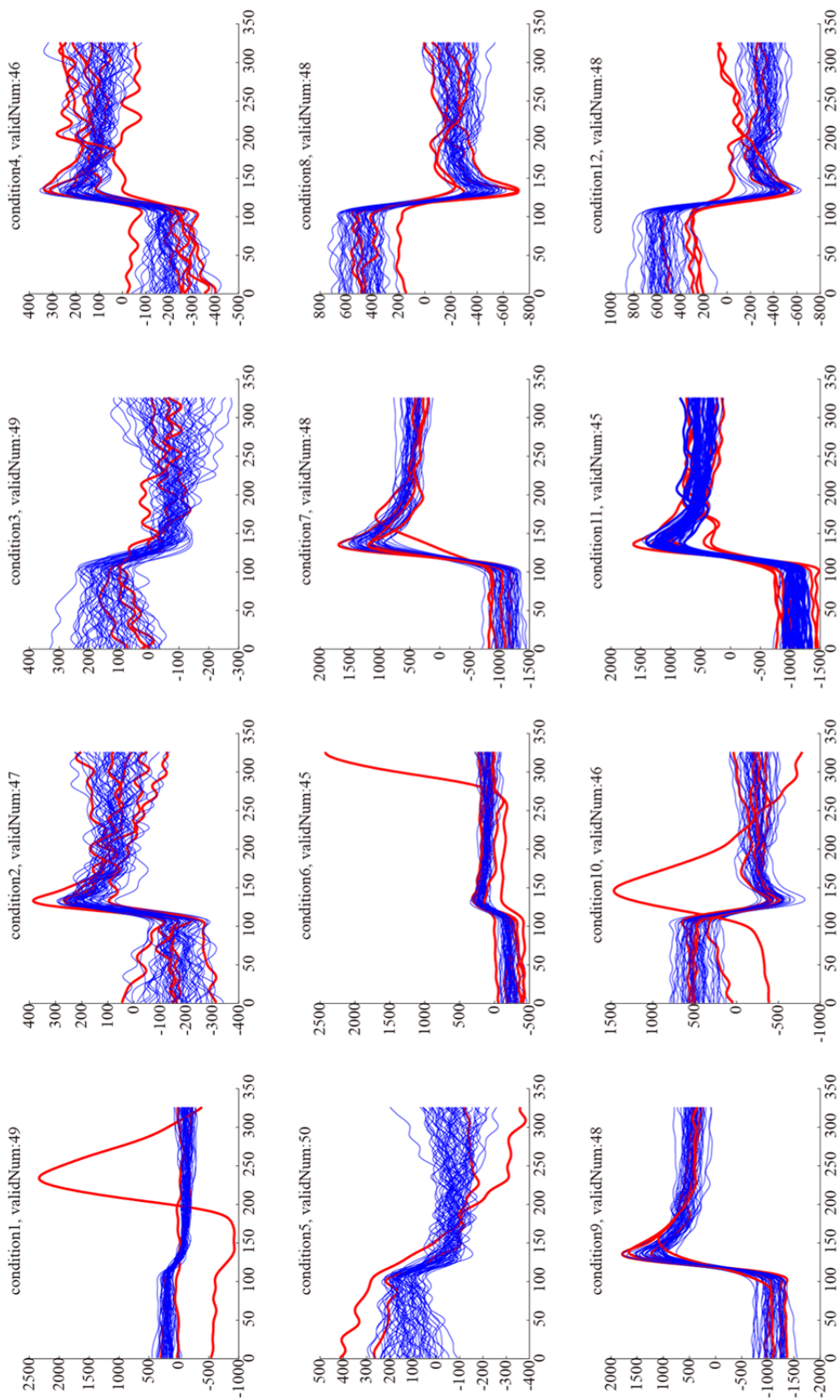Figure 5.5 An example (EOG data) of the dataset containing common bad trials

Figure 5.6 An example (EOG data) of rejected trials in all eye movement conditions

By using obtained ERPs, the propagation coefficients of EOGs were calculated using 'aligned-artifact averages' (AAA) method [77].

4) Linear Regression method:

In agreement with the previous researches [22][25], the model of EEG and EOG can be described by a linear equation:

$$mEEG^{ch}(t) = rEEG^{ch}(t) + \sum_{i=1}^{M} mEOG_i(t) \times b_i^{ch} \qquad (3\text{-}24)$$

Where $mEEG$ represents measured EEG signals on scalp, $rEEG$ represents the 'real' EEG signal which is assumed to reflect brain activities but it is difficult to access due to contaminations of the signals by several types of artifacts. There are three types of EOGs with respect to 3D directions (M in Eq. 1), which corresponds to vertical, horizontal and radial EOGs, if can be measured independently in an ideal way. $mEOG_i$ represents the i-th EOG component and b_i its corresponding propagation coefficient. Croft and Barry [22] suggested that 3 EOG components are necessary for ocular artifact corrections, which consist of vertical, horizontal and radial EOG. Whereas the vertical and horizontal EOGs can be detected easily in saccade tasks, the radial component is too small to be obtained directly [25][98].

In the present study, we focused on the influence of saccade direction specified on individual viewing area in the framework illustrated in Figure 5.3a, and the task dependent regression according to the model of EEGs and EOGs by the linear equation as:

$$rEEG_{***}^{ch} = mEEG_{***}^{ch} - mEOG_{***} \times b_{***}^{ch} \qquad (3\text{-}25)$$

Where *** represents abbreviations of task conditions such as HMR and VLU. The

propagation coefficients b^{ch}_{***} were calculated by the single component regression analysis with the 'AAA' method [77].

5.3 Results

1) EOG influences to EEG channels in vertical and horizontal eye movements

Depending on task conditions, saccade ERPs of VEOG, HEOG and EEGs were obtained by averaging over all trials under each condition. Temporal sequences of task dependent EOGs and the influences on EEGs were shown in Figure 5.7. In horizontal eye movement conditions abbreviated as H** (Figure 7a), which include leftward/rightward eye movement, the HEOG defined as $HL-HR$ changed positively in leftward movements of H*L and negatively in rightward movements of H*R change, exhibiting a consistent range that exceeds $200\mu V$ within a period of 200ms. The flat potential curves under a negligible level in VEOG changes under leftward/rightward movement (H**) conditions suggested that there is almost no eyeball rotation or eyes did movement. Temporal sequences of HEOGs in leftward/rightward movements increased/decreased quickly just before the onset (defined by the highest inclination of the EOG change), while differences depending on fixation positions on top/middle/bottom, abbreviated as HT*, HM* and HD*, are quite small. EOG influences on EEGs were demonstrated with respect to EEG channel positions, such as averaged saccade ERPs on FP1, F7, Fz and Cz as shown in Figure 5.7b. EOG influences appeared in amplitudes of leftward saccade ERPs (HTL, HML and HBL; red lines in the figure) were like F7>FP1>Fz≈Cz≈0 reflected by the distance form eye positions to the channels. In vertical eye movement conditions which include upward/downward eye

movement (V**), the averaged HEOG stayed in a flat way and averaged VEOGs was clearly changed positively/negatively in upward/downward movements (V*U/V*D) as shown in Figure 5.7c. In the upward VEOG showed there is an overshoot around 25ms, which is presumed as an effect of the interaction between eyeballs and the eyelid when eyes were drifting upward [68]. In spite of the same rotation angle 12° of eyeballs, upward and downward eye movements VEOGs showed different amplitudes. This frequently depends on electrode position because muscular structures around eyebrows and cheeks are quite different. In influences on EEG channels (Figure 5.7d), a high amplitude approximately 50μV prominently appeared in the FP1 channel in the upward condition and similarly in the downward condition. In other channels F7, Fz and Cz, the amplitude decrease with the distances increase from eyeball consistently in both upward and downward conditions. These results indicated that EOG influences to EEG potentials maximizing to 50μV in the condition of 12° eyeball rotations are consistent with results of Plöchl et al. [68], which demonstrated in approximately 50μV in the condition of 11.5° eyeball rotation. In vertical eye movement conditions, EEG channels in the midline showed positive/negative amplitudes with tens micro-voltage potentials depending on the upward/downward movements. In horizontal eye movement conditions, F7 showed positive/negative potentials with tens micro-voltage amplitude in both the leftward/rightward movements.

Figure 5.7 Temporal sequences of EOG and saccade ERP changes with respect to the onset timing. Practically the onset shown in the dashed line was defined by the time point of the maximum inclination of the temporal changes. Horizontal EOG (HEOG) and Vertical EOG (VEOG) in (a) and (c). ERPs of FP1, F7, Fz and Cz channels in the horizontal eye movements (b) and vertical eye movements (d).
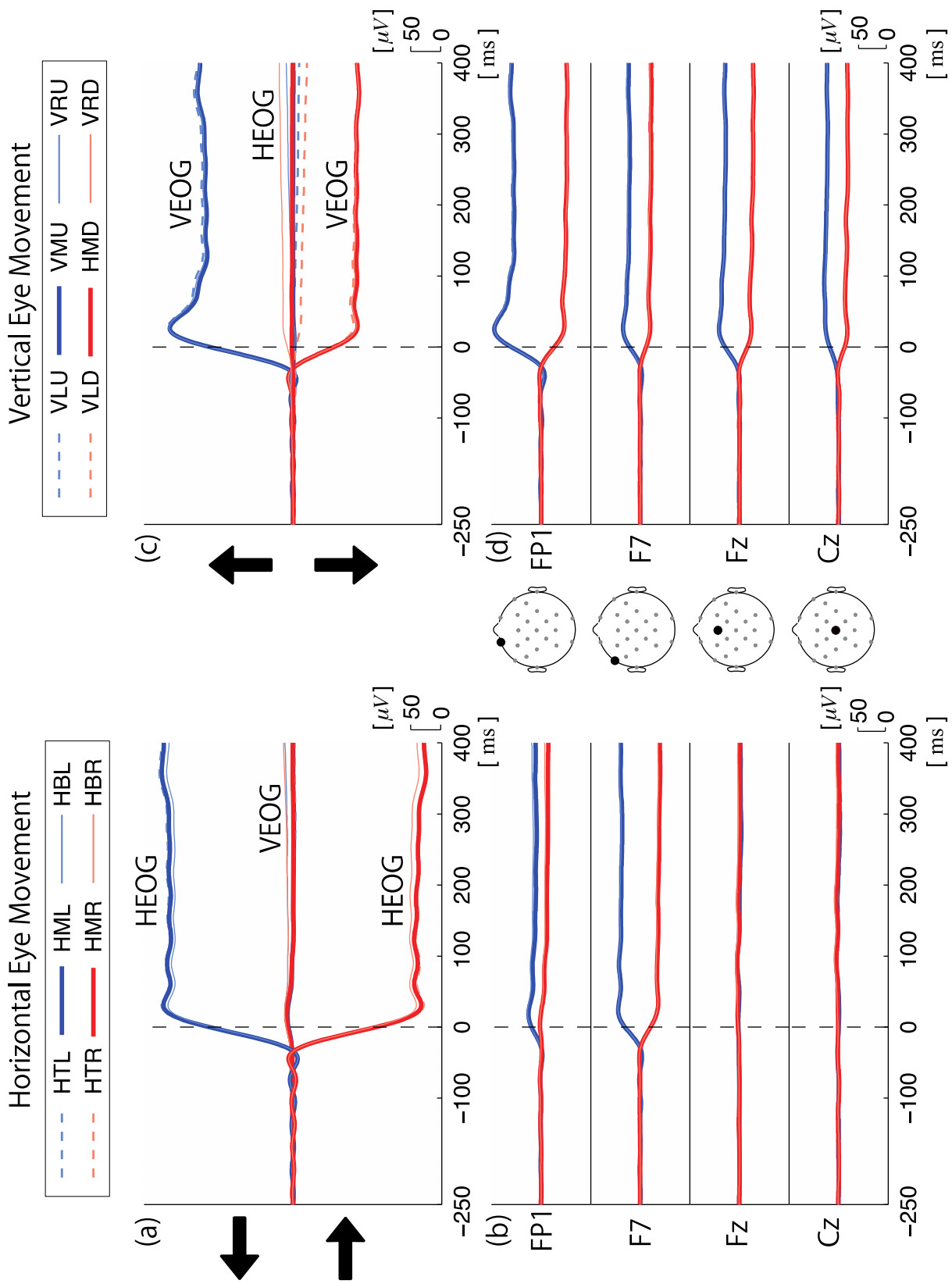
Figure 5.7 An example of eye movement ERPs

2) ERP topographic patterns differentiate depending on eye movement direction and viewing area

ERP topographic patterns depending on task conditions were shown in Figure 5.8, which were replotted from averaged ERP potentials over 150~350ms as a 2D contour map ranging in $\pm 50\mu V$. In horizontal condition of H**, ERP topographic patterns showed nearly reflected images between opposite directions, i.e. leftward/rightward movements abbreviated as H*L and H*R, propagated EOG influences in the head map starting from F7 (with a positive peak of about $50\mu V$ in the leftward group as HTL, HML and HBL and negative peak of about $-50\mu V$ in the rightward group as HTR, HMR and HBR) and F8. The ERP propagations looked larger when in HBL and HBR conditions than in HTL and HTR. In vertical condition of V**, ERP topographic patterns showed nearly symmetric images in upward movements (VLU, VMU and VRU) with different degrees of skew in distribution. While in downward movements (VLD, VMD and VRD), the skew in distribution became much clearer.

3) Direction and viewing area-sensitive propagation coefficients

For the sake of the validation for our hypothesis, propagation coefficients in the regression model were obtained separately depending on conditions, given by the combination of eye movement direction and viewing areas, as shown in Figure 5.9. As the consequence, topographic patterns of the coefficients showed similar distribution patterns with results of the ERP topographic distributions in Figure 5.8, except that the signs of the values. For coefficients topographies the range of values fell into [-0.5, 0.5]. For analyses to testify whether the difference exceeds a significant level or not, the difference between topographies are shown in Figure 5.10 and the result of a pairwise T-test over 8 subjects for all the electrodes were shown in Table 1. Figure 5.10 showed

comparisons depending on four groups as leftward (H*L), rightward (H*R), upward (V*L) and downward (V*D). The * in group labels represents a factor used for comparison such as Top (T), Middle (M) and Bottom (B) in the horizontal case and Left (L), Middle (M) and Right (R) in the horizontal case, and the label in top-right corner of four panels denotes which conditions the differences come from. The difference patterns in groups H*L and H*R showed nearly mirrored-images. In the group of V*U, the difference patterns were not as clear as the other groups. Whereas, in the group of V*D, topographies demonstrated clearly noticeable differences between different fixation conditions. In accordance with judgments on the numeric values, the difference in group V*U (upward eye movements), the differences were relatively small, whereas in group V*D, downward movement, values of the differences in lateral sites are significantly larger, especially in comparison of L-R the differences between left and right hemispheres provide values exceeding 0.03, which means more than 10% percent change in propagation coefficients. Pairwise T-test over 8 subjects on coefficient difference (Table 1) showed the electrodes with significant difference in bold font (t(7)>2.3646; p<0.05).
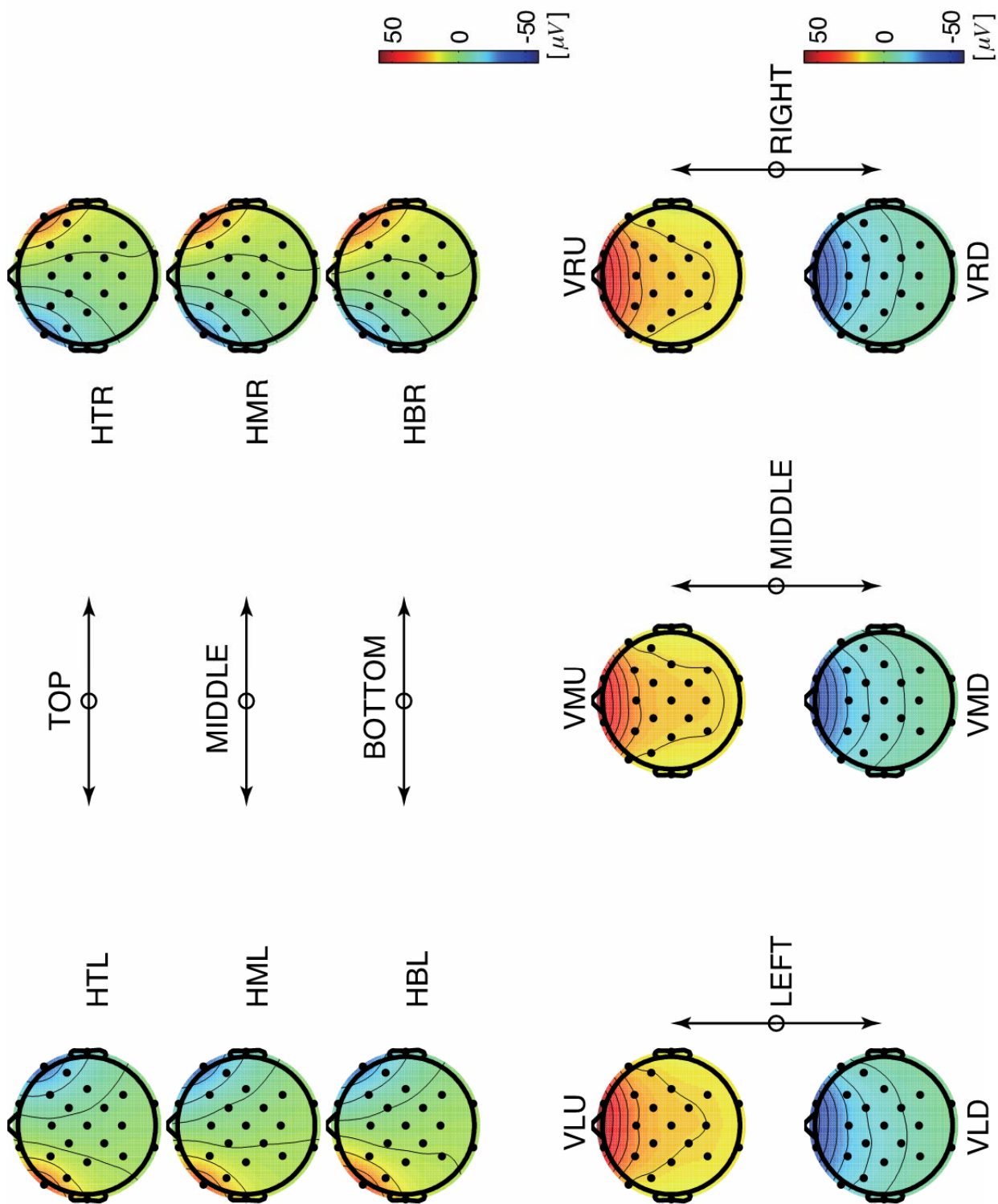
Figure 5.8 Saccade ERP patterns in the head map depending on twelve conditions
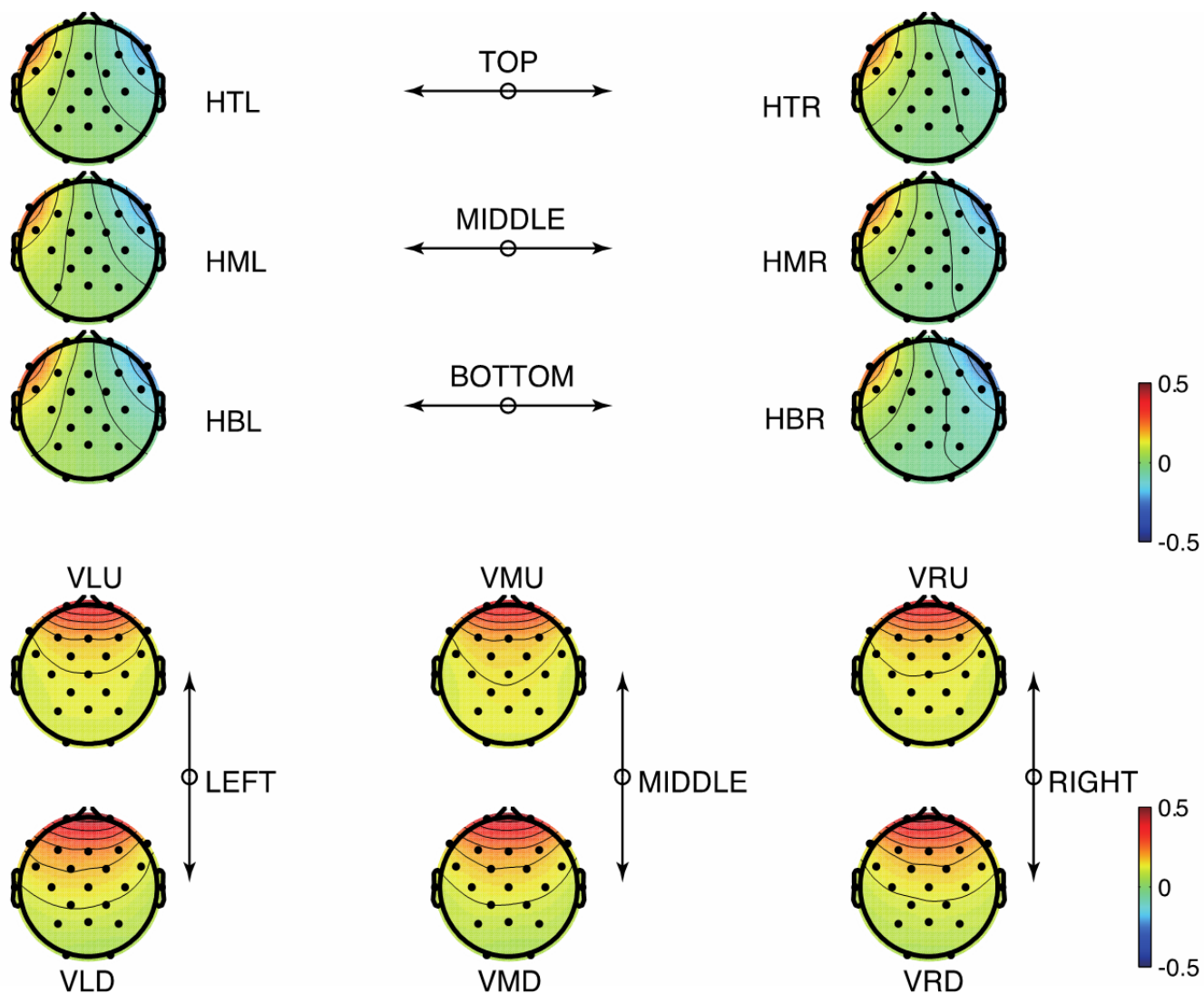
Figure 5.9 Propagation coefficient distribution in the head map depending on twelve conditions.
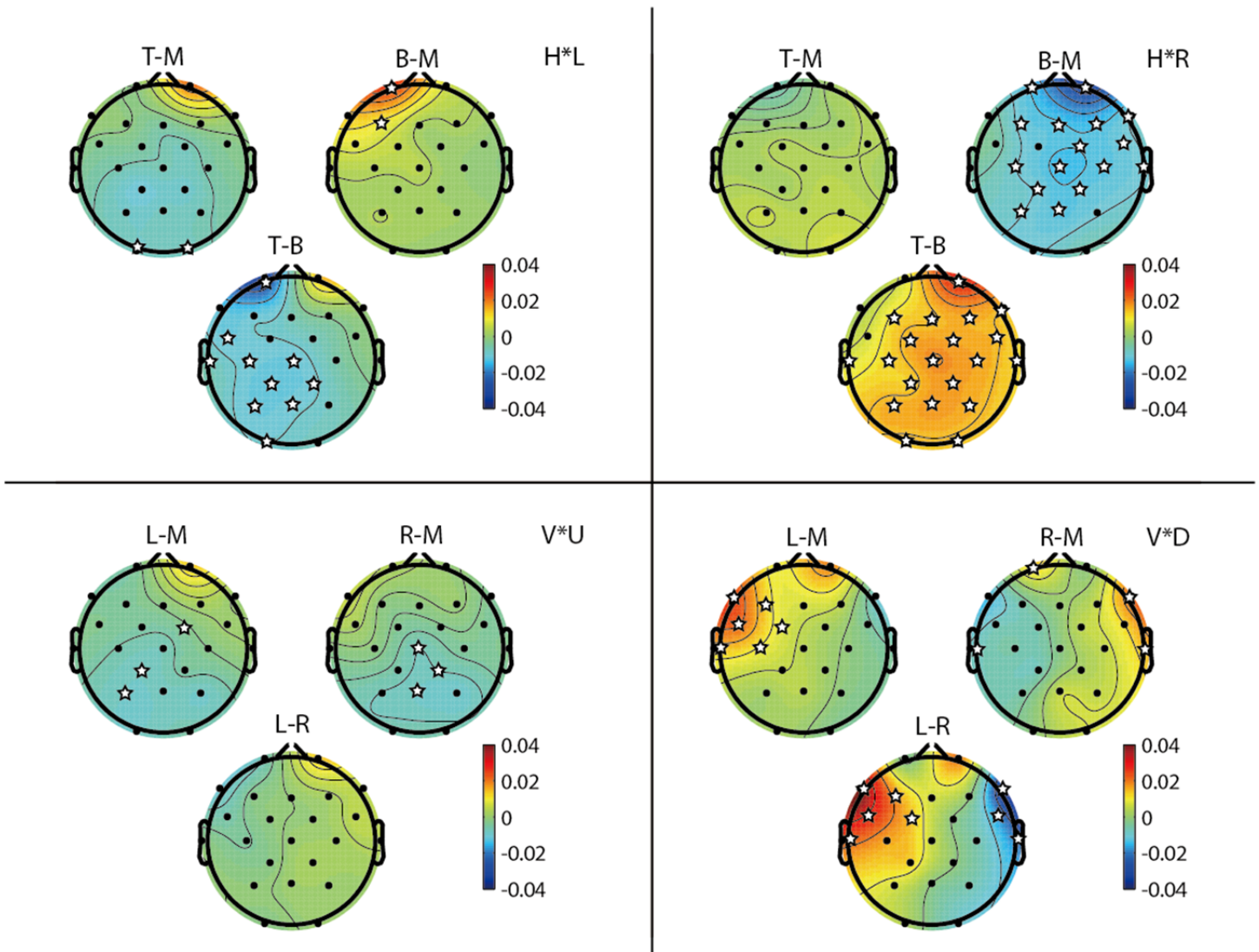
Figure 5.10 Topographic maps of coefficient difference classified by four groups horizontal/vertical and leftward/rightward conditions.

5.4 Discussion

The main aim of the present study is to clarify the influence of eye movement related artifacts to EEG measurements of human subjects who were requested to perform a direction-viewing area depending saccade task. We proposed twelve conditions (abbreviated as H(T/M/B)(R/L) in the horizontal eye movement and V(L/M/R)(U/D) in

the vertical eye movement) to examine a comprehensive set of direction and viewing areas. In the self-paced fixation-and-saccades task, EOG influences differentiated in individual EEG channels when taking viewing area and eye movement direction into account at the same time.

	H*L			H*R			V*U			V*D		
	T-M	B-M	T-B	T-M	B-M	T-B	L-M	R-M	L-R	L-M	R-M	L-R
O1	**-3.70**	0.47	**-4.40**	1.07	**-3.37**	**4.64**	-2.08	**-2.70**	-0.68	0.30	-0.42	0.48
O2	**-5.37**	0.06	**-2.76**	**3.17**	**-3.03**	**5.75**	-1.97	**-2.42**	0.22	-0.52	1.79	-2.26
P3	**-3.22**	1.46	**-3.84**	**2.38**	**-5.17**	**6.51**	**-3.69**	**-3.32**	-0.62	0.41	-1.37	1.71
Pz	**-2.93**	1.25	**-3.58**	2.09	**-5.14**	**5.19**	**-2.79**	**-4.20**	0.41	1.03	1.11	-0.38
P4	**-3.08**	0.81	**-2.93**	2.00	**-3.15**	**4.83**	**-2.69**	**-3.30**	0.41	-0.28	0.91	-1.39
CP1	**-3.27**	0.61	**-3.88**	0.68	**-4.69**	**3.75**	**-3.82**	**-3.01**	-1.12	1.21	-1.50	2.31
CP2	**-2.62**	0.41	**-3.88**	1.30	**-5.16**	**5.02**	-1.97	**-5.02**	1.10	0.32	0.56	-0.22
T7	-1.24	1.55	**-4.43**	0.83	**-3.09**	**3.88**	-1.99	-0.91	-0.70	**5.39**	**-4.29**	**6.83**
C3	-2.21	1.98	**-5.52**	0.66	**-4.36**	**4.29**	**-2.73**	-1.20	-1.95	**3.59**	-1.15	**3.26**
Cz	-2.02	**2.90**	**-3.65**	1.20	**-5.04**	**5.50**	**-3.21**	**-5.64**	0.20	1.25	-0.52	1.97
C4	-2.05	-0.01	**-2.38**	1.13	**-5.03**	**5.21**	-1.15	**-3.45**	0.59	-0.45	1.32	-1.45
T8	-1.31	-0.99	-0.58	0.53	**-9.19**	**3.81**	0.20	-1.59	**2.40**	-2.24	**3.78**	**-4.59**
FC5	-1.22	**3.35**	**-5.03**	0.82	-1.90	**2.73**	-1.87	0.79	-1.40	**3.50**	-2.20	**5.10**
FC1	-1.04	**2.45**	-2.27	1.17	**-3.46**	**5.13**	-1.67	**-2.45**	-0.52	**3.74**	**-2.73**	**3.86**
FC2	-1.37	0.11	-2.08	0.80	**-4.11**	**4.97**	**-4.12**	-1.42	0.02	0.72	1.44	-0.34
FC6	-0.98	-0.27	-0.98	1.87	**-6.65**	**9.62**	0.37	**-2.54**	2.17	-1.65	**2.77**	**-3.76**
F7	0.50	**2.37**	**-2.71**	-0.39	-1.98	0.63	-1.30	1.37	-1.77	**5.24**	**-2.87**	**6.47**
F3	-0.42	**3.94**	**-3.38**	-0.10	**-3.98**	**3.64**	-1.51	-0.39	-1.11	**3.97**	**-2.64**	**3.60**
Fz	-1.04	0.65	**-2.50**	0.19	**-5.17**	**4.83**	-0.94	-1.29	-0.29	1.69	0.01	1.27
F4	-0.02	1.13	-0.79	0.67	**-7.27**	**6.64**	1.17	0.05	0.85	1.72	2.10	-0.15
F8	0.40	0.24	0.18	2.32	**-6.14**	**5.72**	0.14	-1.33	2.02	-2.08	**5.20**	**-4.87**
FP1	-0.19	**4.41**	**-4.26**	-0.88	**-5.46**	1.20	-1.55	0.73	-1.36	1.80	**4.01**	-0.46
FP2	1.50	1.32	0.91	0.47	**-8.40**	**8.48**	2.13	0.02	1.56	**2.90**	-0.18	2.03

Table 1: Pairwise T-values of coefficient difference ($t(7) > 2.3646$; $p < 0.05$). Numbers in bold fonts represented channels/condition with significant difference.

1) Eye movement specificity in the EOG generation

With respect to the morphology of eyeballs and extraocular muscles with nervous controls, eye movement kinematics were modeled with three dimensional properties with horizontal, vertical and radial/torsional axes in a gain control model [99] and three-dimensional kinematics of saccadic and pursuit eye movements [98] which demonstrated all those eye movements can be projected to a horizontal-vertical plane with less interference of torsional changes.   The internal cornea-retinal potential was estimated as a range of 10-30mV [57][71] and recorded as less than 1mV using the skin-surface electrode as EOG recording [72][73]. Even in the millivolt range, it causes a large impact to EEG measurements to be a dominant noise source [22][25][58][61]. The eye movement angle was linearly correlated with the staying EOG potential in a specific range such as less than 30-40° [73], whereas potential fluctuation during saccade and pursuit movements have a dynamic property according to interaction with eyelids [100][101]. For a simplification and phenomenological treatment, the influence of EOGs traditionally were treated by a 3D dipole model of eye movement theoretically [22][25][61] or removed by using multiple EOG channels to enhance the ICA accuracy [102]. In the present study, the experimental design focused on the influence with respect to the specificity in eyeball rotations (the change in orientation of the corneo-retinal dipoles, and extended to a larger framework contains various viewing field conditions. In a preliminary stage, Plöchl et al. [68] investigated the EOG influence in the saccade task. According to their results, the topographic pattern difference did not show any significance between large (~23°) and small (~11.5°) saccadic movement in the same saccade directions, while differences in and upward/downward directions appeared significantly.   In the systematic framework by

combining direction and viewing area, we found a zone-of-gaze sensitivity property of the artifacts, which were demonstrated both in the propagation coefficient and ERP topographic distribution. As a new finding, the differences among top/middle/bottom viewing areas in the horizontal movements were revealed in the coefficient value. The difference value varied from 0.04 to -0.04 as a 10% of the original range of coefficient values, which was estimated as 20μV from the average HEOG amplitude. The same tendency was observed in the difference among left/middle/right viewing areas in the vertical downward movement; however such a difference is negligible in the vertical upward movement. On the particularity of the upward movement, the interaction of eyeballs and eyelids is the plausible candidate to concern. In Plöchl's research [68], they also investigated blink and saccade-related eyelid artifacts. They suggested that two types of artifacts were generated by the same mechanism, and suggested those two kinds of eyelid sliding over the cornea produces the same scalp topography (the typical blink topographic pattern). In the present analyses, we did not treat the eye blinks and eyelid interactions in the model.

2) Possible improvements to artifact correction methods

The effect of viewing area sensitive EOG influence on EEG signals has non-negligible impact on past artifact correction methods. Most of the methods known as regression based methods [22] and component based methods like ICA [83] rely on the mathematical background of the signal processing with less considerations of the cornea-retinal potential change depending eyeball rotations and eyelid interactions. Currently, the eye-tracking system exhibits a high-specification including a 500 Hz sampling rate close to that of the EEG recording system, easily offering an effective

combined analysis [68][103]. Even without EOG recordings, a high-spec eye tracking system detect eyeball rotations and eye blinks accurately, which is used for estimation of the EOG information, opening a new potential of EEG recordings for engineering purposes [3][67].

Combining with the EEG correction methods, even for ICA which has been frequently used for ocular artifact correction [26], the idea of separating coefficient calculations depending the viewing area may improves the accuracy by approximately 10%, without any conflict to the original calculation process. Hopefully, this strategy may be applied to any traditional methods that use fixed propagation coefficients, without only being constrained to regression-based methods and ICA. For simplification of the experimental procedure to test our hypothesis, we segregated three viewing areas horizontally and vertically. This potential can be extended to EEG measurements in the free viewing task and engineering applications of the brain-machine-interface (BCI), by coupling with eye tracking method such as EOG [104] or eye-tracker.

3) Theoretical aspect of the zone-of-gaze sensitivity in the artifact correction

Removing ocular artifacts by adaptive filtering was discussed in contaminated signals of EEG and MEG [105][106][107]. He et al. [108] formulated an adaptive filter with VEOG and HEOG components. Originally the adaptive filter was a generalized method to remove noise from a time-varying signal by using a linear filter with the transfer function defined by finite impulse response (FIR) filters in the concept of the linear model that the signal and noise sources are linearly combined [92][109]. Well-known adaptive filters are the Kalman filter [110], the least mean square (LMS) filter and the recursive least square (RLS) filter [92][109]. The ocular artifact removal

method proposed by He et al. [108] is described with the recorded signal $s(t) = x(t) + z(t)$ where signal $x(t)$ and ocular artifacts $z(t)$ and then error $e(t)$ is defined using FIR filters based on the RLS algorithm as:

$$e(t) = s(t) - \hat{r}_v(t) - \hat{r}_h(t) = x(t) + \left(z(t) - \hat{r}_v(t) - \hat{r}_h(t) \right), \tag{3-26}$$

$$\hat{r}_v(t) = \sum_{m=1}^{M} h_v(m) \cdot r_v(t - m + 1), \tag{3-27}$$

$$\hat{r}_h(t) = \sum_{m=1}^{M} h_h(m) \cdot r_h(t - m + 1). \tag{3-28}$$

where r_v and r_h are VEOG(t) and HEOG(t) respectively. Filter coefficients h_v and h_h are calculated through a minimization of $E[e^2] = E[x^2] + E[(z - \hat{r}_v - \hat{r}_h)^2]$, or $E[(z - \hat{r}_v - \hat{r}_h)^2]$. of $M = 1$ is equivalent to the simple time-domain regression method [23][111]. Theoretically, the selection of M is determined by the characteristics of the EOG–EEG transfer function, and He *et al.* [108] demonstrated that filtering method with the condition of $M > 1$ showed a better performance than that of $M = 1$, which was accompanied with extensive computational cost to obtain target coefficients in recursive calculations determined by M. Finally they concluded that $M = 3$ was suitable in their experimental data. Interestingly, this time-domain regression method can be reconsidered in the viewpoint of the spatial-domain method, and in this sense our result represents a spatial-domain regression method that is categorized in the eye movement direction. In the viewpoint of adaptive filtering methods [92][108][110][112], two dimensional adaptive filter algorithms for image processing have been proposed [113]–[115] by applying the original method of time-varying signals to the spatially-varying information. However, in the consideration of our results, the

combination of the direction specificity and viewing area is crucial for applications to adaptive filtering methods, which need to be treated in multiple layers depending on individual eye movement directions, i.e. direction selective multi-layered spatial adaptive filters. Multi-layered adaptive filters were discussed covering with the learning mechanism of the artificial neural network [116]–[118] yet those were still in the mathematical framework.

Chapter 6   Performance improvement of artifact removal with ocular information

In the previous chapters, the influences from zone-of-gaze or view-field and the way to estimate it were discussed. The biggest difference of in-lab neuroscience researches and free-viewing daily EEG applications can be represented as the level of constraint to eye movements. Traditional methods are able to do the work with respect to a well constrained eye movement condition. However, they never hold the same when being performed in a free-viewing condition. Like showing below, the eye movements taking place out of the center view-field may cause biases in brain activities related EEG estimated (corrected EEG). Here we evaluate the performance improvement from the experimental result obtain from chapter 5.
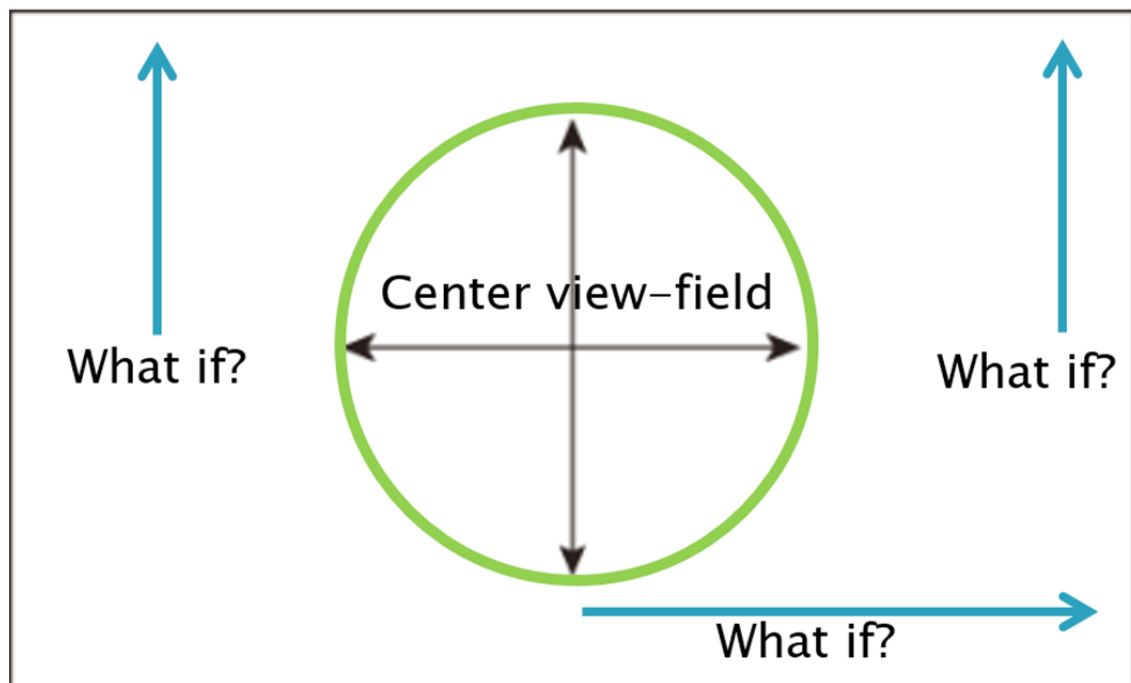

Figure 6.1 Eye movements under different conditions

To evaluate the EOG artifact correction using the specificity of viewing areas and eye movement direction as we focused in this work, the leave-one-out cross-validation method was introduced.

Under each condition, by using the N proper dataset, propagation coefficients of the linear regression were calculated from the $N-1$ dataset and applied to the trial left out. Depending on which trial was left, results of N sets was obtained and then they were used to validate how much EOG influence remains in EEG data after the artifact correction. By connecting corrected N EEG time series in a successive manner and N corresponding EOG time series in the same way, a single value of the correlation coefficient (CC) was calculated by the two time series of the connected N corrected EEG and the corresponding EOG time series.

Therefore, the CC can be used for a measure to evaluate how much EOG influence remains, varying from 0 to 1. Thus, 0 and 1 respectively represent no correlation between corrected EEG and EOG and a high correlation between them. We defined 'proposed method' as the result of the leave-one-out cross-validation and 'normal method' as the consistent procedure applied to the same target EEG signal, but using propagation coefficients obtained from the dataset of the center fixation condition. In every channel and each condition, we finally obtained individual CC form the corrected EEG with the EOG in the proposed method and individual CC for the normal method correspondingly. In other words, the proposed method means EEG corrections calibrated with data of task-sensitive fixation positions. In comparison between the proposed and normal methods, the pairwise T-test over 8 subjects was analyzed after the Fisher's Z-transformation of two sets of CCs for subjects.

Figure 6.2 and 6.3 exhibited an averaged CC (inversed Z-value) over all subjects in every EEG channel in cases of horizontal and vertical conditions, respectively. The figure was highlighted by gray background colors representing ERP absolute amplitudes in corresponding channels as shown in Figure 5.8 under horizontal conditions, the significant difference between proposed and normal methods appeared at lateral 14 channels in leftward eye movements and 21 channels in rightward eye movements [t(7)>3.499; p<0.01]. In comparison between two methods, the difference of CC values in those channels was about 0.1 in average (0.099 in HTL&HBL and 0.093 in HTR&HBR), which can be estimated as 10% of the EOG influence, such as $\pm\, 5\mu V$ in EEG signals if the maximum range of the EOG influence is $\pm\, 50\mu V$. In the same manner, under vertical conditions, the significant difference appeared in 12 channels distributed from parietal to occipital areas in the case of upward eye movements, whereas lateral 12 channels distributed from frontal to parietal areas in the case of downward eye movements. The difference of CC values in those channels was about 0.08 (0.071 in VLU&VRU and 0.093 in VLD&VRD) because of relatively weak differences in the upward case.

These results indicate that fixation position dependent EOG influences are exhibited at propagation coefficients and then the cross-validation based evaluation represents an improvement of the traditional method when the proposed concept is applied to the EEG artifact correction. In the case of the linear regression by using the proposed method, 10% accuracy improvements can be estimated in areas including channels marked in Figure 6.4.
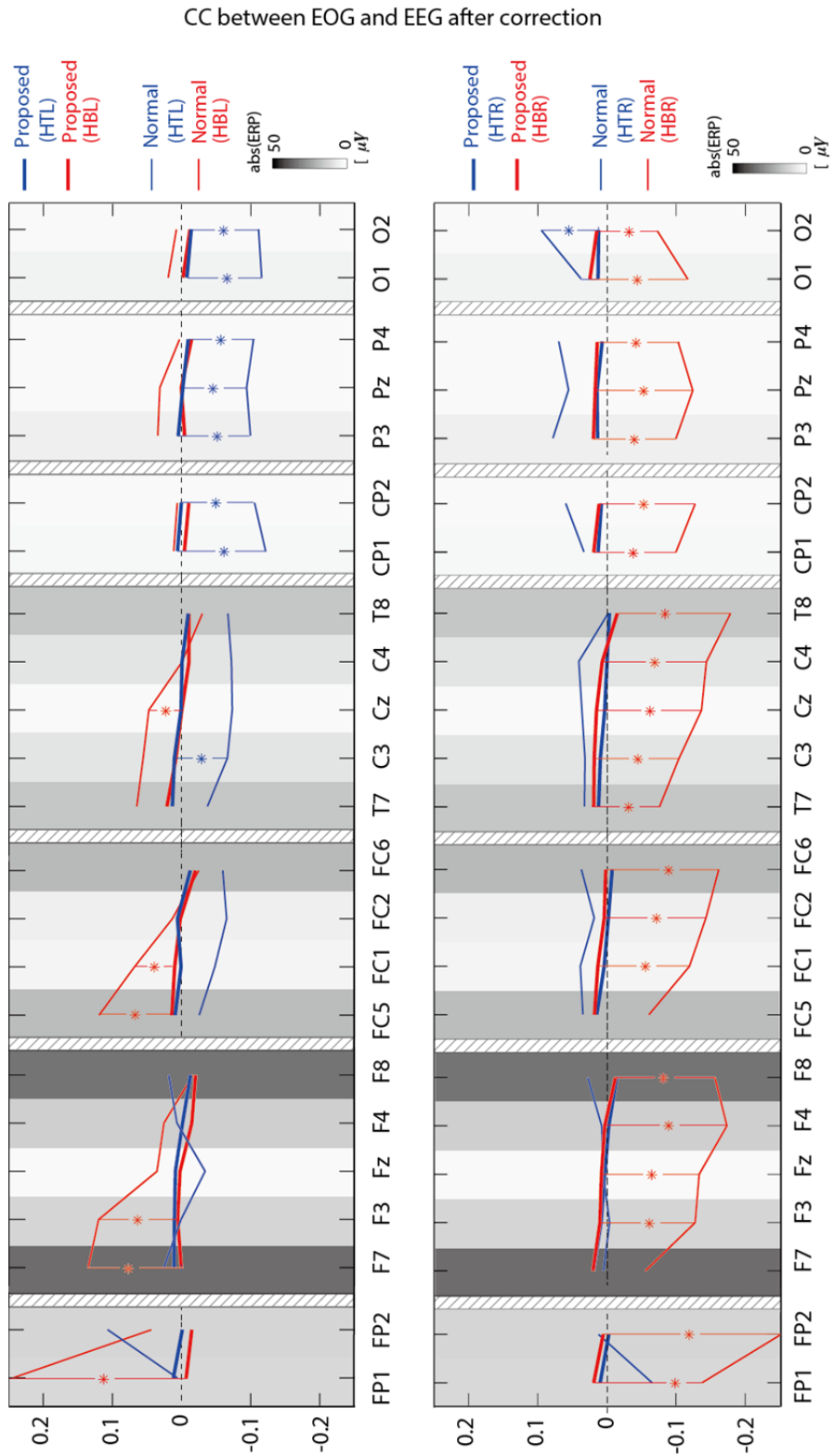
Figure 6.2 Correlation coefficients between proposed methods and traditional methods (horizontal conditions)
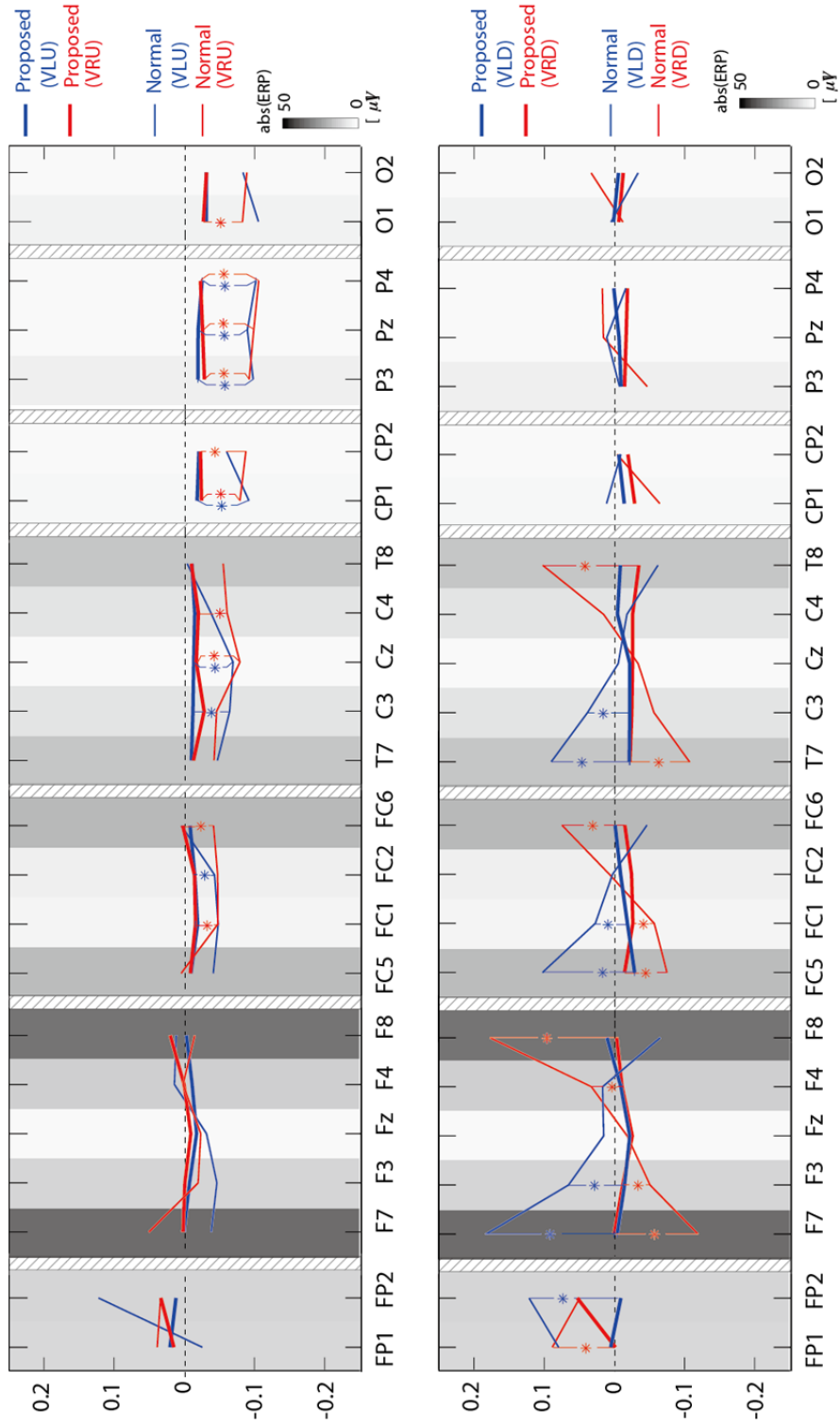
Figure 6.3 Correlation coefficients between proposed methods and traditional methods (conditions
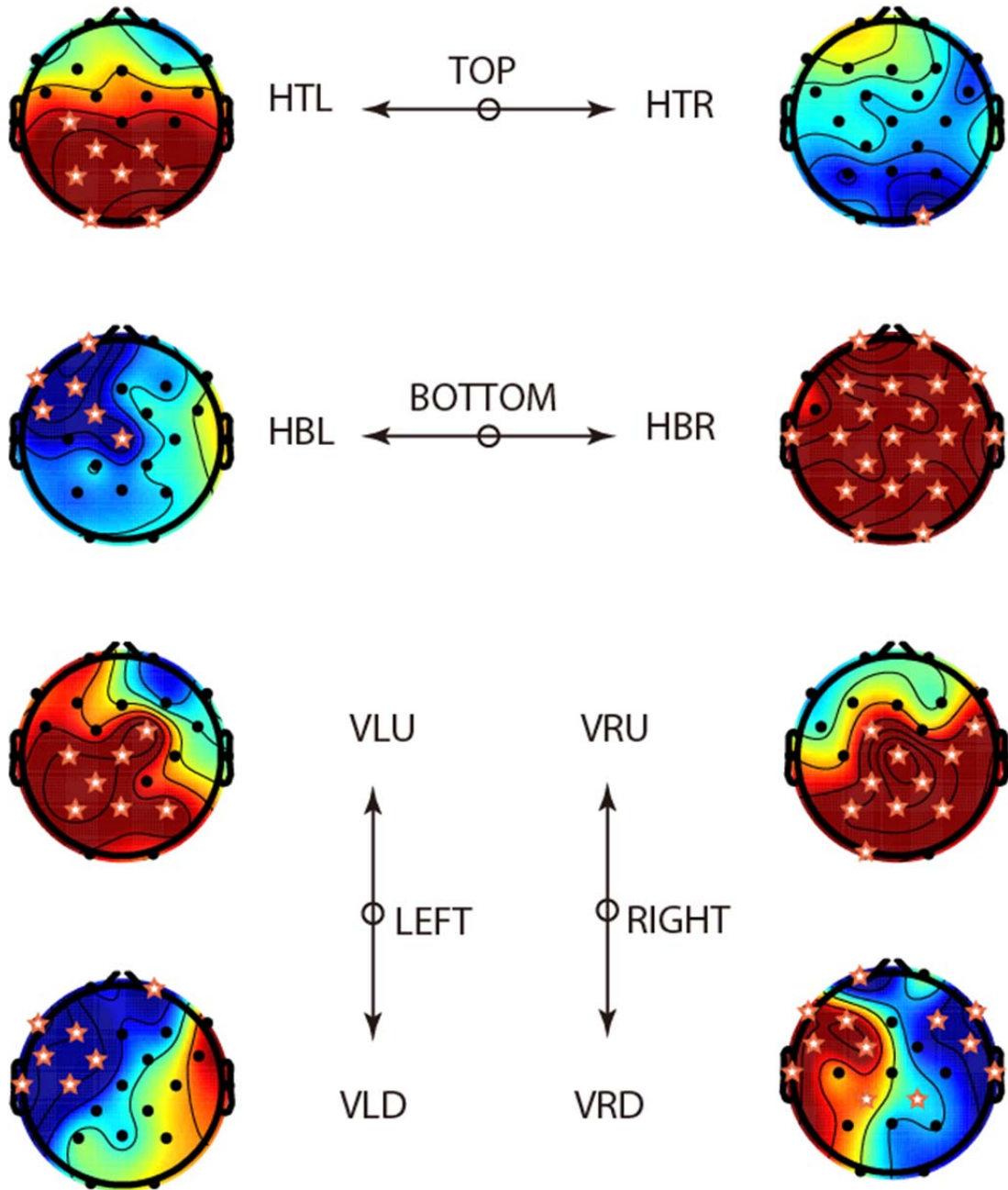
vertical)

Figure 6.4 Electrode locations with significant difference between proposed method and traditional method

In case of the difference between view-field located on opposite sides, the situation becomes more serious as shown in Figure 6.5.
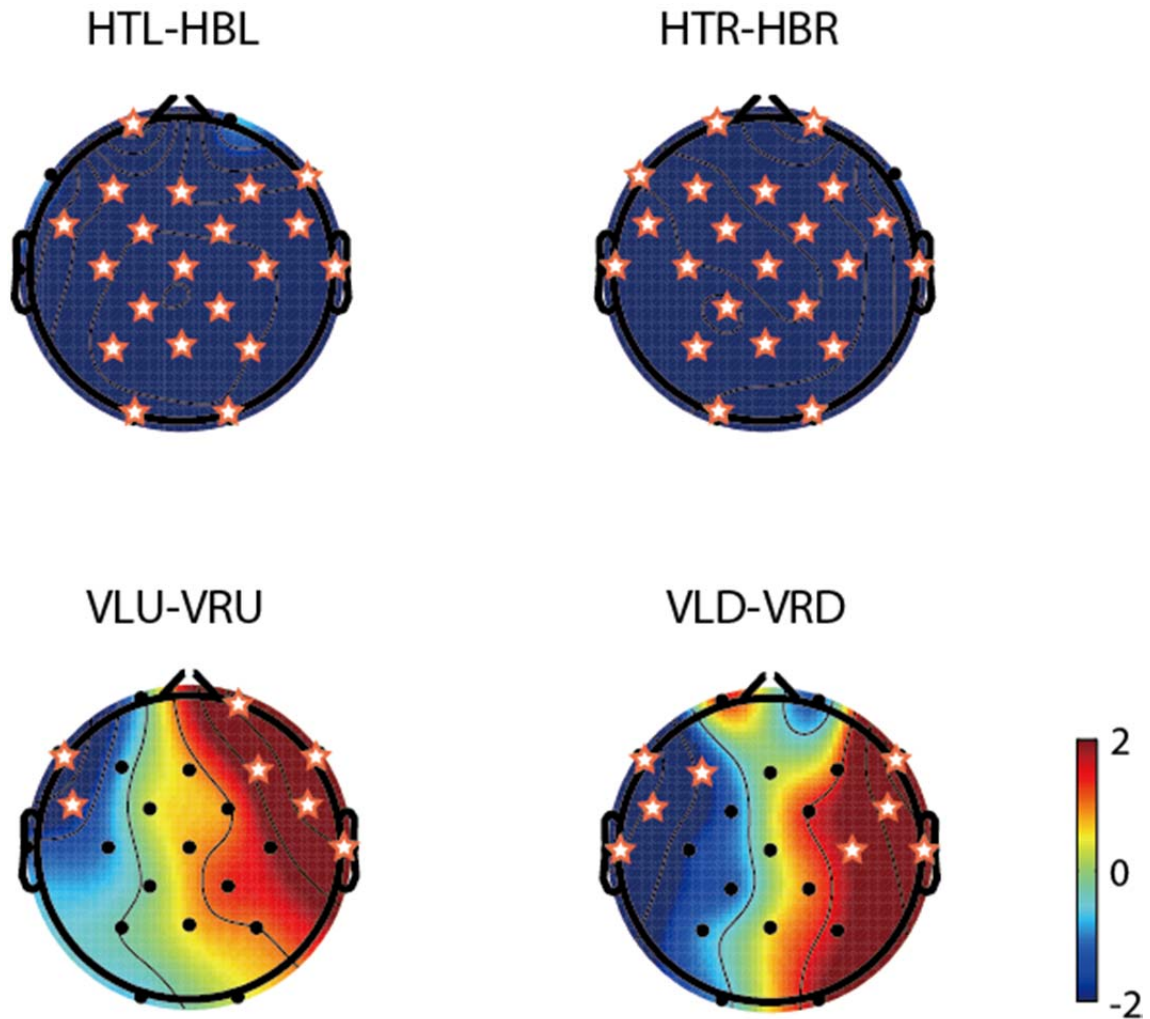
Figure 6.5 Electrode locations with significant difference between opposite sides (color-bar: t-value)

These results confirmed our hypothesis again that when eye movement took place in varied view-field, the propagation coefficient would have significant changes. Furthermore, it also implies the risks of topographic changes when using component based methods. In other word, the stationarity attained (e.g. using high pass filter and well-epoch strategies) actually could not solve this spatial propagation-changes, hence may fail to correct EEG by rejecting one constant topographic pattern for one eye movement type (i.e. horizontal or vertical).

Another conclusion can suggested by Figure 6.5 is that the significance is related to

the angular distance between conditions. When the angular distance increases, the difference gets greater. Note that, it doesn't mean the significance exists when only small angular changes happens. Thus, a reasonable choice for free-viewing EEG applications is to divide the whole view-fields into several zones, for instance a 3-by-3 zones, and obtain propagation coefficients respectively by calibrations. Then, by combining ocular information (e.g. start position and end positions saccades) a stronger ocular artifact removal method can be implemented.

Chapter 7   Summary

In the present study, we hypothesized the existence of direction and viewing area-sensitive EOG influence in the EEG topographic pattern and investigated the influence of eye movement related artifacts in the direction/viewing area depending saccade task. This was evaluated using the systematic protocol to evaluate the dependency by focusing on the coupling effect of eye-movement direction and viewing area and testifying in the framework of the linear regression analysis for EOG corrections. In our experimental results, ERP topographic patterns to evaluate EOG influences in the EEG head map were observed as a reversal structure in the coupling condition between horizontal-rightward and –leftward eye movements and consistently in the coupling condition between vertical-upward and –downward eye movement. Surprisingly, EOG influences are different in comparison between top-viewing and bottom-viewing areas in the horizontal movement condition and consistently are different between right-viewing and left-viewing areas in the vertical movement condition. The result demonstrated that the propagation coefficients were affected differently by the EOG changes depending on viewing fields and the eye movement directions, suggesting the non-trivial contribution to the EOG artifact removal if the coefficient identification is done separately depending on the coupling condition of the viewing area and its direction. Our results indicate that direction and viewing area-sensitive influence of EOG artifacts exhibits in properties appropriate for removing eyeball rotation related artifacts in the context of a visual saccade task. This fact has an impact to past ocular artifact corrections using the constant coefficients in the sense of a possibility of improvements as presumably 10% better performance, which will

contribute to free viewing EEG task availability with frequent eye movements. Our results also enlightened the coming ocular artifact removal/suppression algorithm developments in the future for free-viewing EEG applications.

References

[1]   L. Angell, J. Auflick, P. A. Austria, D. Kochhar, L. Tijerina, W. Biever, T. Diptiman, J. Hogsett, and S. Kiger, "Driver workload metrics task 2 final report - Appendices," *Natl. Highw. Traffic Saf. Adm.*, no. November, 2006.

[2]   T. A. Dingus, S. G. Klauer, V. L. Neale, A. Petersen, S. E. Lee, J. Sudweeks, M. A. Perez, J. Hankey, D. Ramsey, S. Gupta, C. Bucher, Z. R. Doerzaph, J. Jermeland, and R. R. Knipling, "The 100-car naturalistic driving study phase II – Results of the 100-car field experiment," *Chart*, no. April, p. No. HS–810 593, 2006.

[3]   G. Borghini, L. Astolfi, G. Vecchiato, D. Mattia, and F. Babiloni, "Measuring neurophysiological signals in aircraft pilots and car drivers for the assessment of mental workload, fatigue and drowsiness," *Neurosci. Biobehav. Rev.*, vol. 44, pp. 58–75, 2014.

[4]   M. Matousek and I. Petersen, "A method for assessing alertness fluctuations from EEG spectra," *Electroencephalogr. Clin. Neurophysiol.*, vol. 55, no. 1, pp. 108–113, 1983.

[5]   A. S. Gevins, S. L. Bressler, B. A. Cutillo, J. Illes, J. C. Miller, J. Stern, and H. R. Jex, "Effects of prolonged mental work on functional brain topography," *Electroencephalogr. Clin. Neurophysiol.*, vol. 76, no. 4, pp. 339–350, 1990.

[6]   S. Makeig and T. P. Jung, "Changes in alertness are a principal component of variance in the EEG spectrum," *Neuroreport*, vol. 7, no. 1, pp. 213–6, 1995.

[7]   S. Makeig and M. Inlow, "Lapses in alertness: coherence of fluctuations in performance and EEG spectrum," *Electroencephalogr. Clin. Neurophysiol.*, vol. 86, no. 1, pp. 23–35, 1993.

[8]   A. Gale, R. Davies, and A. Smallbone, "EEG correlates of signal rate, time in task and individual differences in reaction time during a five-stage sustained attention task," *Ergonomics*, vol. 20, no. 4, pp. 363–367, 1977.

[9]   O. G. Okogbaa, R. L. Shell, and D. Filipusic, "On the investigation of the neurophysiological correlates of knowledge worker mental fatigue

using the EEG signal," *Appl. Ergon.*, vol. 25, no. 6, pp. 355–365, 1994.

[10] S. H. Fairclough and L. Venables, "Prediction of subjective states from psychophysiology: A multivariate approach," *Biol. Psychol.*, vol. 71, no. 1, pp. 100–110, 2006.

[11] P. Sauseng, W. Klimesch, R. Freunberger, T. Pecherstorfer, S. Hanslmayr, and M. Doppelmayr, "Relevance of EEG alpha and theta oscillations during task switching," *Exp. Brain Res.*, vol. 170, no. 3, pp. 295–301, 2006.

[12] M. A. S. Boksem, T. F. Meijman, and M. M. Lorist, "Effects of mental fatigue on attention : An ERP study," *Time*, vol. 25, no. 1, pp. 107 – 116, 2005.

[13] S. H. Fairclough, L. Venables, and A. Tattersall, "The influence of task demand and learning on the psychophysiological response," *Int. J. Psychophysiol.*, vol. 56, no. 2, pp. 171–184, 2005.

[14] M. Doppelmayr, T. Finkenzeller, and P. Sauseng, "Frontal midline theta in the pre-shot phase of rifle shooting: Differences between experts and novices," *Neuropsychologia*, vol. 46, no. 5, pp. 1463–1467, 2008.

[15] S. M. Slobounov, K. Fukada, R. Simon, M. Rearick, and W. Ray, "Neurophysiological and behavioral indices of time pressure effects on visuomotor task performance," *Brain Res. Cogn. Brain Res.*, vol. 9, no. 3, pp. 287–98, 2000.

[16] S. K. L. Lal and A. Craig, "A critical review of the psychophysiology of driver fatigue," *Biol. Psychol.*, vol. 55, no. 3, pp. 173–194, 2001.

[17] A. Steptoe and D. Macready, "Negative transfer of heart rate control following biofeedback training: a partial replication," *Biofeedback Self. Regul.*, vol. 10, no. 3, pp. 269–74, Sep. 1985.

[18] S. A. Grossman, V. R. Sheidler, K. Swedeen, J. Mucenski, and S. Piantadosi, "Correlation of patient and caregiver ratings of cancer pain," *J. Pain Symptom Manage.*, vol. 6, no. 2, pp. 53–7, 1991.

[19] G. F. Wilson and F. Fisher, "The use of cardiac and eye blink measures to determine flight segment in F4 crews," *Aviat. Sp. Environ. Med.*, vol. 62, no. 10, pp. 959–962, 1991.

[20] G. F. Wilson, "Air-to-ground training missions: A psychophysiological workload analysis," *Ergonomics*, vol. 36, no. 9, pp. 1071–1087, 1993.

[21] J. B. Brookings and J. F. Wilson, "Personality and family-environment

predictors of self-reported eating attitudes and behaviors," *J. Pers. Assess.*, vol. 63, no. 2, pp. 313–326, 1994.

[22] R. J. Croft and R. J. Barry, "Removal of ocular artifact from the EEG: A review," *Neurophysiol. Clin.*, vol. 30, no. 1, pp. 5–19, 2000.

[23] G. Gratton, M. G. Coles, and E. Donchin, "A new method for off-line removal of ocular artifact," *Electroencephalogr. Clin. Neurophysiol.*, vol. 55, no. 4, pp. 468–84, Apr. 1983.

[24] G. Gratton, "Dealing with artifacts: The EOG contamination of the event-related brain potential," *Behav. Res. Methods, Instruments, Comput.*, vol. 30, no. 1, pp. 44–53, 1998.

[25] A. Schlögl, C. Keinrath, D. Zimmermann, R. Scherer, R. Leeb, and G. Pfurtscheller, "A fully automated correction method of EOG artifacts in EEG recordings," *Clin. Neurophysiol.*, vol. 118, no. 1, pp. 98–104, 2007.

[26] J. A. Urigüen and B. Garcia-Zapirain, "EEG artifact removal state-of-the-art and guidelines," *J. Neural Eng.*, vol. 12, no. 3, p. 31001, 2015.

[27] H. D. Lux, "Neurophysiological basis of the EEG and DC potentials," *Electroencephalogr. Basic Princ. Clin. Appl. Relat. Fields*, pp. 24–28, 1981.

[28] R. Kuś, M. Kamiński, and K. J. Blinowska, "Determination of EEG activity propagation: pair-wise versus multichannel estimate," *IEEE Trans. Biomed. Eng.*, vol. 51, no. 9, pp. 1501–10, Sep. 2004.

[29] H. Aurlien, I. O. Gjerde, J. H. Aarseth, G. Eldøen, B. Karlsen, H. Skeidsvoll, and N. E. Gilhus, "EEG background activity described by a large computerized database," *Clin. Neurophysiol.*, vol. 115, no. 3, pp. 665–673, 2004.

[30] E. Kirmizi-Alsan, Z. Bayraktaroglu, H. Gurvit, Y. H. Keskin, M. Emre, and T. Demiralp, "Comparative analysis of event-related potentials during Go/NoGo and CPT: decomposition of electrophysiological markers of response inhibition and sustained attention," *Brain Res.*, vol. 1104, no. 1, pp. 114–28, 2006.

[31] H. Zhang and J. Jacobs, "Traveling theta waves in the human hippocampus," *J. Neurosci.*, vol. 35, no. 36, pp. 12477–87, Sep. 2015.

[32] Z. Shi, X. Gao, and R. Zhou, "Frontal theta activity during working memory in test anxiety," *Neuroreport*, vol. 26, no. 4, pp. 228–232, 2015.

[33] A. Maglione, G. Borghini, P. Aricò, F. Borgia, I. Graziani, A. Colosimo,

W. Kong, and G. Vecchiato, "Evaluation of the workload and drowsiness during car driving by using high resolution EEG activity and neurophysiologic indices," *Eng. Med. Biol. Soc.*, pp. 6238–6241, 2014.

[34] G. Luca, J. Haba Rubio, D. Andries, N. Tobback, P. Vollenweider, G. Waeber, P. Marques Vidal, M. Preisig, R. Heinzer, and M. Tafti, "Age and gender variations of sleep in subjects without sleep disorders," *Ann. Med.*, vol. 47, no. 6, pp. 482–491, 2015.

[35] B. Van Hal, S. Rhodes, B. Dunne, and R. Bossemeyer, "Low-cost EEG-based sleep detection," *IEEE Eng. Med. Biol. Soc. Annu. Conf.*, vol. 2014, pp. 4571–4, 2014.

[36] T. P. Rao, M. Ozeki, and L. R. Juneja, "In search of a safe natural sleep aid," *J. Am. Coll. Nutr.*, vol. 34, no. 5, pp. 1–12, 2015.

[37] E. H. S. Choy, "The role of sleep in pain and fibromyalgia," *Nat. Rev. Rheumatol.*, pp. 1–8, 2015.

[38] D. Neu, O. Mairesse, P. Verbanck, P. Linkowski, and O. Le Bon, "Non-REM sleep EEG power distribution in fatigue and sleepiness," *J. Psychosom. Res.*, vol. 76, no. 4, pp. 286–91, Apr. 2014.

[39] J.-L. Zhang, J. Li, G. Meng, and M.-G. Li, "Study on fatigue of pilots during simulated flight training based on electroencephalogram," *Chinese J. Appl. Physiol.*, vol. 29, no. 3, p. 267—270, 2013.

[40] A. Kalauzi, A. Vuckovic, and T. Bojić, "Topographic distribution of EEG alpha attractor correlation dimension values in wake and drowsy states in humans," *Int. J. Psychophysiol.*, vol. 95, no. 3, pp. 278–91, 2015.

[41] B. W. Hsu, M. J. J. Wang, C. Y. Chen, and F. Chen, "Effective indices for monitoring mental workload while performing multiple tasks," *Percept. Mot. Skills*, vol. 121, no. 1, pp. 94–117, Aug. 2015.

[42] R. Luijcks, C. J. Vossen, H. J. Hermens, J. van Os, and R. Lousberg, "The influence of perceived stress on cortical reactivity: A proof-of-principle study," *PLoS One*, vol. 10, no. 6, p. e0129220, 2015.

[43] L. Sherlin, F. Muench, and S. Wyckoff, "Respiratory sinus arrhythmia feedback in a stressed population exposed to a brief stressor demonstrated by quantitative EEG and sLORETA," *Appl. Psychophysiol. Biofeedback*, vol. 35, no. 3, pp. 219–228, 2010.

[44] L. F. H. Basile, "Complex, multifocal, individual-specific

attention-related cortical functional circuits," *Biol. Res.*, vol. 40, no. 4, pp. 451–70, 2007.

[45] M. Corsi-Cabrera, Z. Muñoz-Torres, Y. del Río-Portilla, and M. A. Guevara, "Power and coherent oscillations distinguish REM sleep, stage 1 and wakefulness," *Int. J. Psychophysiol.*, vol. 60, pp. 59–66, 2006.

[46] F. Cassim, W. Szurhaj, H. Sediri, D. Devos, J. Bourriez, I. Poirot, P. Derambure, L. Defebvre, and J. Guieu, "Brief and sustained movements: Differences in event-related (de)synchronization (ERD/ERS) patterns," *Clin. Neurophysiol.*, vol. 111, no. 11, pp. 2032–9, Nov. 2000.

[47] D. J. McFarland and J. R. Wolpaw, "Sensorimotor rhythm-based brain-computer interface (BCI): feature selection by regression improves performance," *IEEE Trans. neural Syst. Rehabil. Eng.*, vol. 13, no. 3, pp. 372–9, Sep. 2005.

[48] D. J. Mcfarland, W. A. Sarnacki, and J. R. Wolpaw, "Brain computer interface (BCI) operation : Optimizing information transfer rates," vol. 63, no. 3, pp. 237–251, 2003.

[49] R. Ortner, D. C. Irimia, J. Scharinger, and C. Guger, "A motor imagery based brain-computer interface for stroke rehabilitation," *Stud. Health Technol. Inform.*, vol. 181, pp. 319–323, 2012.

[50] L. Michels, K. Bucher, R. Lüchinger, P. Klaver, E. Martin, D. Jeanmonod, and D. Brandeis, "Simultaneous EEG-fMRI during a Working Memory Task: Modulations in Low and High Frequency Bands," *PLoS One*, vol. 5, no. 4, p. e10298, 2010.

[51] T. I. Laine, K. W. Bauer, J. W. Lanning, C. A. Russell, and G. F. Wilson, "Selection of input features across subjects for classifying crewmember workload using artificial neural networks," *IEEE Trans. Syst. Man, Cybern. Part ASystems Humans.*, vol. 32, no. 6, pp. 691–704, 2002.

[52] F. Babiloni, F. Cincotti, D. Mattia, M. Mattiocco, S. Bufalari, F. De Vico Fallani, A. Tocci, L. Bianchi, M. G. Marciani, V. Meroni, and L. Astolfi, "Neural basis for the brain responses to the marketing messages: An high resolution EEG study," *Annu. Int. Conf. IEEE Eng. Med. Biol. - Proc.*, pp. 3676–3679, 2006.

[53] G. Li, B. Lee, and W. Chung, "Smartwatch-based wearable EEG system for driver drowsiness detection," *IEEE Sens. J.*, vol. 15, no. 12,

pp. 7169–7180, 2015.

[54] T. Nakano, H. Watanabe, F. Homae, and G. Taga, "Prefrontal cortical involvement in young infants' analysis of novelty," *Cereb. Cortex*, vol. 19, no. 2, pp. 455–463, 2009.

[55] M. A. Jatoi, N. Kamel, A. S. Malik, I. Faye, and T. Begum, "A survey of methods used for source localization using EEG signals," *Biomed. Signal Process. Control*, vol. 11, pp. 42–52, 2014.

[56] A. S. Keren, S. Yuval-Greenberg, and L. Y. Deouell, "Saccadic spike potentials in gamma-band EEG: Characterization, detection and suppression," *Neuroimage*, vol. 49, no. 3, pp. 2248–2263, 2010.

[57] M. F. Marmor and E. Zrenner, "Standard for clinical electro-oculography," *Arch Ophthalmol*, vol. 111, no. 5, pp. 601–604, 1993.

[58] P. Berg and M. Scherg, "Dipole models of eye movements and blinks," *Electroencephalogr. Clin. Neurophysiol.*, vol. 79, no. 1, pp. 36–44, 1991.

[59] A. Delorme, J. Palmer, J. Onton, R. Oostenveld, and S. Makeig, "Independent EEG sources are dipolar," *PLoS One*, vol. 7, no. 2, p. e30135, 2012.

[60] R. K. S. Kwan, A. C. Evans, and B. Pike, "MRI simulation-based evaluation of image-processing and classification methods," *IEEE Trans. Med. Imaging*, vol. 18, no. 11, pp. 1085–1097, 1999.

[61] T. W. Picton, P. Van Roon, M. L. Armilio, P. Berg, N. Ille, and M. Scherg, "The correction of ocular artifacts: A topographic perspective," *Clin. Neurophysiol.*, vol. 111, no. 1, pp. 53–65, 2000.

[62] W. Becker and a F. Fuchs, "Lid-eye coordination during vertical gaze changes in man and monkey," *J. Neurophysiol.*, vol. 60, no. 4, pp. 1227–1252, 1988.

[63] R. J. Croft and R. J. Barry, "EOG correction : A new perspective," vol. 107, no. May, pp. 387–394, 1998.

[64] B. Hu, H. Peng, Q. Zhao, B. Hu, D. Majoe, F. Zheng, and P. Moore, "Signal quality assessment model for wearable EEG sensor on prediction of mental stress," *IEEE Trans. Nanobioscience*, vol. PP, no. 99, p. 1, 2015.

[65] M. Yoshida, H. Shinohara, and H. Kodama, "Assessment of nocturnal sleep architecture by actigraphy and one-channel electroencephalography in early infancy," *Early Hum. Dev.*, vol. 91, no.

9, pp. 519–26, 2015.

[66] A. R. Teixeira, A. M. Tomé, E. W. Lang, P. Gruber, and A. Martins da Silva, "Automatic removal of high-amplitude artefacts from single-channel electroencephalograms," *Comput. Methods Programs Biomed.*, vol. 83, no. 2, pp. 125–138, 2006.

[67] H. Wang, Y. Li, J. Long, T. Yu, and Z. Gu, "An asynchronous wheelchair control by hybrid EEG-EOG brain-computer interface," *Cogn. Neurodyn.*, vol. 8, no. 5, pp. 399–409, 2014.

[68] M. Plöchl, J. P. Ossandón, and P. König, "Combining EEG and eye tracking: Identification, characterization, and correction of eye movement artifacts in electroencephalographic data," *Front. Hum. Neurosci.*, vol. 6, no. October, pp. 1–23, 2012.

[69] J. M. Henderson, S. G. Luke, J. Schmidt, and J. E. Richards, "Co-registration of eye movements and event-related potentials in connected-text paragraph reading," *Front. Syst. Neurosci.*, vol. 7, no. July, pp. 1–13, 2013.

[70] J. E. Kamienkowski, M. J. Ison, R. Q. Quiroga, and M. Sigman, "Fixation-related potentials in visual search: A combined EEG and eye tracking study," *J. Vis.*, vol. 12, no. 7, p. 4, 2012.

[71] Q. Ding, K. Tong, and G. Li, "Development of an EOG (Electro-Oculography) based Human-Computer Interface," *IEEE Eng. Med. Biol. Soc. Conf.*, vol. 7, pp. 6829–31, 2005.

[72] R. C. Dorf, *CRC handbook of engineering tables*, New. CRC Press, 2003.

[73] K. Shinomiya, N. Itsuki, M. Kubo, and H. Shiota, "Analyses of the characteristics of potential and cross-talk at each electrode in electro-oculogram," *J. Med. Investig.*, vol. 55, pp. 120–126, 2008.

[74] O. G. Lins, T. W. Picton, P. Berg, and M. Scherg, "Ocular artifacts in EEG and event-related potentials I: Scalp topography," *Brain Topogr.*, vol. 6, no. 1, pp. 51–63, 1993.

[75] J. L. Kenemans, P. C. M. Molenaar, M. N. Verbaten, and J. L. Slangen, "Removal of the ocular artifact from the EEG: A comparison of time and frequency domain methods with simulated and real data," *Psychophysiology*, vol. 28, no. 1. pp. 114–121, 1991.

[76] T. Elbert, W. Lutzenberger, B. Rockstroh, and N. Birbaumer, "Removal of ocular artifacts from the EEG--A biophysical approach to the EOG,"

Electroencephalogr Clin Neurophysiol, vol. 60, no. 5, pp. 455–463, 1985.

[77] R. J. Croft and R. J. Barry, "EOG correction: A new aligned-artifact average solution," *Electroencephalogr. Clin. Neurophysiol.*, vol. 107, no. 6, pp. 395–401, 1998.

[78] I. DiMatteo, C. R. Genovese, and R. E. Kass, "Bayesian curve-fitting with free-knot splines," *Biometrika*, vol. 88, p. 1055—1071, 2001.

[79] G. L. Wallstrom, R. E. Kass, A. Miller, J. F. Cohn, and N. A. Fox, "Automatic correction of ocular artifacts in the EEG: A comparison of regression-based and component-based methods," *Int. J. Psychophysiol.*, vol. 53, no. 2, pp. 105–119, 2004.

[80] G. Wallstrom, J. Liebner, and R. E. Kass, "An implementation of bayesian adaptive regression splines (BARS) in C with S and R wrappers," *J. Stat. Softw.*, vol. 26, no. 1, pp. 1–21, 2008.

[81] A. Cichocki, "Generalized component analysis and blind source separation methods for analyzing multichannel brain signals," in *Statistical and Process Models for Cognitive Neuroscience and Aging*, 1st ed., M. J. Wenger and C. Schuster, Eds. Psychology Press, 2006.

[82] P. K. Sadasivan and D. Narayana Dutt, "SVD based technique for noise reduction in electroencephalographic signals," *Signal Processing*, vol. 55, no. 2, pp. 179–189, 1996.

[83] T. P. Jung, S. Makeig, M. Westerfield, J. Townsend, E. Courchesne, and T. J. Sejnowski, "Removal of eye activity artifacts from visual event-related potentials in normal and clinical subjects," *Clin. Neurophysiol.*, vol. 111, no. 10, pp. 1745–1758, 2000.

[84] T. P. Jung, S. Makeig, C. Humphries, T. W. Lee, M. J. McKeown, V. Iragui, and T. J. Sejnowski, "Removing electroencephalographic artifacts by blind source separation," *Psychophysiology*, vol. 37, no. 2, pp. 163–178, 2000.

[85] A. Hyvärinen, "Fast and robust fixed-point algorithms for independent component analysis," *IEEE Trans. neural networks*, vol. 10, no. 3, pp. 626–34, 1999.

[86] I. Winkler, S. Haufe, and M. Tangermann, "Automatic classification of artifactual ICA-components for artifact removal in EEG signals," *Behav. Brain Funct.*, vol. 7, no. 1, p. 30, 2011.

[87] D. Girton and J. Kamiya, "A simple on-line technique for removing eye

movement artifacts from the EEG," *Electroencephalogr. Clin. Neurophysiol.*, vol. 34, no. 2, pp. 212–216, Feb. 1973.

[88] C. Vidaurre, T. H. Sander, and A. Schlögl, "BioSig: The free and open source software library for biomedical signal processing," *Comput. Intell. Neurosci.*, vol. 2011, no. 2011, p. 12, 2011.

[89] R. J. Croft and R. J. Barry, "Issues relating to the subtraction phase in EOG artefact correction of the EEG," *Int. J. Psychophysiol.*, vol. 44, no. 3, pp. 187–195, 2002.

[90] T. T. H. Pham, R. J. Croft, P. J. Cadusch, and R. J. Barry, "A test of four EOG correction methods using an improved validation technique," *Int. J. Psychophysiol.*, vol. 79, no. 2, pp. 203–10, 2011.

[91] R. J. Croft and R. J. Barry, "EOG correction of blinks with saccade coefficients: A test and revision of the aligned-artefact average solution," *Clin. Neurophysiol.*, vol. 111, no. 3, pp. 444–451, 2000.

[92] A. Zaknich, *Principles of adaptive filters and self-learning systems*. Springer London, 2005.

[93] J. Kayser and C. E. Tenke, "Principal components analysis of Laplacian waveforms as a generic method for identifying ERP generator patterns II: Adequacy of low-density estimates," *Clin. Neurophysiol.*, vol. 117, no. 2, pp. 369–380, 2006.

[94] S. Makeig and J. Onton, "ERP features and EEG dynamics," *Oxford Handb. Event-Related Potential Components*, no. July, pp. 1–37, 2011.

[95] A. Delorme and S. Makeig, "EEGLAB: An open source toolbox for analysis of single-trial EEG dynamics including independent component analysis," *J. Neurosci. Methods*, vol. 134, no. 1, pp. 9–21, 2004.

[96] C. Carl, A. Açik, P. König, A. K. Engel, and J. F. Hipp, "The saccadic spike artifact in MEG," *Neuroimage*, vol. 59, no. 2, pp. 1657–1667, 2012.

[97] D. H. Brainard, "The psychophysics toolbox," *Spat. Vis.*, vol. 10, no. 4, pp. 433–436, 1997.

[98] M. J. Thurtell, A. C. Joshi, and M. F. Walker, "Three-dimensional kinematics of saccadic and pursuit eye movements in humans: Relationship between Donders' and Listing's laws," *Vision Res.*, vol. 60, pp. 7–15, 2012.

[99] T. Haslwanter, R. Jaeger, S. Mayr, and M. Fetter, "Three-dimensional

eye-movement responses to off-vertical axis rotations in humans," *Exp. Brain Res.*, vol. 134, no. 1, pp. 96–106, 2000.

[100] L. J. Bour, M. Aramideh, and B. W. de Visser, "Neurophysiological aspects of eye and eyelid movements during blinking in humans," *J. Neurophysiol.*, vol. 83, no. 1, pp. 166–176, 2000.

[101] F. VanderWerf, P. Brassinga, D. Reits, M. Aramideh, and B. Ongerboer de Visser, "Eyelid movements: behavioral studies of blinking in humans under different stimulus conditions," *J. Neurophysiol.*, vol. 89, no. December 2002, pp. 2784–2796, 2003.

[102] C. A. Joyce, I. F. Gorodnitsky, and M. Kutas, "Automatic removal of eye movement and blink artifacts from EEG data using blind component separation," *Psychophysiology*, vol. 41, no. 2, pp. 313–25, Mar. 2004.

[103] A. T. Duchowski, *Eye Tracking Methodology: Theory and Practice. Second edition.* Spriger, 2007.

[104] R. Barea, L. Boquete, M. Mazo, and E. López, "System for assisted mobility using eye movements based on electrooculography," *IEEE Trans. Neural Syst. Rehabil. Eng.*, vol. 10, no. 4, pp. 209–218, 2002.

[105] S. D. Georgiadis, P. O. Ranta-aho, M. P. Tarvainen, and P. A. Karjalainen, "Single-trial dynamical estimation of event-related potentials: A Kalman filter-based approach," *IEEE Trans. Biomed. Eng.*, vol. 52, no. 8, pp. 1397–406, Aug. 2005.

[106] S. Sanei and J. Chambers, *EEG signal processing, 1st edition*, vol. 1. Wiley, 2007.

[107] J. R. Gentili, H. Oh, T. J., B. D., and J. L., "Signal processing for non-invasive brain biomarkers of sensorimotor performance and brain monitoring," in *Signal Processing*, InTech, 2010, pp. 1–6.

[108] P. He, G. F. Wilson, and C. A. Russell, "Removal of ocular artifacts from electro-encephalogram by adaptive filtering," *Med. Biol. Eng. Comput.*, vol. 42, pp. 407–412, 2004.

[109] J. Gerardo, J. C., and J. Velazquez, "Applications of adaptive filtering," in *Adaptive Filtering Applications*, InTech, 2011, pp. 1–20.

[110] B. D. O. Anderson and J. B. Moore, *Optimal Filtering*, vol. 16, no. 1. Dover Publications, 2005.

[111] R. Verleger, T. Gasser, and J. Mocks, "Correction of EOG artifacts in event-related potentials of the EEG: Aspects of reliability and validity,"

Psychophysiology, vol. 19, no. 4, pp. 472–480, 1982.

[112] B. Noureddin, P. D. Lawrence, and G. E. Birch, "Online removal of eye movement and blink EEG artifacts using a high-speed eye tracker," *IEEE Trans. Biomed. Eng.*, vol. 59, no. 8, pp. 2103–10, 2012.

[113] A. C. Tan and S.-T. Chen, "Two-dimensional adaptive LMS IIR filter," in *1993 IEEE International Symposium on Circuits and Systems*, 1993, no. 0, pp. 299–302.

[114] M. Muneyasu, E. Uemoto, and T. Hinamoto, "A novel 2-D adaptive filter based on the 1-D RLS algorithm," in *Proceedings of 1997 IEEE International Symposium on Circuits and Systems. Circuits and Systems in the Information Age ISCAS '97*, 1997, vol. 4, no. 0, pp. 2317–2320.

[115] M. Shams Esfand Abadi and S. Nikbakht, "Image denoising with two-dimensional adaptive filter algorithms," *Iran. J. Electr. Electron. Eng.*, vol. 7, no. 2, pp. 84–105, 2011.

[116] M. Ibn Kahla, Z. Faraj, F. Castanie, and J. C. Hoffmann, "Multi-layer adaptive filters trained with back propagation: A statistical approach," *Signal Processing*, vol. 40, no. 1, pp. 65–85, 1994.

[117] M. I. Kahla, Z. Faraj, and F. Castanie, "Mathematical properties of multi-layer adaptive filters," in *ICANN '93*, London: Springer London, 1993, pp. 778–778.

[118] J. I. S. de Oliveira, S. Y. C. Catunda, A. K. Barros, and J.-F. Naviner, "Multi-layer level measurement using adaptive filtering," in *2005 IEEE Instrumentationand Measurement Technology Conference Proceedings*, 2005, vol. 1, no. 0, pp. 732–736.